California Energy Commission

Geothermal Exploration, Economic Analysis and Distributed Energy Resource Demonstration

Final Project Report

California Energy Commission

Edmund G. Brown Jr., Governor

September 2018 | CEC-GEO-14-003

Primary Author(s):

Dr. Ismail Kuscu
Lisa Safford
Dr. Roy Mink
Curtis Rose
Warner Mountain Energy Corporation
State Highway 299
Cedarville, CA 96104

Dr. James McClain
University of California Davis
1 Shields Ave.
Davis, CA 95616

Daniel Hand
Sustainable Engineering
13801 120th St. E
Puyallup, WA 98374

Chester Robertson
Project Director, County of Modoc

Elisabeth de Jong

Commission Agreement Manager, California Energy Commission

Natalie Lee

Deputy Director

Renewable Energy Division, California Energy Commission

Drew Bohan

Executive Director, California Energy Commission

ABSTRACT

An extensive geoscientific investigation of geothermal resources in the eastern Surprise Valley was made to gain information on the potential for electric power development, followed by a demonstration of a distributed energy resource. Geological, geophysical and geochemical surveys were conducted to acquire information about the geological features and structures in an area of approximately 800 acres. Based on the findings, three sites were selected for temperature gradient drilling. The holes were used to obtain temperature gradient data and construct stratigraphic sections of the area. Water samples provided information about the geochemistry and the upflow pattern of the area's hot water circulation. A conceptual model on how the geothermal systems worked in central eastern part of Surprise Valley was developed based on the geoscientific investigation.

A Distributed Energy Resource (DER) unit was installed to demonstrate the benefits of a small distributed electric energy resource utilizing low temperature and low flow thermal fluids discharging to the surface. The unit was designed to produce 20 kW. A hot spring, with a temperature of 190°F and flow of about 150 gallons was used for the demonstration project. Although the unit demonstrated that electricity can be created at very low temperatures and flow, a six-minute test performed, using ten 100-watt light bulbs, resulted in surging and non-continuous power capabilities. Commissioning of the DER unit did not occur because consistent and adequate electrical power could not be supplied by the unit.

Assumptions derived from the temperature gradient drilling and geoscientific data were used to conduct economic feasibility studies identifying and quantifying development opportunities for the geothermal resource. In this context, electric, agricultural and aquaculture production potential of the study area were examined. Market feasibility studies for development opportunities were completed by determining the cost, economic merit, and sensitive variables both for the development and the market.

Keywords: geothermal, distributed energy resource unit, hot springs, California Energy Commission, temperature gradient drilling, geophysics, Warner Mountain Energy, Welsco Drilling, Sustainable Engineering, Cornerstone Sustainable Energy, PwrCor, economic analysis, market analysis, Modoc County, geochemistry, direct use

Please use the following citation for this report:

Ismail Kuscu, Lisa Safford, Roy Mink, Warner Mountain Energy Corporation, Daniel Hand, Sustainable Engineering, James McClain, University of California Davis, 2018. *Final Project Report: Geothermal Exploration, Economic Analysis and Distributed Geothermal Energy Resource Demonstration Project.* California Energy Commission. Publication Number: CEC-GEO-14-003.

ACRONYMS

Acronym/Abbreviation	Definition
AMT	acoustic magnetotelluric
ARFVTP	Alternative and Renewable Fuel and Vehicle Technology Program
AB	Assembly Bill
BPA	Bonneville Power Administration
Btu's	British thermal units
Btu/kWH	British thermal units per kilowatt-hour
Btu/(SF-Hr.)	British thermal units per square-foot-hour
BLM	Bureau of Land Management
Energy Commission	California Energy Commission
CAISO	California Independent System Operator
CO_2	carbon dioxide
CPS	counts per second
CSEM	controlled source electromagnetic
˚C	Degrees Celsius
˚F	Degrees Fahrenheit
DC	Direct Current
DUP	Duplicate sample
$/kWh	Dollars per kilowatt-hour
gpm	gallons per minute
>	greater than
HPS	high pressure sodium
HDPE	high-density polyethylene
(Hr. Ft2. ˚F)/BTU	hours-square feet-degrees Fahrenheit per British thermal unit
ICP-AES	Inductively coupled plasma atomic emission spectroscopy
ICP-MS	Interdisciplinary Center for Plasma Mass Spectrometry using Inductively Coupled Plasma Mass Spectrometry
kW	Kilowatt
kWHs	Kilowatt-hours
KGRA	Known Geothermal Resource Area
LOD	Limit of detection
LOI	loss on ignition
Tlb	low-potassium, high-alumina olivine tholeiites
MPR	Market Price Referent
MW	megawatt
MWhs	megawatt-hours
µg/L	micrograms per liter
(mS/cm)	microsiemens per centimeter
MPH	miles per hour
Acronym/Abbreviation	**Definition**

mg/L	milligrams per liter
mls	milliliters
mmole	millimole
Ma	million years
MSWA	Multichannel Surface Wave Analysis
NOPA	Notice of Proposed Awards
NFT	Nutrient Film Technique
MMBtu/Hr.	one million British thermal units per hour
O&M	Operation and maintenance
OIT	Oregon Institute of Technology
ORC	Organic Rankine Cycle
ppb	parts per billion
ppm	parts per million
lbs/Hr.	pounds per hour
PPA	Power purchase agreement
REE	rare earth element
RPS	Renewables Portfolio Standard
REAP	Rural Energy for America Program
km^2	square kilometers
SVEC	Surprise Valley Electrification Corp
SVHS	Surprise Valley Hot Springs
SVMW	Surprise Valley Mineral Wells
TDS	total dissolved solids
USDA	United States Department of Agriculture
USGS	United States Geological Survey
UAS	unmanned aerial system
WME	Warner Mountain Energy Corporation
XRF	X-Ray Fluorescence

TABLE OF CONTENTS

LIST OF FIGURES

LIST OF TABLES

EXECUTIVE SUMMARY

Background

Surprise Valley is located in northeast California, in the County of Modoc which lies at the intersection of the borders of California, Oregon and Nevada. The project site is located five miles east of Cedarville and 20 miles east of Alturas in the vicinity of Surprise Valley Hot Springs (SVHS) resort.

Geologically, Surprise Valley is a part of the Great Basin that extends across most of the northern half of Nevada. The Surprise Valley geothermal system is located within a geological escarpment, known as a graben. It is a fluid-producing system bounded by the Surprise Valley Fault to the west and Hays Canyon fault to the east. The graben basin is filled with alluvium and lake deposits interbedded with numerous volcanic flows, tuffs, and breccias. Basin fill ranges in thickness from less than 100 ft. to over 6,250 ft.

Geothermal activity in Surprise Valley has long been known. Archaeologists have found that the first known human inhabitants of the valley constructed dwellings selectively in hot spring areas 5000 to 6000 years ago. In the early 1900s spas were widely used by the locals but the geothermal potential of the area was highlighted around 1951, following investigations after the eruption of a mud volcano in nearby Lake City. In 1974, an area of 295 km^2 (72,940 acres) in Surprise Valley was classified as a “Known Geothermal Resource Area” by the U.S. Geological Survey.

Recently detailed geochemical and geophysical studies have been conducted, largely focusing on the west side of the valley, to better understand how geothermal fluids flow through the subsurface and where the faults that circulate these fluids exist. Results of these studies indicate the potential for large-scale geothermal development in Surprise Valley. The geothermal reservoir temperature throughout Surprise Valley is estimated to be about 347˚F. Deep exploration wells have been drilled on the west side of the valley with the intent to develop a large-scale geothermal power plant.

Out of 304 hot springs in the State the SVHS site is listed as the third hottest with a total flow of about 3,000 gallons per minute. Two geothermal wells are located at the site along with several hot springs. Existing resource flow is about 3,000 gallons per minute with temperatures as high as 217˚F.

Purpose

Although geothermal resources are abundant in Surprise Valley and much research has been conducted, geothermal electricity is not yet being produced in this part of Northern California. The overall purpose of the project is to reveal the geothermal potential of the eastern side of the Surprise Valley and assess the economic value of the potential. The goals of this project were to conduct geologic exploration with the long-term goal of marketing Modoc County’s large-scale geothermal potential and, concurrently, to demonstrate the technical feasibility of a distributed energy resource. The ultimate goal is to reduce dependence on fossil fuels.

Objectives

The objectives of this project were to acquire geoscientific information on the east side of Surprise Valley using multiple geologic approaches including drilling, to install and demonstrate the effectiveness of a distributed energy geothermal unit to generate electricity, to generate an economic feasibility and market analysis, and to engage public in creating an interest in geothermal development.

Conclusions and Recommendations

Warner Mountain Energy (WME), under contract with Modoc County, conducted geoscientific investigation to evaluate the geothermal potential in the study area. Investigations included surficial geology reconnaissance, mapping, fault analysis, 2-m soil temperature probe survey of 123 sites, soil gas survey, limited shallow auger surveys, geophysical surveys, and water sampling.

Three holes were drilled at the sites selected based on the results of the WME and UCD surveys. Depths of holes ranged from 750-1416 feet below ground surface. The holes were logged for temperature gradients with increasing gradients seen in all holes.

Development of a hot spring resource discharging at 190˚F and flowing at about 150 gallons per minute was undertaken to facilitate the demonstration of a 20kW Distributed Energy Resource (DER) unit. The DER unit engine operates based on the thermal expansion or compression of supercritical CO2. It is designed to generate power from low temperature (below 165˚F) heat sources based on the expansion/contraction of supercritical CO_2 when heat is added or removed.

The County of Modoc contracted with WME to supply the geothermal resource and site infrastructure, and with Cornerstone Sustainable Energy doing business as PwrCor to supply the DER unit. Southwest Research Institute (SWRI) Laboratory assisted PwrCor to design, build and demonstrate the DER unit.

A demonstration leading to commissioning of the PwrCor machine was conducted on March 9, 2018. This demonstration involved running the machine and lighting ten 100-watt light bulbs for about 6 minutes and 25 seconds. During the test the machine powered up and down lighting the bulbs 18 times. The power bursts from four to six seconds each with approximately three power bursts per minute.

Although the unit demonstrated that electricity can be created at very low temperatures and flows for several minutes, commissioning of the unit did not occur because the power was not consistent and the unit could not be connected for a net metering system.

An economic feasibility study was completed in order to identify and quantify development opportunities for the geothermal resource. Electric production, agricultural and aquaculture potential were evaluated.

Electric production potential, assuming a single producer/injector pair of wells with typical binary power plant technology, was estimated to be capable of approximately a 22 MW power plant if a flow of 10,000 GPM at 285 ˚F is developed. The estimated cost for 22 MWs is about $100 million; the estimated cost for a smaller, nominal 6.4 MW plant is about $25.8 million.

Economic feasibility for greenhouse and aquaculture operations are favorable considering the availability of geothermal heating.

A market feasibility study was performed to determine the cost of development opportunities. The cost of developing electric power is high, as in any development. The potential to put electric power on the grid under economically-favorable conditions for larger power markets is limited at the present time, due to the low cost of natural gas and gap in transmission line between the County and the electricity market to larger user bases to the South. However, bringing a power user to Modoc County to utilize power on site is a viable option. The market for agricultural and aquaculture products is favorable given the availability of the geothermal resource for production. Development of the resource could result in jobs and economic benefits to the County.

Numerous public outreach activities occurred with good attendance by the public. Many questions were asked during the outreach activities. Outreach events occurred at the project site (open house during drilling); community meetings at the local Senior Center, the local church; several newspaper articles were published; and handouts on the basics of geothermal energy were provided to the local schools.

As for the scientific outputs of the project, the University of California Davis (UCD) delivered a presentation at the American Geophysical Union in 2015 on the geochemistry of the area and following this, an article was published in Applied Geochemistry magazine. WME has submitted two abstracts discussing the findings in the study area to the Geothermal Resource Council meeting held in October 2018.

CHAPTER 1: Introduction

1.1 Background

1.1.1 Project Need

Geology and geothermal possibilities of the Surprise Valley have been studied since the 1970's with a substantial increase of research in the past decade. Recent research groups have included the UCD; University of Nevada, Reno; National Space and Aeronautics Administration (NASA); Stanford University; University of Central Washington; Carnegie-Mellon University; and the United States Geological Survey (USGS).

Detailed geochemical and geophysical studies have been conducted, largely focusing on the west side of the valley to better understand how geothermal fluids flow through the subsurface and where the faults exist that circulate these fluids. Results of these studies indicate the potential for large-scale geothermal development in Surprise Valley. Scientists have identified some major fault structures and have estimated that the geothermal reservoir temperature throughout Surprise Valley is about 347˚F. Deep exploration wells have been drilled on the west side of the valley with the intent to develop a large-scale geothermal power plant.

Out of 304 hot springs in the State, this project site, Surprise Valley Hot Springs, is listed as the third hottest. A 160-ft well at the Surprise Valley Hot Springs resort measures 217˚F.

Most of the studies thus far have focused on the Lake City Fault Zone area on the west side of the valley. These works do not address the details of the geothermal system beneath the Surprise Valley Hot Springs on the east side of the valley.

To effectively characterize the east side of the valley for power production potential, more geological information is needed. The area in the vicinity of Surprise Valley Hot Springs provides an excellent opportunity to learn about the relationship of the eastern valley geothermal system relative to the western valley geothermal system. This project will build upon existing geophysical and geochemical studies focused on the west side of the valley.

1.1.2 Scope of Work

The scope of work for this project includes deep subsurface exploration, shallow subsurface exploration, temperature gradient drilling, demonstration of small distributed energy resource unit, economic and market feasibility, and public outreach.

1.1.3 Site Description

Surprise Valley is located in northern California, in the east of Modoc County, east of Alturas. Locals refer to the area as the *Tricorner Region* because of the region's location at the intersection of California, Oregon and Nevada state lines (Figure 1).

The area is part of the Great Basin that extends across most of the northern half of Nevada. Most of the valley is over 4,000 feet above mean sea level and could be characterized as a high-altitude desert valley. The Warner Mountains are located on the west side of the valley and the Hays Canyon Range is located on the east side of the valley. Communities in Surprise Valley include Eagleville, Cedarville, Lake City and Fort Bidwell.

The project site, Surprise Valley Mineral Wells (SVMW), also referred to as "Surprise Valley Hot Springs", is located five miles east of Cedarville and 20 miles east of Alturas in Modoc County, California (Figure 1).

Figure 1: Location of Surprise Valley.

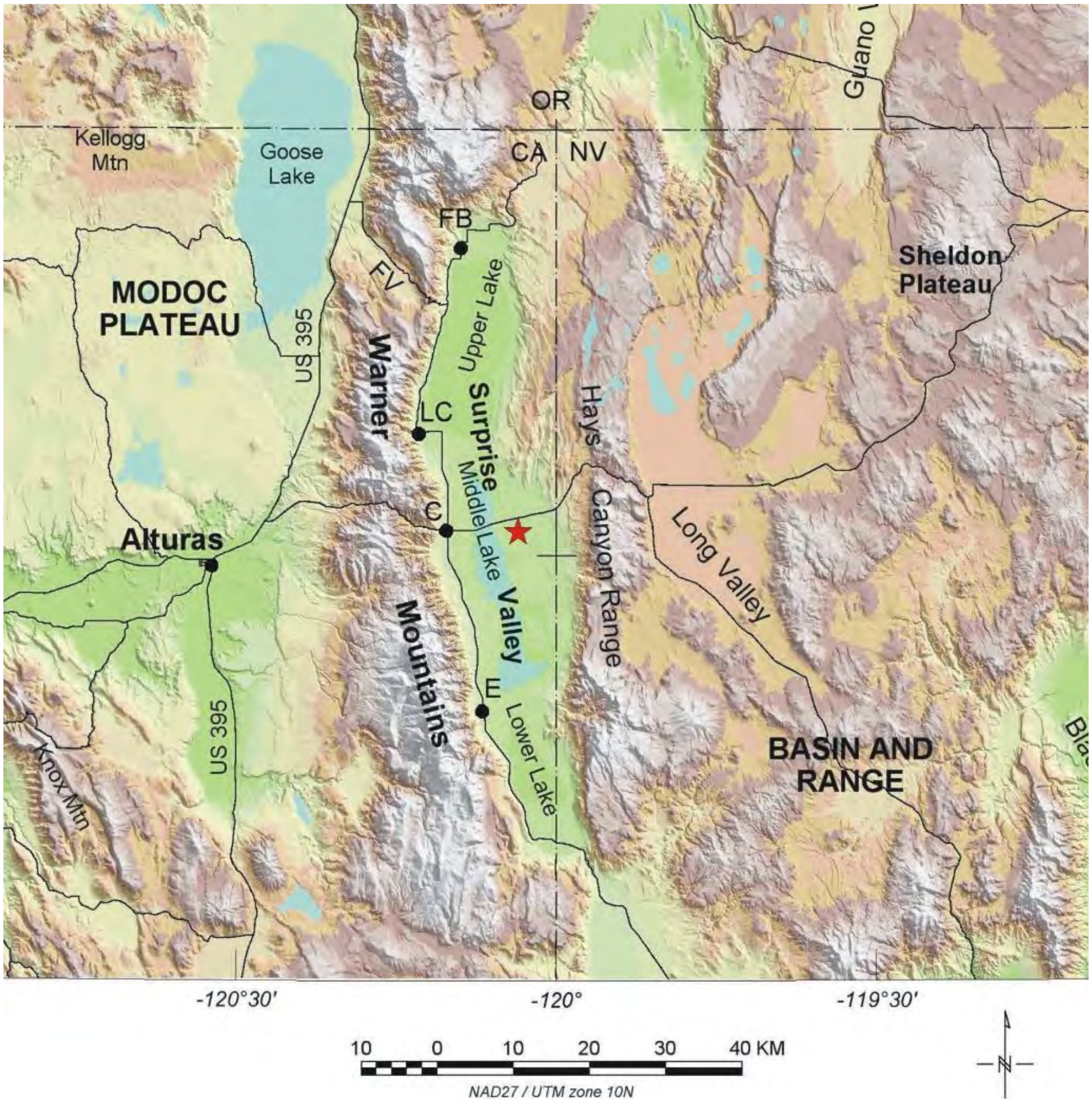

The red star denotes the Surprise Valley Mineral Wells (SVMW).

The study area is on about 800 acres of private land and includes the surficial property surrounding the Surprise Valley Hot Springs resort. Geothermal rights are leased to Warner Mountain Energy Corporation. Figure 2 shows a Bureau of Land Management map of the general project location as located within Township 42 N, Range 17 E, Section 06, Modoc County, Mount Diablo Meridian; private lands are shown with a white background, public lands are shown with a gold background.

Figure 2: Location of project site on Bureau of Land Management map showing land status.

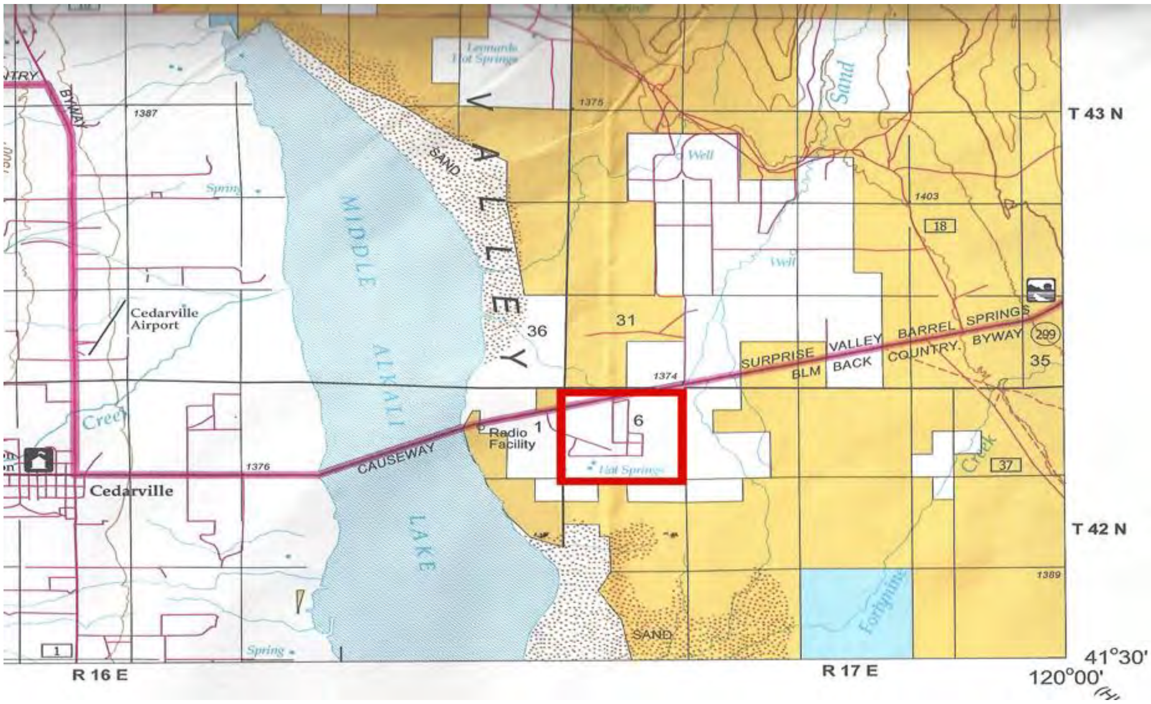

1.2 Goals and Objectives

1.2.1 Goals

Although geothermal resources are abundant in Surprise Valley and much research has been conducted, geothermal electricity is not yet being produced in Northern California. In the past, geothermal development has been focused in Central and Southern California.

The *goals* of this project were to conduct geologic exploration with the long-term goal of marketing Modoc County's large-scale geothermal potential and, concurrently, to demonstrate the technical feasibility of a distributed energy resource unit. This aligns with the Geothermal Grant and Loan Program goals of offsetting costs of developing geothermal resources within local jurisdictions and reducing dependence on fossil fuels. Geologic exploration and temperature gradient drilling proves the technical feasibility of the resource; economic feasibility lays the foundation for geothermal development planning and financing; and successful demonstration of a distributed energy resource serves as an example for other Modoc County geothermal sites.

1.2.2 Objectives

The *objectives* of this project were 1) fill in scientific data gaps on the east side of Surprise Valley in the vicinity of Surprise Valley Hot Springs (SVHS) using an integration of multiple geologic approaches including geochemical, geophysical, two-meter soil probe temperature survey, soil gas survey, and exploratory drilling; 2) install and demonstrate the effectiveness of a distributed energy geothermal unit to generate electricity immediately; 3) generate an economic feasibility and market analysis to facilitate steps in long-range planning; and 4) effectively engage the public in creating a strong interest in geothermal development.

For a detailed discussion on the history of geothermal activity, previous studies, and regional geology see Appendix A.

1.3 Regional Structural Geology

Within the Great Basin of the western United Sates, geothermal fields are in greatest abundance in northern Nevada and neighboring parts of northeast California and southeastern Oregon (Figure 3). The fields can be grouped into four northeast-trending major fault zones and one northwest-

Figure 3: Geothermal fields in Great Basin.

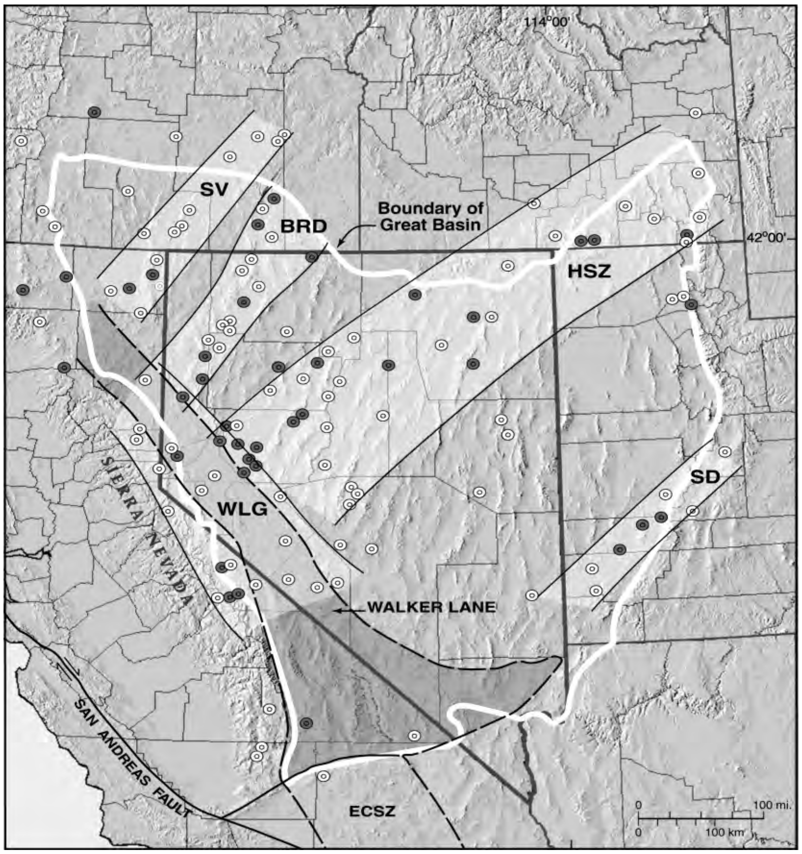

Geothermal fields cluster in the Sevier Desert (SD), Humboldt Structural Zone (HSZ), Blackrock desert (BRD), Surprise Valley (SV), and Walker Lane (WLG) belts. White circles are geothermal systems with maximum temperatures of 100-160 °C, gray circles have maximum temperatures >160 °C. ECSZ: eastern California Shear Zone.
Credit: Faulds et al., 2004.

trending fault zone. From southeast to northwest, the northeast-trending belts are referred to as Sevier Desert, Humboldt, Black Rock Desert, and Surprise Valley geothermal belts (Faulds, et al., 2004). This clustering of geothermal fields lies within a much broader region of high heat flow that covers much of the western USA (Blackwell and Richards, 2004). Surprise Valley of northeastern California is the westernmost graben of the Basin and Range province.

Surprise Valley of northeastern California marks a major tectonic transition between the relatively un-extended Modoc Plateau and a region of 10-15 percent extension to the east. In addition, it sits just north of the Walker Lane, which accommodates up to 20 percent of dextral slip associated with Pacific-North American plate interactions, and just south of the Cascades back-arc that is undergoing extension and clock-wise rotation.

On the western margin of the valley, the east-dipping Surprise Valley fault (SVF) separates the valley from the Warner Mountains and may accommodate over 7 km of normal slip (

Figure 4). The SVF includes several major segments connected by step-overs that primarily step to the left, likely reflecting the growth and connection of a system of en echelon fault segments. An en echelon segment is identified as a formation of rock showing movement in a particular direction. The most significant of these step-overs coincides with minor topographic highs in Surprise Valley, dividing the valley into a series of three sub-basins that host the upper, middle, and lower lakes. Numerous Quaternary fault scarps occur as far as 2 km from the main range-front, cutting and displacing basin sediments by as much as 15 m (Hedel, 1980). The scarps are concentrated at the step-overs of the range-front fault, propagating into the basin and may be fault splays that initiate at the juncture of en echelon segment boundaries.

Figure 4: Cenozoic fault map draped over shaded relief of Surprise Valley and surrounding regions.

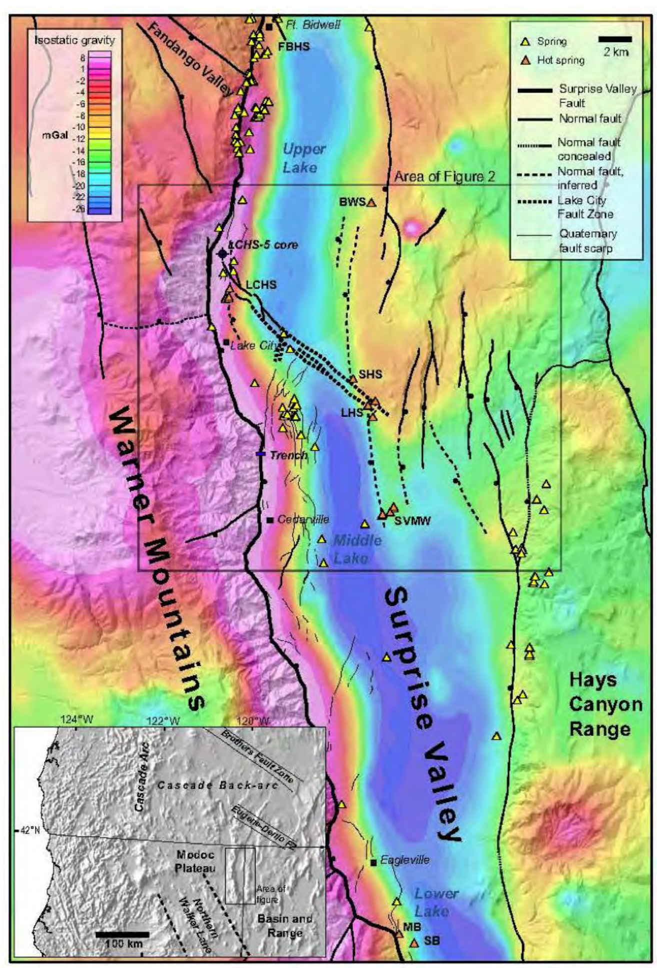

BWS: Boyd Warm Springs, FBHS: Fort Bidwell Hot Springs, LCHS: Lake City Hot Springs, LHS: Leonard Hot Springs, MB: Menlo Baths, SB: Squaw Bath Hot Springs, SHS: Seifert Hot Springs, SVMW: Surprise Valley Mineral Wells. Inset shows a regional index map. Colors indicate isostatic gravity. *Credit: Glen et al., 2008).*

Roughly parallel to the SVF, a series of closely spaced normal faults cuts the late Miocene to Pliocene volcanic rocks in the low hills north of the Hays Canyon Range (

Figure 4). The dip direction of these faults, as well as the amount of offset and tilt they accommodate, varies considerably along the length of the range, creating several tilt domains.

Between the major range-front faults is a set of northwest-trending structures referred to as the Lake City Fault Zone (LCFZ) (

Figure 4), a half-km wide zone of low-relief alluvial scarps and photo-lineaments that crosses the subdued topographic high separating the Upper and Middle Lakes (Hedel,1984; Glen et al., 2008). This network of scarps appears to connect the eastern and western basin-bounding faults. The close correspondence of this feature with most hot springs in the valleys suggests it plays a key role in hydrothermal circulation. On the eastern margin of the Upper Lake basin, offset of normal faults reaches several hundred meters and fault-bounded blocks are tilted and rotated up to 15° to the west. These faults die out and dips on the flows flatten to the north. These faults are most numerous and have the greatest offset just north of the road between Cedarville and Vya, where several conjugate (west-dipping) faults have also developed, resulting in a series of inter-fingering horsts and grabens. This zone of more faulting likely represents a transverse antithetic accommodation zone, which accommodates the transition from a half-graben in the upper lake basin to a full graben in the middle and lower lake basins.

1.4 Surprise Valley Mineral Wells

Surprise Valley Mineral Wells is a name historically given to the area in the vicinity of Surprise Valley Hot Springs resort. There are several hot springs of various size in the area (Figure 5).

Figure 5: Surprise Valley Mineral Wells. Red pushpins show hot spring locations.

1.4.1 Local Geology

The springs are located on a rather flat area which is covered by Quaternary (Holocene) alluvium (Qal) comprised of unconsolidated sedimentary deposits associated with modern sediments. This widespread unit overlies the Quaternary eolian deposits (Qe) (Holocene) which is comprised of eolian sand dunes, mostly stabilized as indicated by vegetation growth. Quaternary lake and playa (Qp) deposits (Holocene) which are evaporites and clay deposits in ephemeral lakes. The oldest unit in the area is Quaternary pluvial lake deposits (Qpl) (Pleistocene) and denotes the lake sediments deposited in Pleistocene Lake Surprise. These are primarily fine-grained sediments, often tuffaceous, but also include minor gravels and waterlain tuffs (Figure 6). The question mark associated with Qpl in Figure 6 indicates that the unit needs further ground-truthing.

The north-south trending faults in Figure 6 are observed as rather deep seated faults, however, they do not have significant vertical offsets along the cross-section. The westerly situated, west-dipping fault cuts the Surprise Valley Fault at depth. The other fault, located easterly, dips east.

Figure 6: Geologic map of the area surrounding Surprise Valley Mineral Wells.

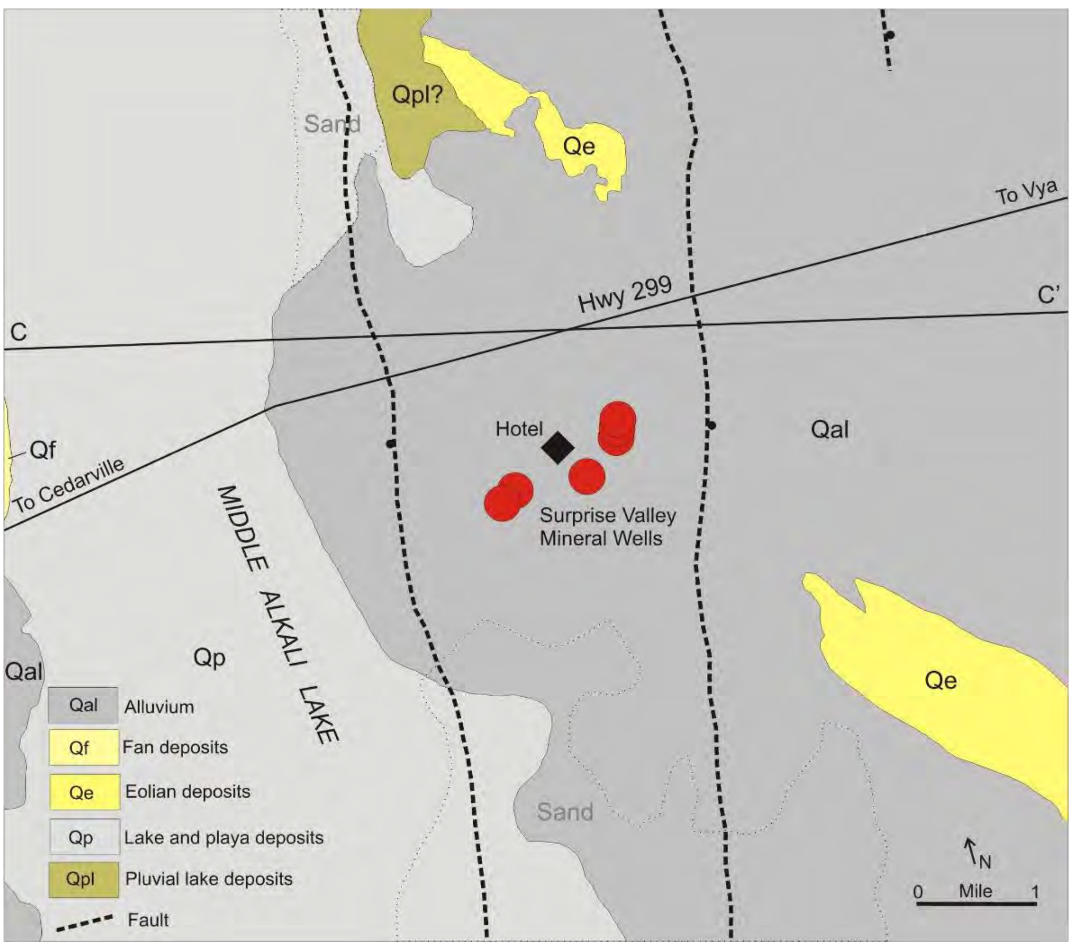

Red dots show the springs and wells. *Credit: Egger and Miller, 2011.*

1.4.2 Geophysical Studies Covering the Surprise Valley Mineral Wells

No previous site specific geophysical studies were conducted in close proximity of the SVMW, however, those carried out basinwide have been useful in revealing some information about the site.

Glen et al. (2013) collected high-resolution magnetic data from the air using a UAS to provide continuous coverage and combined ground and air data. In order to reveal the origin of the magnetic high, the authors made use of high-resolution reflection seismic data along a stretch of the magnetic high (Fontiveros, 2010), and a gravity model along the same profile (Athens, 2011). Consequently, they revealed the presence of a tabular magnetic body aligned with a fault that was interpreted to be a strongly magnetic mafic dike, which is a dark colored volcanic rock cut into the geologic formation horizontally (Glen et al., 2013) (

Figure 7). A detailed survey in the middle basin reveals that the magnetic high is locally discontinuous, consisting of segments with splays and spurs that bend or abruptly terminate (

Figure 7).

Figure 7: Magnetic residual map of combined ground and UAS data of the Surprise Valley area.

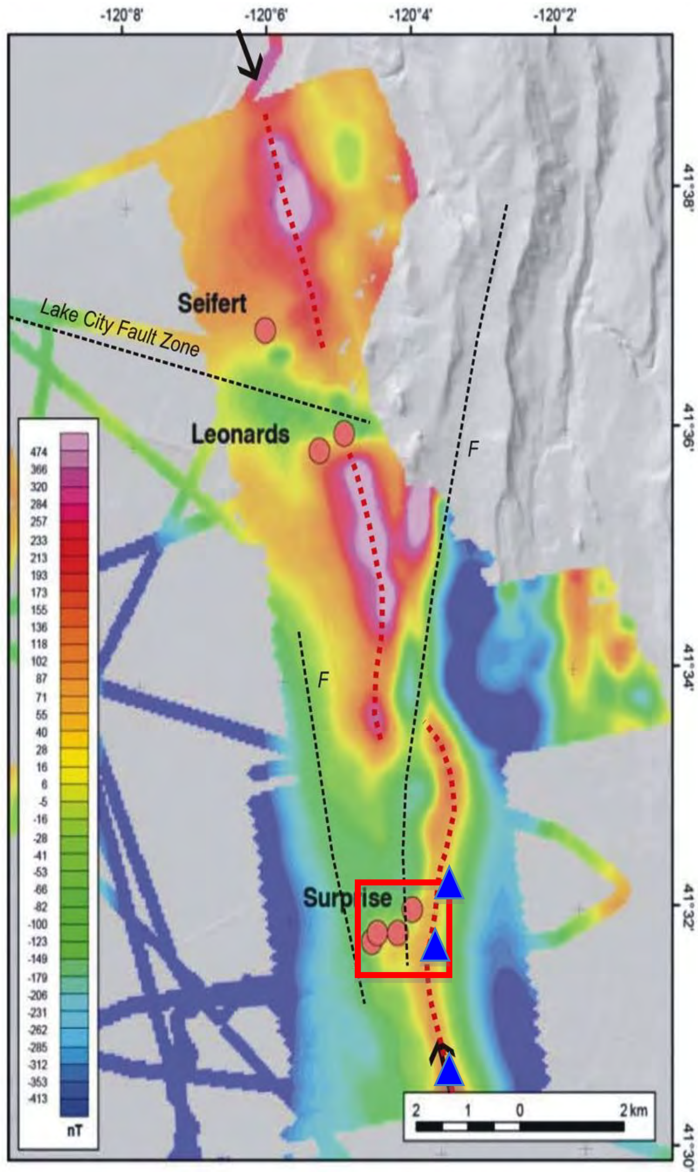

The red rectangle indicates the study area at Surprise Valley Hot Springs (SVHS, labeled "Surprise" on the figure). The orange circles denote the locations of hot springs. The red dotted lines and the black arrows indicate the linear magnetic anomaly that may play a role in hydrothermal system. The blue triangles are the locations of basalt outcrops observed in the area. Note that the hot springs lie along the magnetic anomaly, but also along the faults, labelled "F" that bound the eastern border of the valley. *Credit: Glen et al., 2013.*

Terminations of in-line segments such as between Seyferth and Leonard hot springs (

Figure 7) appear as abrupt lows crossing the magnetic high. Similarly, the easterly fault passing near SVMW hot springs cut the magnetic high and cause another abrupt magnetic low. These segmented structures have the potential for facilitating the presence of geothermal fluids by creating stress perturbations around fault tips and interaction zones. They also maintain porosity and permeability in the surrounding rocks and sediments as strain accumulates.

CHAPTER 2:

Geoscientific Studies Conducted to Reveal the Geothermal Potential of the Study Area

2.1 Deep Subsurface Geological Exploration

2.1.1 Geophysical Surveys

An exploration of the shallow subsurface beneath the SVHS property was conducted during this study. The goals were to identify the "plumbing" related to the hot springs, and to characterize how that plumbing may be connected to the deeper source of thermal waters. Before the study it was known that the hot springs took place near faults that could provide a conduit for hot fluid upwelling. But the springs also took place over a magnetic high that could indicate the presence of a volcanic dike or lava flow that also could provide a conduit for upflow of the fluid. This geophysical study represents an attempt to better constrain models for the hydraulic system. The study consisted of a magnetotelluric survey technique known as "acoustic magnetotelluric" (AMT) and controlled source electromagnetic (CSEM). In addition, a shallow seismic experiment was conducted in effort to better understand the local structures, and to mitigate a fundamental ambiguity in the interpretation of magnetotelluric information. Finally, an array for a long period magnetotellurics was deployed to provide information from deeper in the Earth.

2.1.1.1 Short-Period Magnetotelluric Survey

For the purposes of this report, the AMT technique and the CSEM technique were combined referring to them as the "short-period magnetotelluric survey". The short-period study exploited electromagnetic waves produced either by atmospheric fluctuations (e.g. distant lighting storms) or a controlled source antenna. The waves, assumed to be vertically incident, have a broad spectrum of frequencies. As they propagate into the Earth the electromagnetic waves "feel" the conductivity structure of the Earth, with contributions dependent on the conductivity and frequency of the incident waves. In general, the lower the frequency the deeper waves will penetrate more deeply into the Earth. Similarly, the lower the conductivity, the deeper the waves may penetrate. The penetration depth is usually characterized by a "skin depth" (δ). The skin depth is defined as,

$$\delta = (2/\mu_o\sigma\omega)^{1/2} = (\rho T/\mu_o\pi)^{1/2} \qquad \text{Eq. 1}$$

In these equations ω is the radial frequency of the incident electromagnetic waves, with $\omega=2\pi/T$, and T is the period. σ is the electrical conductivity of the material, and ρ is electrical resistivity such that $\rho=1/\sigma$. μ_o is the magnetic permeability of the Earth, assumed to be small and almost constant. Each frequency contained in the incident electromagnetic wave has its own skin depth; that is, each "feels" the Earth at different depths. For this report the resistivity structure is discussed rather than the conductivity structure keeping in mind that they are reciprocals of each other.

These equations are strictly true only for an Earth that is a homogenous half space. For the real Earth where conductivity or resistivity varies with depth, an effective skin depth can be defined that provides an informal estimate of the contribution of each level to an estimate of the conductivity as a function of depth. By measuring the north-south components of the electric potential (E_y), and magnetic field (H_y). Similarly, the east-west components (E_x and H_x) can be measured. For a homogeneous Earth an impedance Z can be defined such that,

$$Z = \frac{E_x}{H_y} = - \frac{E_y}{H_x} \qquad \text{Eq. 2}$$

and from this we can solve for the resistivity in the subsurface, where

$$r = \frac{1}{wm_0}|Z|^2. \qquad \text{Eq. 3}$$

As stated above, this value of resistivity is only the true resistivity for a homogeneous Earth. For a more realistic Earth, such as one that is vertically stratified or layered, this is only an "apparent resistivity" (ρ_a). Because each frequency samples the Earth differently (each frequency has its own skin depth) the apparent resistivity was found to be varying with frequency, w, or period (T). That is, apparent resistivity has the relationship.

$$\rho_a = \rho_a(\omega) = \rho_a(T) \qquad \text{Eq. 4}$$

The inverse problem for magnetotellurics for a stratified Earth is to convert the apparent resistivity $\rho(\omega)$ into the true resistivity as a function of depth, ρ (z). The Niblett-Bostic approximation was used here (Bostic, 1977) to make this calculation, using the relation,

$$\rho(z) = \rho_a \frac{(2+f)}{(2-f)}, \qquad \text{Eq. 5}$$

where f is given by the derivative,

$$f = \frac{d[\log(\rho_a)]}{d[log\sqrt{T}]} \qquad \text{Eq. 6}$$

This project uses the assumption that under each of the magnetotelluric stations the Earth is locally vertically stratified. Lateral variability can be determined by comparing stations distributed over the field area.

a) Survey details

For the survey a Geometrics Strategem EH4^T system was leased. This system records the two orthogonal magnetic field components (H_x and H_y), where "x" refers to the east-west direction and "y" refers to the north-south direction of the magnetic field. Simultaneously, two potential field components (E_x and E_y) are recorded using electrode pairs. The system exploits both natural sources from 10 to 92000 Hz, and includes a transmitter source, generating signal from 800 to 64000 Hz.

The system was deployed throughout the study area at 33 locations (Figure 8) over two seasons of fieldwork. The measurements from the natural sources and the antenna source are combined in the analysis. Deployments are over the hot spring area and are combined into profiles (Figure 8).

Figure 8: Deployment plan for the short- and long-period magnetotelluric survey.

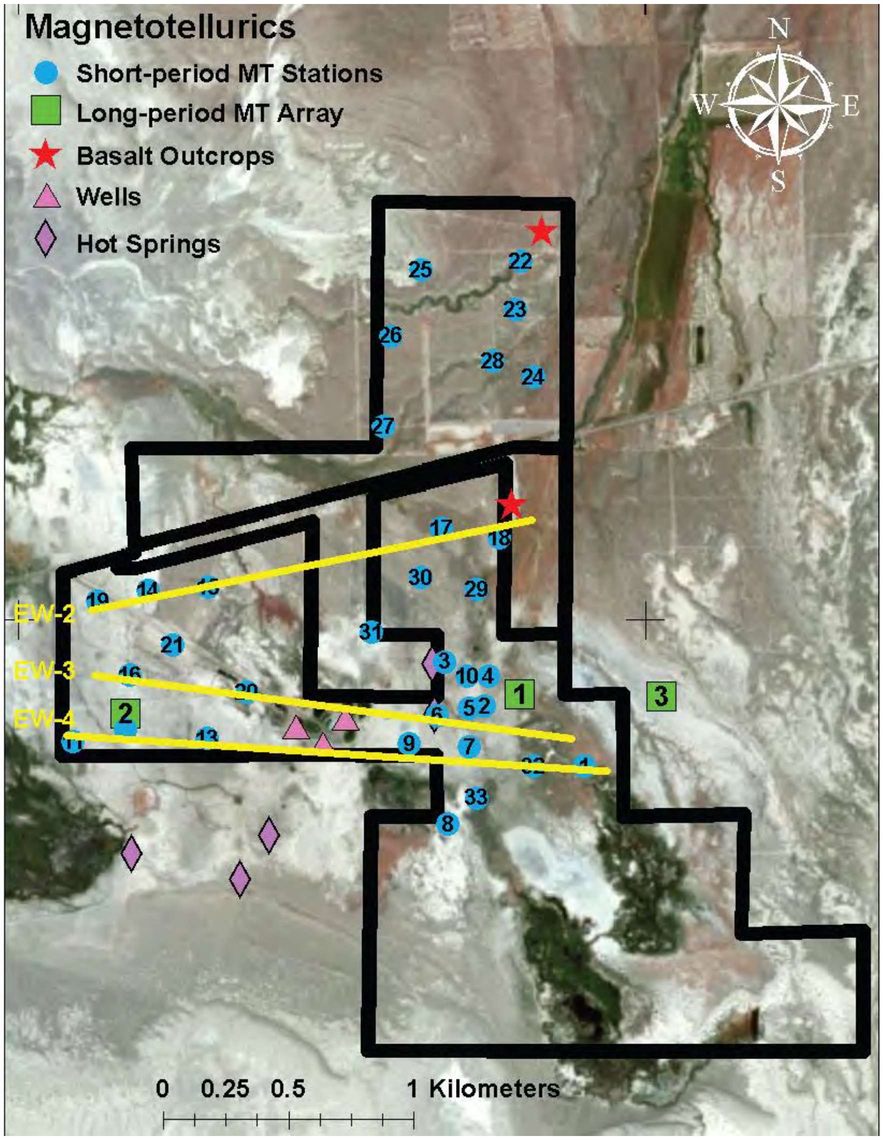

The station locations are shown by blue dots. Black lines indicate the property boundaries. Thermal wells and natural hot springs are denoted by purple diamonds and the location of the basalt outcrops is indicated by a red star. The stations are grouped into three profiles, EW-2, EW-3 and EW-4, for ease of discussion in the text.

b) Results

Results are presented as a series of east-west cross sections below (Figure 9 to Figure 11). For each section, one-dimensional inversion and interpolation was used for each station. This can show the trends along the sections. The resistivity values are represented by colors with warmer colors representing the low resistivity. Low resistivity may indicate presence of ground water and/or thermal waters beneath the surface. These would presumably be present in porous or permeable materials. However, low resistivity values could represent impermeable clays in the sediments. These contradictory interpretations are fundamental. In volcanic regions impermeable clays result from hydrothermal alteration of the overlying volcanic rocks, and thus form a cap beneath which thermal waters are trapped. However, it is perhaps unlikely that such a mechanism is at work in Surprise Valley where lake sediments dominate.

A number of features can be seen on all three cross sections. On the west end of the three pseudo-profiles a high resistivity layer (~150 m) lies under a thin intermediate resistivity layer (~10 to 20 m). It is believed that this was caused by recently dampened surface layers (vadose zones) perched above sediments that appear low in fluid content (high resistivity). At the east end of all three profiles (These can be seen under station 17 on EW-2, under station 10 on EW-3, and under station 32 on EW-4), the same high resistivity layer is present, and appears to reach the surface. It is suggested that this was caused by dry alluvium and/or lake sediments.

Figure 9: Resistivity cross-section EW-2.

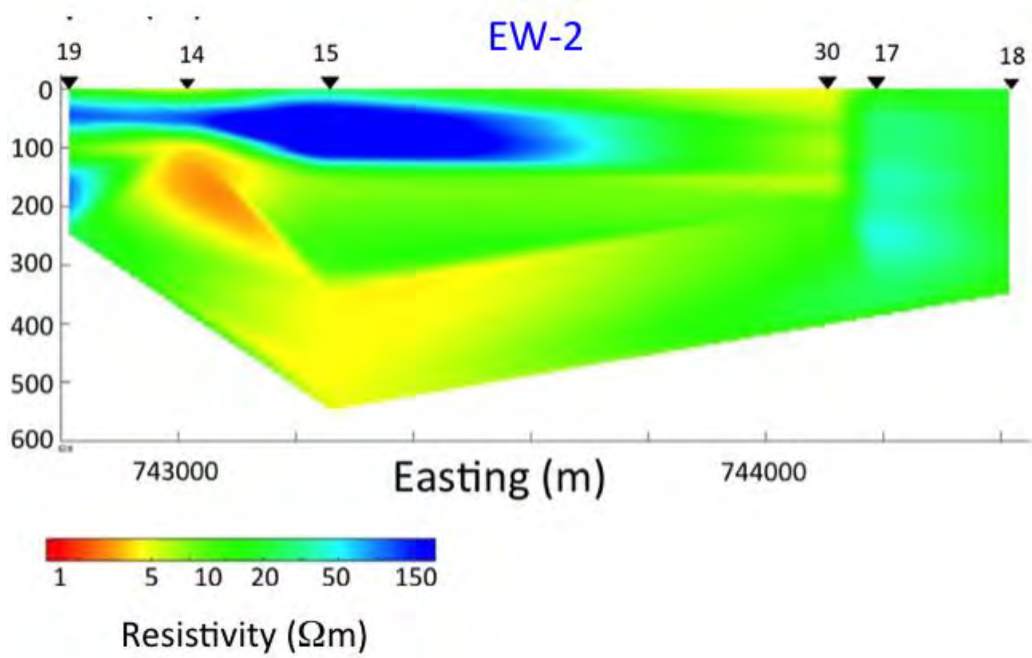

The stations used to construct this section are shown as black triangles at the top of the section. Blue represents the highest resistivity, and probably represents loose alluvium near the surface. The gap between station 15 and 30 is the least reliable of this interpolated cross section. No hot springs or wells were near this cross section. On all these cross sections west is to the left and east is to the right.

At the central part of each profile, the surface is characterized by lower resistivity values (5- 10 Ωm). This is poorly resolved on profile EW-2 because the property was not accessible. There also are gaps between stations on EW-3 and EW-4 because of the proximity of the resort, with its buried infrastructure and electrical lines. However, for both lines, the area near the hot springs included stations and reveals the lower resistivity values (Figure 10 and Figure 11). The interpretation of this co-existence of high temperature springs and low resistivity values is caused by upflow zones for the thermal waters. As part of the overall project elevated temperatures in the subsurface on drill sites TG-3 and TG-4 were found.

All three profiles reveal low resistivity values (1-30 Ωm) beneath the high resistivity zones at the west end of each profile. This is particularly true to the west ends of profiles EW-3 and EW-4, where resistivity values of 1-5 Ωm are present. As discussed above, the presence of such low resistivity values may indicate presence of ground water, including thermal fluids. Alternatively, the presence of a clay layer that could form an impermeable barrier to upwelling fluids could cause low resistivity. Clay minerals tend to be good conductors and can result from geochemical alteration by prior exposure to thermal waters. This has been observed in volcanically-hosted geothermal areas. The fluids occur beneath the impermeable cap and display somewhat higher resistivity values. These two somewhat contradictory interpretations are fundamental ambiguity in the interpretation of resistivity values observed in the field.

Figure 10: Resistivity cross-section EW-3.

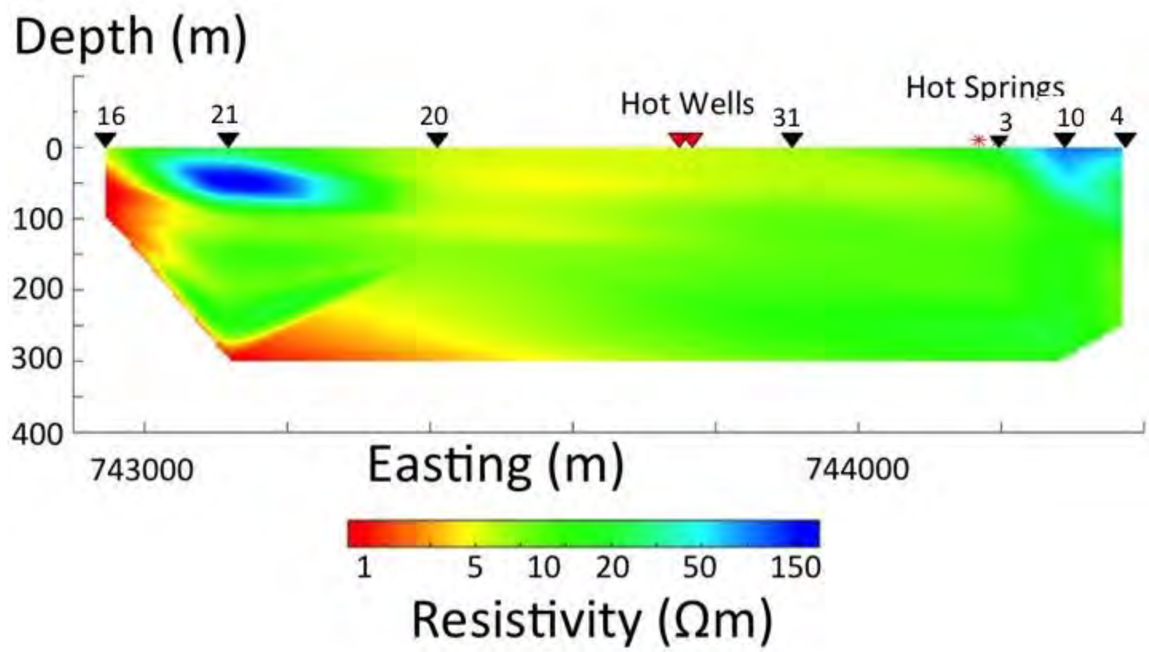

The locations of associated stations are denoted by black triangles. The positions of the hot wells at SVHS are denoted by red triangles and the hot springs are denoted by red stars. Note that the entire areas around the hot springs and wells have relatively low resistivity, possibly because of upwelling geothermal fluids. To the west and east are high resistivity zones that may represent dry lake sediments or sediments filled with relatively fresh (high resistivity) water. However, farthest west (Station 16) has low resistivity at shallow depths. This could result from the impermeable clay layer becoming shallow toward the lake, or it could be additional basalts allowing geothermal fluids near the surface. There are additional hot springs immediately south of these sites, but not on the SVHS property (see Figure 8).

In Surprise Valley, clay and silt may provide the low permeability cap to underlying thermal waters. However, the low resistivity values associated with clay and silt observed are connected to the surface zones that lie under hot springs. The low resistivity values observed to the west are most likely the hot water trapped beneath the lake sediments that leak to the surface. This implies that the reservoir of hot water is larger and extends under the Middle Lake.

Figure 11: Resistivity cross-section EW-4.

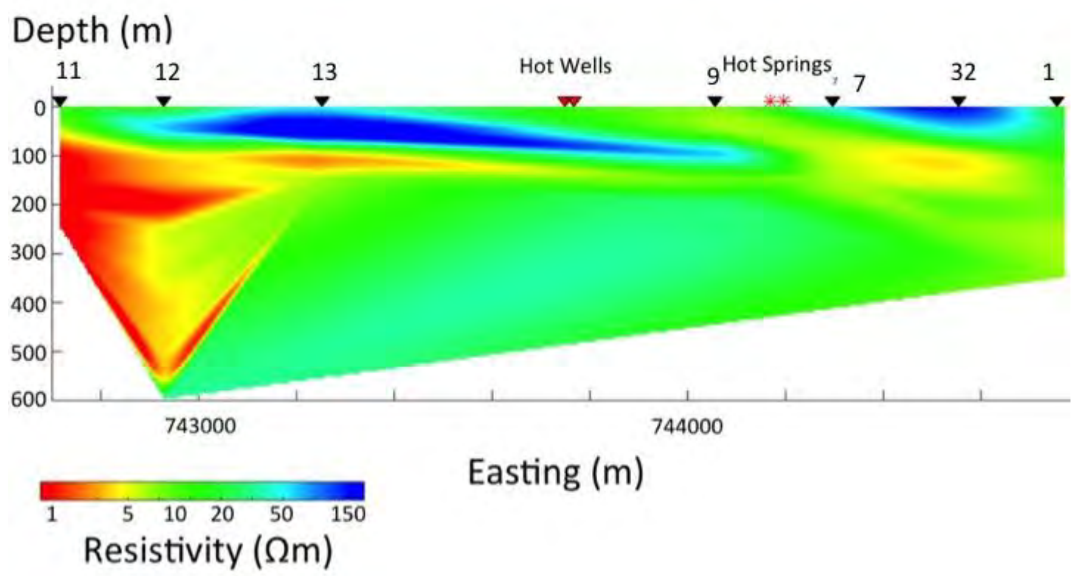

Note that the gap in the near-surface high resistivity zone that appears below the hot springs. While it is tempting to extend this gap to the hot wells, it is noted that the Earth beneath the wells is not well imaged. Stations in the actual resort area were avoided because of the presence of plumbing and high noise.

2.1.1.2 Long-Period Magnetotelluric Survey

In addition to the short-period magnetotelluric surveys, some newly acquired equipment were tested to detect the electrical and magnetic fields associated with longer period electromagnetic waves generated by fluctuations in the Earth's magnetosphere. These fluctuations are generally caused by variations in the solar wind, the charged particles emanating from the sun's surface. The advantage of the longer period waves is that they penetrate more deeply into the Earth and yield information about the Earth's conductivity (or resistivity) structure.

a) Survey details

Equipment to conduct long-period magnetotelluric surveys are similar to that used for the short-period studies. In addition to the two magnetometers measuring the horizontal components of the magnetic field (H_x and H_y), a third magnetometer measures the vertical component of the field (H_z). To measure the horizontal components of the electric field at long periods, electrodes are spaced about 100 meters apart. The field data is recorded over days to weeks and stacked to improve the signal to noise ratio. At these low frequencies and large electrode spacing, near surface resistivity values are not well constrained and the long period measurements complement the short-period measurements discussed above.

Three deployments of the long period array were made (locations are shown in Figure 8). They were deployed along an east-west line. Two stations successfully recorded data, while the third station was partly unsuccessful for recording because the cables were chewed, probably by rabbits. In general, large differences between stations were not expected since they were relatively close together for the long period waves.

For the array LEMI-701T potential electrodes were used. The data from all five channels (H_x, H_y, H_z, E_x, E_y) were recorded on a RefteкT recorder and then processed to determine apparent resistivity values as described for the short-period survey. A sample from the dataset is shown in Figure 12.

b) Results

All of the arrays yield similar results (Figure 13). This is expected because the arrays, by virtue of the long wavelengths used, average over a lateral area that is broad compared to the size of the study area. In Figure 11 the results for array 3 are shown. The figure shows resistivity as a

Figure 12: Sample of a time series from the long-period magnetotelluric array.

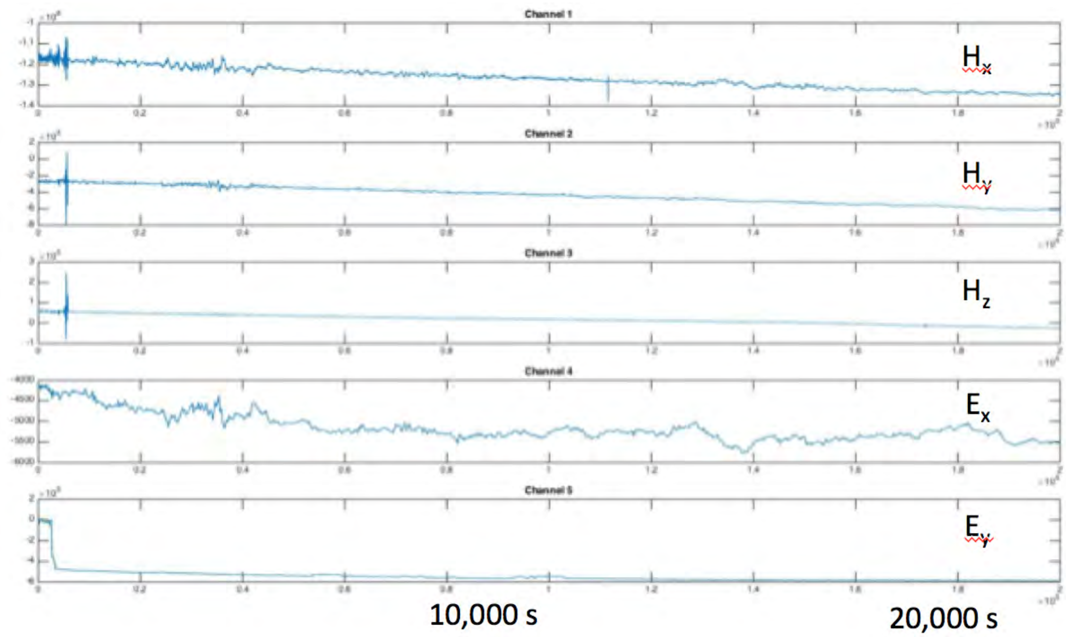

The data are sampled at 10 hz, so the total time represented here is 20,000 seconds or about 5.5 hours.

function of depth computed using the East-West electrodes (E_x) and Equation 1 in blue, and resistivity using the North-South electrodes (E_y) and Equation 2 in red. Although the two directions display differences, there is no systematic variation one would associate with an anisotropic resistivity structure.

All of the results for the long-period study reveal low and highly variable resistivity values at the surface, increasing to moderate resistivity values at depth. By two kilometers depth, the resistivity values have risen to about 100 Ωm and then rise more slowly to resistivity values over 1000-5000 Ωm at a depth of 5 kilometers. It is interpreted that this result indicates the hydrothermal fluids and/or lake sediments (clays) were present to a depth of about one kilometer but give way to more resistant basement rocks below that depth.

In Figure 13 two values for resistivity plotted for the same location are seen. The red dots are resistivity values computed from impedances using the ratio:

$$Zred = -\frac{H_y}{E_x}.$$

The blue dots are the resistivity values computed from impedances that use the ratio:

$$Z_{blue} == \frac{H_x}{E_y}$$

The fact that these values tend to be different implies an anisotropy (typically from a preferred orientation of fractures in the subsurface). However, the range of the differences is not particularly great, so these differences may not be important.

Figure 13: Results of the long-period array deployment for resistivity as a function of depth.

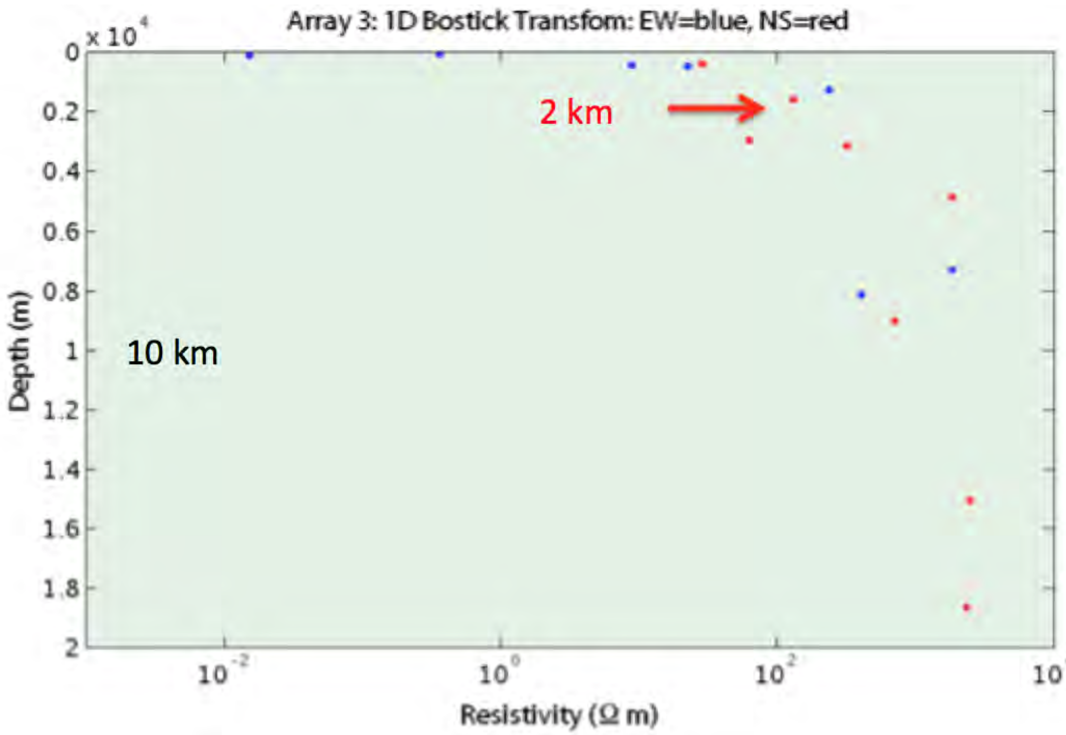

Depths are given in units of 10^4m, so the 10 km and 2 km depths denoted for ease of viewing. Notice that at 2 and 4 km the resistivity values increase abruptly to 100 Ωm and 1000 Ωm respectively. Although these results are preliminary, it is likely that this increase results from the transition to basement rocks and/or the decrease in fluid content.

2.1.1.3 Shallow Seismic Survey

As a component of this study a shallow seismic survey was conducted. The goals of this survey were to:

1) Determine the depths to structures that may accommodate upwelling of geothermal fluids to the hot springs. The characteristics of these structures are expected to affect the estimates of the capacity of the thermal reserve. In general, the important structures were expected to be shallow faults and/or basalt outcrops in the area. It was planned to use both seismic refraction and reflection processing to determine depths and velocities,
2) Determine the stratigraphy of the units on the SVMW property. This is expected to allow determination of the depositional history of the sediments in the area,
3) And use newly developed Multichannel Surface Wave Analysis (MSWA) to utilize the usually ignored surface waves (ground roll) part of the signal to determine the shear-wave structure beneath the study area.

a) Survey details

For shallow seismic survey, a Geometrics Strataview R-24 recorder which can record up to 24 independent geophone channels was used. The channels were connected to 14 Hz vertical geophones spaced approximately 20 feet (6.1 m) apart. The maximum source-receiver offset was 480 feet (146 m), although the actual maximum useful distance for any particular profile depended on the ground conditions at the source.

UCD developed an in-house version of a source known as "Betsy Gun" that relied on energy from an 8-gauge shotgun blank to generate seismic waves (Figure 14). The seismic survey was conducted on 7 profiles (

No evidence for coherent P-wave reflections from subsurface interfaces was detected. In fact, a reflection from the sediment-basalt interface and even interfaces within the sediments was expected. The fact that the reflections were not observed suggests that the basalt surfaces are irregular and rough and very shallow. Internal reflections in a basalt body are unlikely. This is consistent with observations of surface outcrops.

Figure 15). No evidence for coherent P-wave reflections from subsurface interfaces was detected. In fact, a reflection from the sediment-basalt interface and even interfaces within the sediments was expected. The fact that the reflections were not observed suggests that the basalt surfaces are irregular and rough and very shallow. Internal reflections in a basalt body are unlikely. This is consistent with observations of surface outcrops. Each profile consisted of one to four spreads of 24 geophones each. At every two or three geophone locations a source was set off and each source was recorded on the full geophone spread.

Figure 14: "Betsy Gun" apparatus used as a source for the seismic array.

The gun relied on an 8-gauge shotgun blank for impulsive energy. The device is mechanically triggered. Simultaneously with the shell ignition, an electronic triggering signal is sent to the seismic recorder that initiated recording, essentially setting time=0 for each shot. Multiple shots could be fired at a single source point and the resulting signals stacked to provide improved signal to noise ratio for a given shot point.

For each deployment of the 24-channel geophone array a shot point was selected at every second or third geophone location and each shot thus generated 24 seismograms (Figure 15 and

The picked P-wave travel times were combined with up to 7 used in one analysis. They were processed using a 2-D tomographic scheme where the model structure is divided into constant velocity layers as a function of depth. Then lateral heterogeneities were incorporated into the resulting models by varying the depths of the boundaries between layers. An example is given in Figure 18.

Figure 16). The picked P-wave travel times were combined with up to 7 used in one analysis. They were processed using a 2-D tomographic scheme where the model structure is divided into constant velocity layers as a function of depth. Then lateral heterogeneities were incorporated into the resulting models by varying the depths of the boundaries between layers. An example is given in Figure 18. Three arrivals are easily visible on the seismograms. The earliest are the compressional waves (P-waves) that propagate through the Earth. The second obvious arrival is the "air-wave" that is the acoustic wave that travels through the air. It is the highest amplitude on the waves. Finally, there are the surface waves or "ground roll". These waves, normally treated as "noise", have recently been exploited to determine the shallow shear waves structure. Using an approach known as Multichannel Surface Wave Analysis (MSWA), the dispersion curves (phase velocity versus velocity) are inverted for near-surface structure.

No evidence for coherent P-wave reflections from subsurface interfaces was detected. In fact, a reflection from the sediment-basalt interface and even interfaces within the sediments was expected. The fact that the reflections were not observed suggests that the basalt surfaces are irregular and rough and very shallow. Internal reflections in a basalt body are unlikely. This is consistent with observations of surface outcrops.

Figure 15: Shallow seismic profiles shot during the survey.

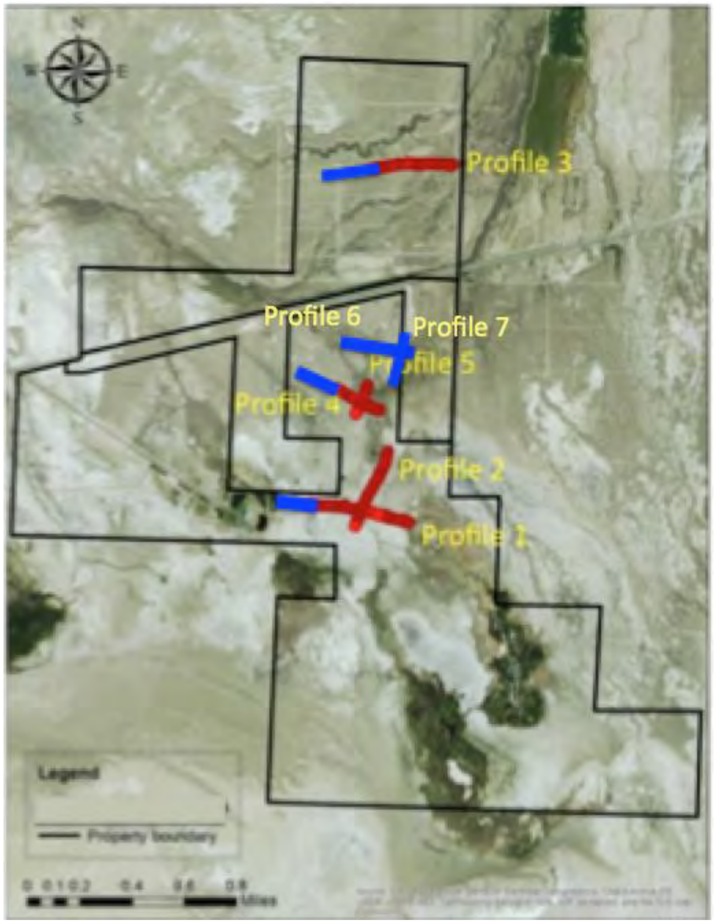

Seven profiles were shot during this survey. Each profile included 1 to 4 spreads of 24 geophones each. Along each profile, shot points were placed at every two or three geophone locations. It is estimated that approximately 3500 seismograms were collected in the course of two field seasons. The red and blue lines were shot in 2015 and 2016 field seasons, respectively.

The refraction analysis was accomplished by using the compressional waves (P-waves in

The picked P-wave travel times were combined with up to 7 used in one analysis. They were processed using a 2-D tomographic scheme where the model structure is divided into constant velocity layers as a function of depth. Then lateral heterogeneities were incorporated into the resulting models by varying the depths of the boundaries between layers. An example is given in Figure 18.

Figure 16 and Figure 17). The picked P-wave travel times were combined with up to 7 used in one analysis. They were processed using a 2-D tomographic scheme where the model structure is divided into constant velocity layers as a function of depth. Then lateral heterogeneities were incorporated into the resulting models by varying the depths of the boundaries between layers. An example is given in Figure 18.

In general, the P-waves were easily picked and resulting travel times can be used to infer velocity structure. Several shot points along a given profile and picked arrivals were used in refraction analysis.

The picked P-wave travel times were combined with up to 7 used in one analysis. They were processed using a 2-D tomographic scheme where the model structure is divided into constant velocity layers as a function of depth. Then lateral heterogeneities were incorporated into the resulting models by varying the depths of the boundaries between layers. An example is given in Figure 18.

Figure 16: Example of seismogram record section generated by a single shot.

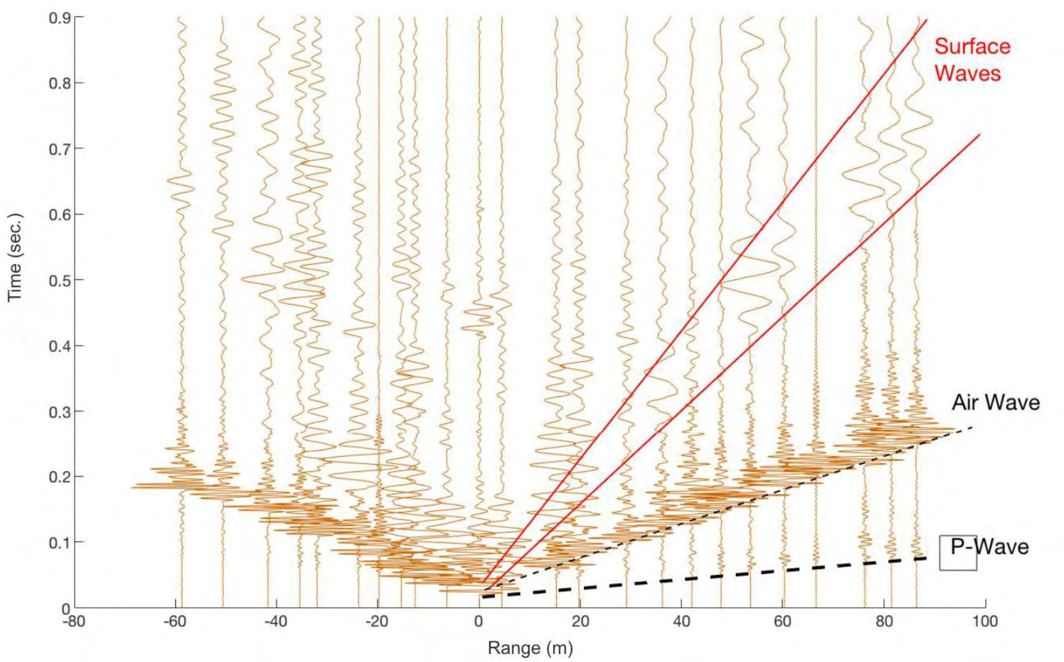

The entire set of 24 seismograms is displayed, and each is plotted at a horizontal position corresponding to the distance between the source (at Range =0) and the geophone location. The vertical axis is the time after the source generation (Time=0*).* Like most seismic experiments. P wave travel times were used as the primary data to determine subsurface velocity structure.

Figure 17: Example of a seismogram from a single shot as recorded on geophones for one spread of 24 geophones.

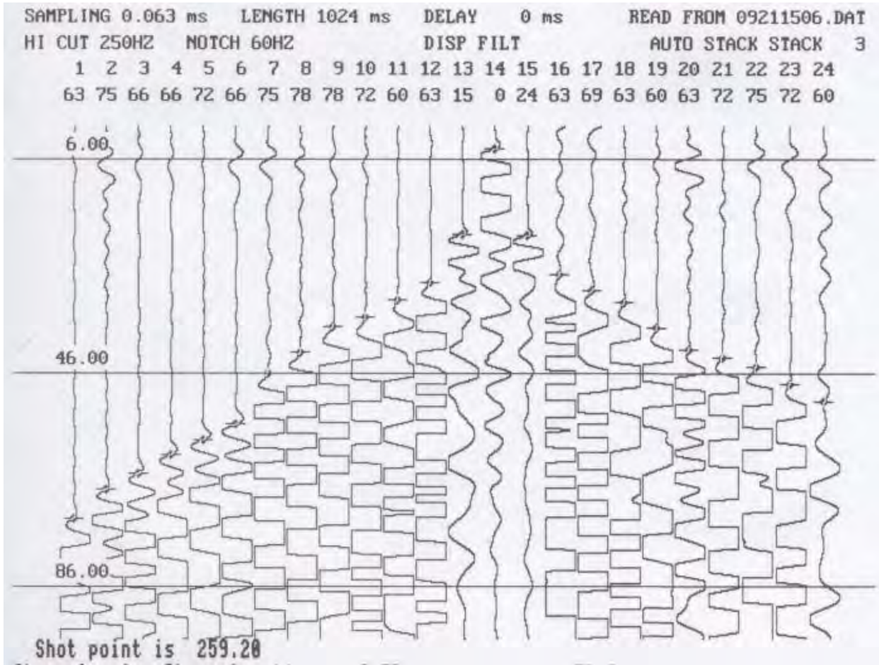

The air waves do not dominate here in this projection because they are "clipped". Thus, the P waves are easily observed. The P-wave arrivals times are picked (small bar) for each of the channels shown here. Note that travel time is positive downward in this projection.

Figure 18: Example of inversion for layer velocities and depths for a portion of the profile 3.

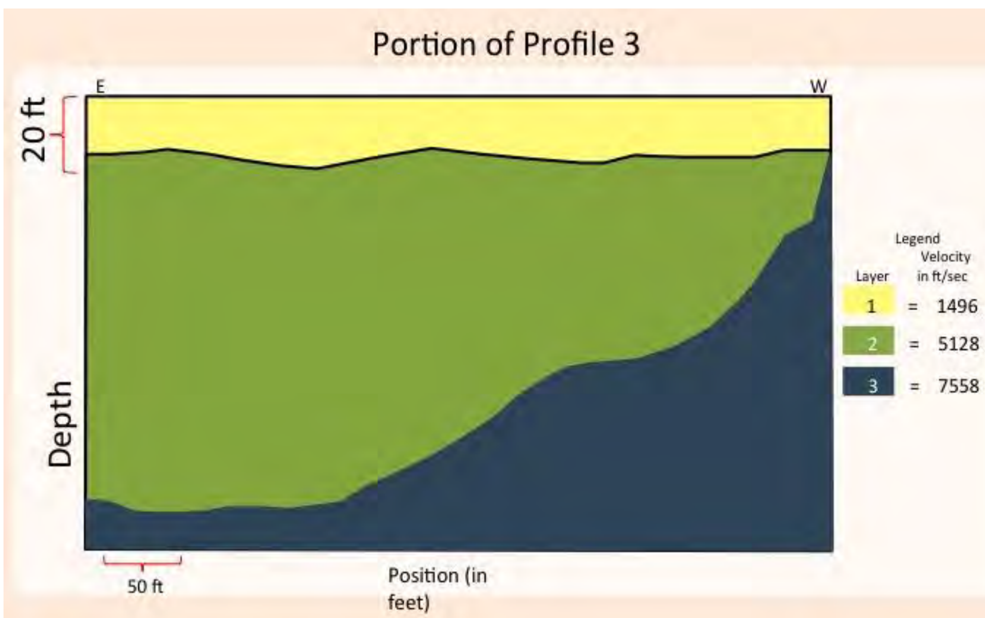

This example is for two geophone spreads (24 channels each) and 8 shot points. The arrival times plot along straight-line segments. The slopes of those lines are the inverses of the layer velocities and the line intercepts correspond to the depth to the layers. For this model the tomographic inversion resulted in a three-layer approximation to the velocity structure. Lateral heterogeneities in the structure are accommodated in the tomographic inversion by varying the depth of the different layer boundaries. Each layer is presumed to have a constant velocity. The velocities for the three layers are given on the right. The shallowest layer has a velocity of (456 m/s (1496 ft/s), corresponding to uncompacted dry sediments. Note that the highest velocity here is about 2306 m/s (7558 ft./s) and corresponds to compacted sediments.

b) Results

In the tomographic cross sections, structures which were approximated by two or three layers, were detected. The velocities for the first layer were typically around 1500 to 4000 feet per second (450-900 m/s). These velocities are appropriate for uncompacted and relatively dry sediments at the surface.

The second layer velocities were typically between 6000 and 8000 feet per second (1800-2450 m/s). These velocities are characteristic of compacted sediments. However, these velocities are found at shallow depths, and such velocities in sediments are unlikely. It is possible that the higher velocities may indicate the presence of porous or fractured basalts or both basalts and sediments. Thermal gradient holes included basalts at relatively shallow depths.

The third layer, when present in the model, include velocities of 10000 to over 12000 feet per second (3000 to over 3650 m/s). These velocities are too high for shallow sediments and then must indicate the presence of fractured or porous basalt. Basalt outcrops have been discovered on or near the field area. In addition, the thermal gradient holes reveal substantial basalt in the shallow subsurface. Finally, presence of a strong magnetic anomaly high (

Figure 7) supports a model that includes fractured or porous basalt.

One way of folding all of the seismic data together is to show the estimated depths to Layer 3 as a contour map (Figure 19). These show the depths in meters and reveal layer 3 depths range from less than 20 (actually zero at the outcrop site) to 40 meters. This is consistent with all of the above-mentioned observations, and it is postulated the SVHS property is underlain by basalt. It may be further postulated that the basalt, along with any faults present, provides conduits allowing thermal waters to come to the surface from under the compacted lake sediments that otherwise trap the thermal waters.

Figure 19: Contours showing the depth velocities of 2500 m/s (8200 ft/s) or greater.

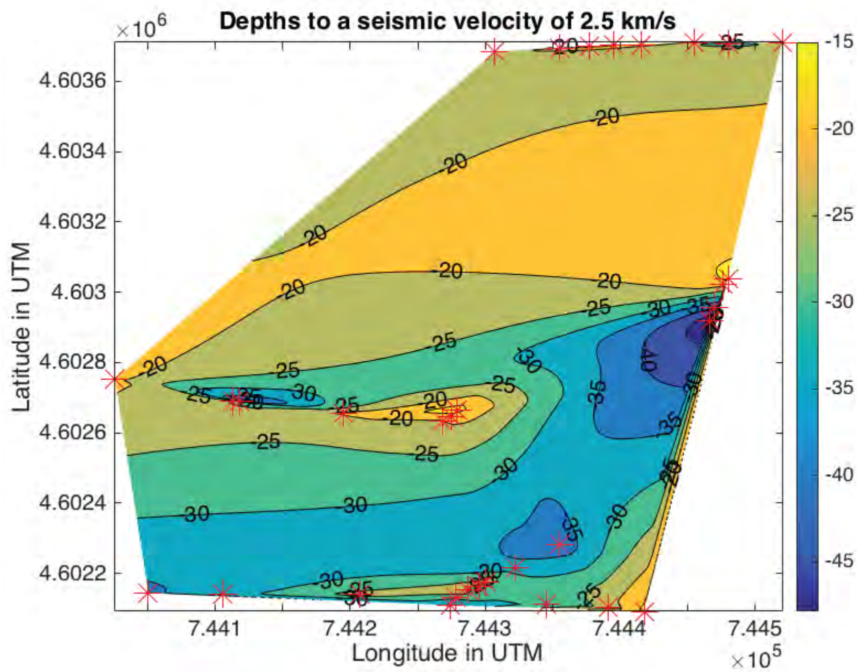

These velocities are too high for sediments located at such shallow depths. It is likely they reflect porous basalts, perhaps associated with the hot springs present. The red stars are the location of shot points where these high velocities were observed. Note that the region is between UTM 4603000 and 4603450N.

2.1.2 Geochemical Survey

2.1.2.1 Water Sampling Collection

In the scope of geochemical data collection and analysis, water samples were collected from a temperature gradient hole (TG 2) drilled at the study area and from numerous other hot springs in the valley (Figure 20).

Water samples from hot springs were collected using high-density polyethylene (HDPE) syringes (NormJect®), dedicated Tygon® tubing, HDPE luer stop-cock valves and were stored in acid-cleaned HDPE bottles. Samples from the temperature gradient well (TG-2) were retrieved from a depth of 274 m in the auger barrel using the airlift method. Separate sample aliquots were used for field pH and conductivity measurements. Samples for cation and trace element analysis were filtered (0.45μm) and acidified in the field using 1 ml HNO_3 (67-69 percent Optima™ grade, Fisher Scientific) per 120 mls samples for stable isotope, anion, pH and conductivity measurements were filtered in the field, but not acidified. They were stored on ice during transport and refrigerated until the analyses were performed.

Figure 20: Water sampling locations.

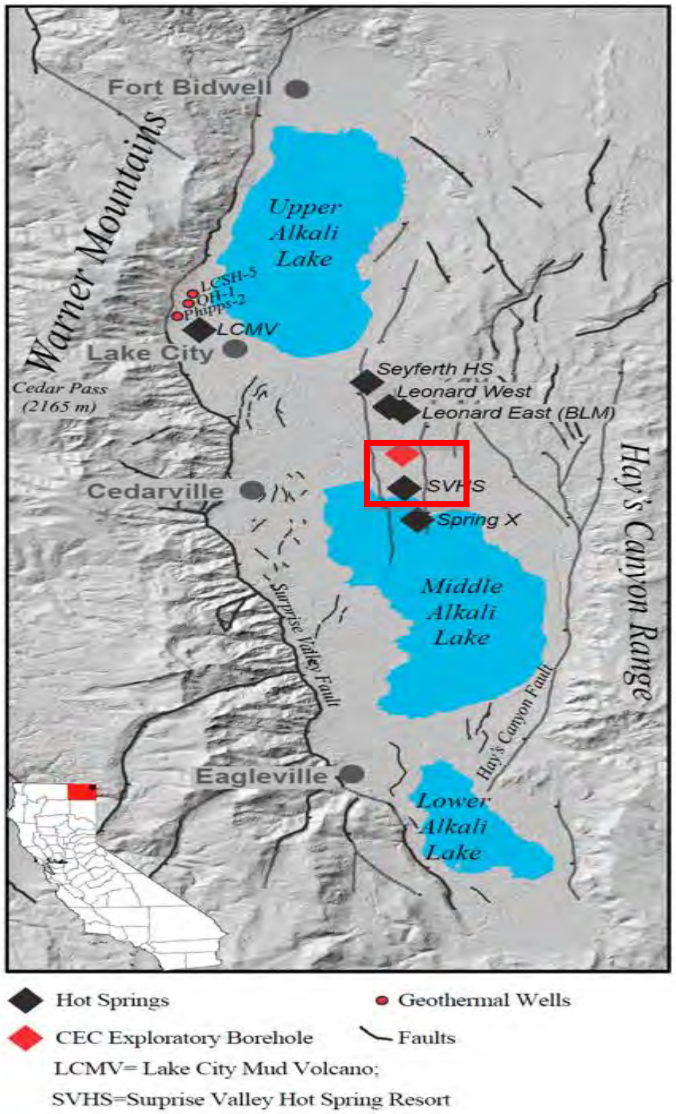

Surprise Valley consists of three basins filled with ephemeral lakes. Red diamond denotes the location of the thermal gradient hole where subsurface fluids were sampled. To the west are the Warner Mountains and the Surprise Valley Fault (SVF). To the east are the Hays Canyon Mountains and a variety of west-dipping normal faults, including the Hays Canyon Fault (HCF). The study area, the Surprise Valley Hot Springs (SVHS) resort property, is denoted by the red box. *Credit: Modified from Fowler et al., 2017.*

2.1.2.2 Analyses and Results

Cation and trace element analyses were made at the University of California Interdisciplinary Center for Plasma Mass Spectrometry using Inductively Coupled Plasma Mass Spectrometry (ICP-MS; Agilent 4500 quadrupole). Boron and anion (Cl^-, SO_4^{-4}, NO_3, HCO_3^{-1}, and $CO_3)^{-2}$ measurements along with sodium, calcium, and magnesium measurements for selected samples, were made at the UC Davis Analytical Laboratory (AnLab) using ICP Atomic Emission Spectrometry (ICP-AES). Laboratory measurements of electrical conductivity and pH were also made at AnLab. Fluid stable isotope (oxygen and hydrogen) analyses were conducted at the UC Davis Stable Isotope

Facility using laser spectroscopy (Los Gatos Instruments). Fluid samples for rare earth element (REE) analysis were prepared using a modified (offline) version of the pre-concentration method. Analytical accuracy and detection limits for REE analyses were quantified through repeated analyses of the NASS-6 seawater standard. The detection limit is defined as three times the standard deviation of six replicate analysis of the NASS-6 seawater standard. Table 1 provides information on locations and field measurements of the samples.

Table 1: Water sampling locations (UTM grid 10T) and field parameters.

Sample ID	Sample Date	Site Name	Easting	Northing	Elev (m)	Temp (°C)	Field pH	Field Cond. (mS/cm)
20150824-1	8/24/15	SVHS Hot Well	743766	4602055	1373	97	8.46	1.372
20150824-2	8/24/15	Spring E of SVHS (northern)	744167	4602264	1377	91	8.29	1.432
20150824-3	8/24/15	Spring E of SVHS (southern)	744200	4602174	1371	89	8.20	1.39
20150824-4	8/24/15	Spring SW of SVHS	743386	4601797	1368	97	8.17	1.404
20150824-5	8/24/15	Cold water well at Desert Rose	744634	4603365	1369	14	8.47	0.293
20150824-6	8/24/15	Spring X	744332	4599812	1354	55	9.33	1.52
20150825-1	8/25/15	Seyferth Hot Spring	741317	4611137	1395	83	7.81	1.69
20150825-2	8/25/15	Leonard Hot Spring East	742898	4609625	1381	62	7.85	1.647
20150825-3	8/25/15	Leonard Hot Spring West (BLM)	743354	4609507	1400	69	8.29	1.32
20150825-4	8/25/15	LCMV	732275	4616634	1362	99	7.47	1.721
20160321-1	3/21/16	SVHS Hot Well	743765	4602052	1380	79	8.51	1.505
20160321-2	3/21/16	SVHS Reed Spring	743896	4601867	1372	40	7.95	1.321
20160321-3	3/21/16	Spring SW of SVHS	743381	4601796	1375	90	8.12	1.72
20160321-4	3/21/16	SVHS Flat Shack Spring	742965	4601684	1372	83	8.17	1.573
20160321-5	3/21/16	Spring E of SVHS (Small)	744193	4602244	1374	76	8.15	1.637
20160321-6	3/21/16	Spring E of SVHS (Northern)	744168	4602263	1374	77	8.06	1.553
20160321-7	3/21/16	Spring E of SVHS (Tiny)	744170	4602199	1376	68	8.16	1.779
20160321-8	3/21/16	Spring E of SVHS (Southern)	744194	4602181	1377	82	8.03	1.751
20160321-9	3/21/16	SVHS Cold Well	743765	4602052	1380	13	8.81	0.367
20160321-10	3/21/16	SVHS Hot Wellhead Near Ponds	743602	4602110	1383	81	8.05	1.714
	11/2016	SVHS TG-2					--	--

SVHS = Surprise Valley Hot Springs (TGW=Thermal Gradient Well-2)

BLM = Bureau of Land Management

LCMV = Lake City Mud Volcano

Results for major element and anion abundances are provided in

Table 2. The rare earth abundances and the trace element abundances are shown in Table 3, and Table 4, respectively. Light stable isotope rations (δD and $\delta^{18}O$) are shown in Table 5.

Table 2: Major and anion results (in mg/l) for SVHS waters.

	SVHS Well	Seyferth HS	Leonard HS	LCMV	SVHS TG-2	Spring E of SVHS (north)	Spring E of SVHS (south)	Spring SW of SVHS	Spring X SSW of SVHS	*LOD*[2] *(ppm)*
Temperature (°C)	97	83	69	99	~50	91	89	97	55	--
Conductivity (Field) (mS)	1.372	1.69	1.32	1.721		1.43	1.39	1.40	1.52	--
Conductivity (Lab) (mS)						1.39	1.38	1.38	1.56	--
pH (Field)	8.46	7.81	8.288	7.47		8.29	8.20	8.17	9.33	--
pH (Lab)	8.64	8.05	8.47	8.05	8.6	8.45	8.48	8.5	9.46	--
Major Elements (ICP MS)										
Si	44.8	49.8	49.2	89.0	44.6	--	--	--	--	0.068
Na	266	306	320	316	282	--	--	--	--	0.0086
K	5.2	8.9	8.3	16.2	5.4	--	--	--	--	0.0048
Ca	16.7	29.5	26.9	24.8	19.2	--	--	--	--	0.0071
Mg	0.03	0.20	0.54	0.36	0.12	--	--	--	--	0.00016
Ca (Soluble)	--	--	--	--	--	18.8	19.0	18.6	1.2	
Mg (Soluble)	--	--	--	--	--	<	<	<	<	0.01
B (Soluble)	5.9	7.8	5.3	6.6	5.8	5.9	5.9	5.8	6.0	0.01
Anions (GC) Cl	178	197	164	201	186	174	173	173	217	0.10
SO_4	327	407	312	333	333	--	--	--	--	0.1
NO_3	<	<	<	<	<	--	--	--	--	0.05
HCO_3	36.6	67.1	42.7	164.7	48.8	--	--	--	--	0.1
CO_3	9.0	<	3.0	<	9.0	--	--	--	--	0.1
Charge Balance Error	-0.8	-0.4	13.1	0.4	0.4	--	--	--	--	

1. Na, Ca and Si exceeded the calibration range at 1X dilution, thus values are reported for a 40X dilution.

2. The limit of detection (LOD) is 3σB/a, where 'σB' is the standard deviation of the replicate analyses of the ratio of the analyte counts per second (CPS) to the internal standard (IS) CPS found in the calibration blank, and 'a' is the coefficient from the IS corrected calibration curve's regression equation: y=ax+blank.

3. percent Recovery is the average (n=5) percent recovery of a 100-ppb standard solution (1000 ppb for Na, Al, Si, P, K, and Ca)

-- **Not analyzed**

< **Less than the specified LOD**

Table 3: Trace element abundances (in mg/l).

	SVHS Well	Seyferth HS	Leonard HS (BLM)	LCMV	SVHS TG-2	*LOD*[2] *(ppm)*
Li	85.1	140	127	251	90.8	0.007
Al	51.7	3.9	<	12.4	163	0.69
P	8.1	8.7	11.5	23.4	52.7	1.57
V	0.39	0.49	0.22	0.26	0.89	0.003
Cr	0.05	0.07	0.09	0.06	0.23	0.010
Mn	0.6	7.9	94.9	69.1	110.4	0.012
Fe	1.08	2.02	5.46	12.64	2682	0.12
Cu	0.17	0.06	0.07	0.13	0.31	0.02
Zn	1.10	0.16	14.44	0.24	82	0.16
As	191	365	378	305	71	0.16
Se	2.7	3.2	2.8	2.0	<	0.7
Rb	18.8	35.4	26.9	78.7	21.0	0.01
Sr	219	542	170	1162	155	0.05
Mo	33.0	37.7	39.1	36.2	20.9	0.03
Cd	0.05	0.05	0.05	0.03	0.02	0.02
Sb	3.5	7.4	5.4	14.8	2.7	0.02
Cs	9.4	20.2	14.6	61.4	11.8	0.02
Ba	5.8	21.4	6.3	31.9	6.1	0.03
Pb	<	<	0.102	<	2.3	0.07
U	<	<	<	<	0.01	0.01

1. Na, Ca and Si exceeded the calibration range at 1X dilution, thus values are reported for a 40X dilution.

2. The limit of detection (LOD) is 3σB/a, where 'σB' is the standard deviation of the replicate analyses of the ratio of the analyte counts per second (CPS) to the internal standard (IS) CPS found in the calibration blank and 'a' is the coefficient from the IS corrected calibration curve's regression equation: y=ax+blank.

3. percent Recovery is the average (n=5) percent recovery of a 100 ppb standard solution (1000 ppb for B, Mn, and P)

-- **Not analyzed**

< **Less than the specified LOD**

Table 4: Analyses results for rare earth elements.

Units	SVHS Well	Seyferth HS	Seyferth HS	Seyferth HS	LCMV	LCMV	NASS-6 Seawater	*LOD*
	20150824-1 (F)	20150825-1 (F)	20150825-1 (F-DUP)	20150825-1 (U)	20150825-4 (F)	20150825-4 (F-DUP)		
Y	<	<	<	<	7.9	7.8	18.3	2.4
La	2.1	2.5	2.3	2.0	7.3	7.0	10.4	1.4
Ce	3.5	3.9	3.8	3.4	13.6	13.2	4.0	0.6
Pr	0.27	0.3	0.29	0.28	1.26	1.22	1.3	0.2
Nd	<	<	<	<	3.9	4.0	5.7	0.8
Sm	0.36	<	<	<	0.84	0.84	1.0	0.2
Eu	<	<	<	<	<	<	0.21	0.04
Gd	<	<	<	<	1.2	1.1	1.3	0.3
Tb	<	<	<	<	0.16	0.16	0.2	0.02
Dy	<	<	<	<	0.9	0.9	1.4	0.2
Ho	<	<	<	<	0.2	0.2	0.4	0.1
Er	<	<	<	<	0.6	0.6	1.2	0.2
Tm	--	--	--	--	--	--	--	--
Yb	<	<	<	<	0.5	0.5	1.1	0.1
Lu	<	<	<	<	0.08	0.08	0.2	0.02
percent Tm Spike Recovery	98	98	99	92	93	92	95-107	--

Values in parts per trillion (pictogram/kg)

(F) **Filtered**

(U) **Unfiltered**

(DUP) **Duplicate sample run independently through entire preconcentration method percent recovery based on a 5 ppb TM spike**

LOD **Limit of detection**

Table 5: Analyses results for stable isotopes (δD and $\delta^{18}O$) for SVHS waters.

Sample ID	Site Name	δD (VSMOW)	$\delta^{18}O$ (VSMOW)
Sample			
20150824-1	Surprise Valley Hot Springs Well (SVHS)	-119	-14.3
20150824-2	Spring S of SVHS (northern)	-117	-14.2
20150824-3	Spring S of SVHS (southern)	-117	-14.2
20150824-4	Spring NW of SVHS	-119	-14.4
20150824-5	Cold water well at Desert Rose	-115	-14.9
20150824-6	Spring X	-119	-14.6
20150825-1	Seyferth/Chicken Hot Spring	-120	-14.2
20150825-2	Leonard's Hot Spring East	-119	-14.1
20150825-3	Leonard's Hot Spring West (BLM)	-117	-14.2
20150825-4	Lake City Mud Volcano (LCMV)	-114	-13.5
20160321-1	SVHS Hot Well	-117	-14.2
20160321-2	SVHS Reed Spring	-115	-13.5
20160321-3	Spring SW of SVHS	-119	-14.3
20160321-4	SVHS Flat Shack Spring	-118	-14.2
20160321-5	Spring E of SVHS (Small)	-116	-14.0
20160321-6	Spring E of SVHS (Northern)	-117	-14.2
20160321-7	Spring E of SVHS (Tiny)	-117	-13.9
20160321-8	Spring E of SVHS (Southern)	-118	-14.2
20160321-9	SVHS Cold Well	-113	-14.7
20160321-10	SVHS Hot Wellhead Near Ponds	-118	-14.4
	SVHS TG-2	-116	-14.0
	Laboratory Standard		
	Known value	-55.7	-8.04
	Mean (n=11)	-55.3	-7.80
	1 SD	0.9	0.11

H2O stable isotope analysis by laser spectroscopy (Los Gatos Research Instruments).

2.1.3 Drill-Cut Sample Collection and Analysis

The source of heat and the permeability paths that allow fluids to migrate to and from the heat source are the essential questions in geothermal systems. For the geothermal system beneath the Surprise Valley Hot Springs permeability paths are not clearly known. For this reason, petrographic composition of the drill-cuttings collected from the temperature gradient holes (TG-2, TG-3, and TG-4) along with the rock samples collected from nearby outcrops were studied to provide information to constrain models for the geothermal system.

In order to collect information on the origin of the basalts which crop out in the vicinity of the Surprise Valley Hot Springs area, samples were collected and analyzed from these outcrops (Figure 21). Results of analysis (Figure 22) showed that the basalt samples did not have similar compositions, therefore, they appear to have resulted from different eruptions and do not correspond to a single dike.

Figure 21: Magnetic anomaly map of the study area.

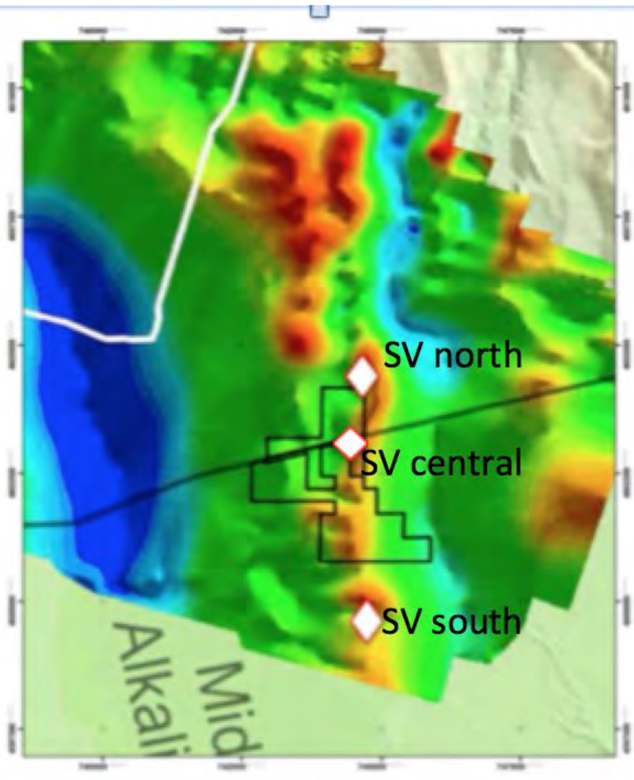

Magnetic anomaly highs are shown in warmer colors. Grey lines denote the Surprise Valley Hot Springs property boundaries. The diamonds show the locations of the basalt outcrops in vicinity of the study area. Note the outcrops lie along the magnetic anomaly high. *Credit: (Glenn et al., 2011).*

Figure 22: Compositions in magnesium/potassium spaces for key basalts of the study area.

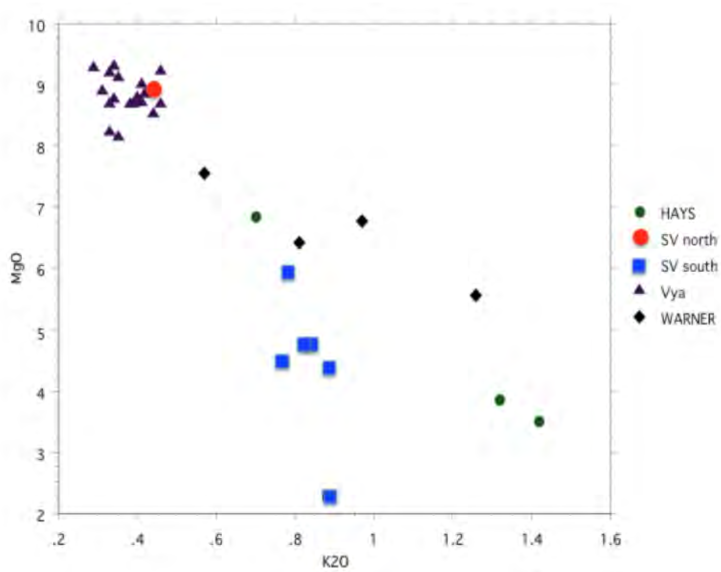

Note the compositions for the basalts located in the south of Surprise Valley (blue) and in the north of the Surprise valley (red circle). The former appears to be similar to the Warner or Hays basalts, while the latter appears to be similar to the younger Vya basalts.

Drill-cuttings were collected at each 10-foot interval from temperature gradient holes TG-2, TG-3, and TG-4. A subset of samples were examined under a petrographic microscope. All the hard rock chips were identified as basalt with no confirmation of the presence of andesite. As for alteration minerals, zeolite, smectite, and chlorite phases were observed. No epidote was detected in the samples. Epidote alteration begins to occur at temperatures at about 220˚C (428˚F).

A representative of 9 samples were selected to examine bulk rock compositions. Each sample included a large number of chips from 10-foot intervals. The samples were ground and subjected to Inductively Coupled Plasma Mass Spectrometer (ICPMS) and X-Ray Fluorescence (XRF) analysis. All analyses were done using loss on ignition (LOI) measurements. The samples were also analyzed for major elements.

The major element analyses show quite clearly that all drill-cuttings, including those identified as andesite, were basalt. In addition, the range of drill-cutting compositions was relatively narrow (Figure 23). They appear to be similar in composition to the basalt outcrops located in the south of Surprise Valley and Warner basalts.

The ICPMS results provided rare earth elements that could be compared to those from the outcrops located to the north and south of Surprise Valley Hot Springs (Figure 24).

Figure 23: Compositions in barium/strontium space that include drill-cutting samples (blue pentagons).

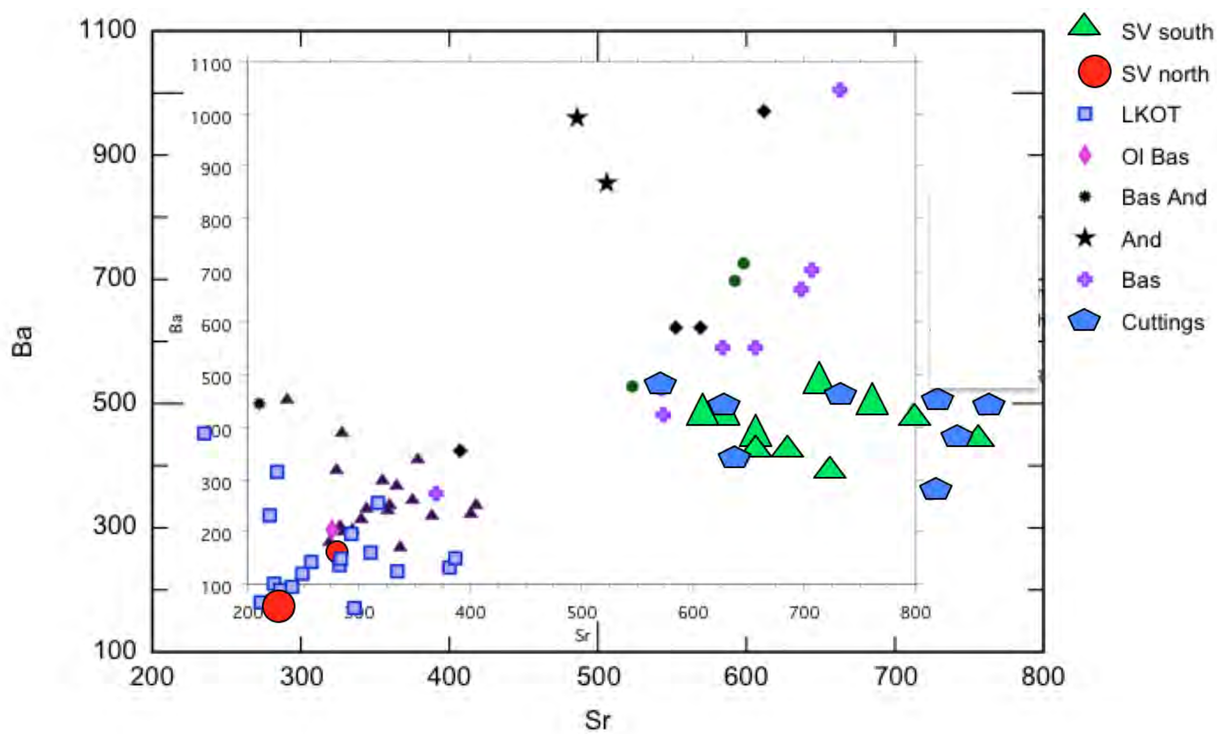

The cuttings are definitely from the same lavas that produced the outcrops located to the south of Surprise Valley (green triangles), even though they are farther than the lavas from the outcrops located to the north of the Surprise valley (large red circle).

Figure 24: Rare earth element abundances (spider diagram).

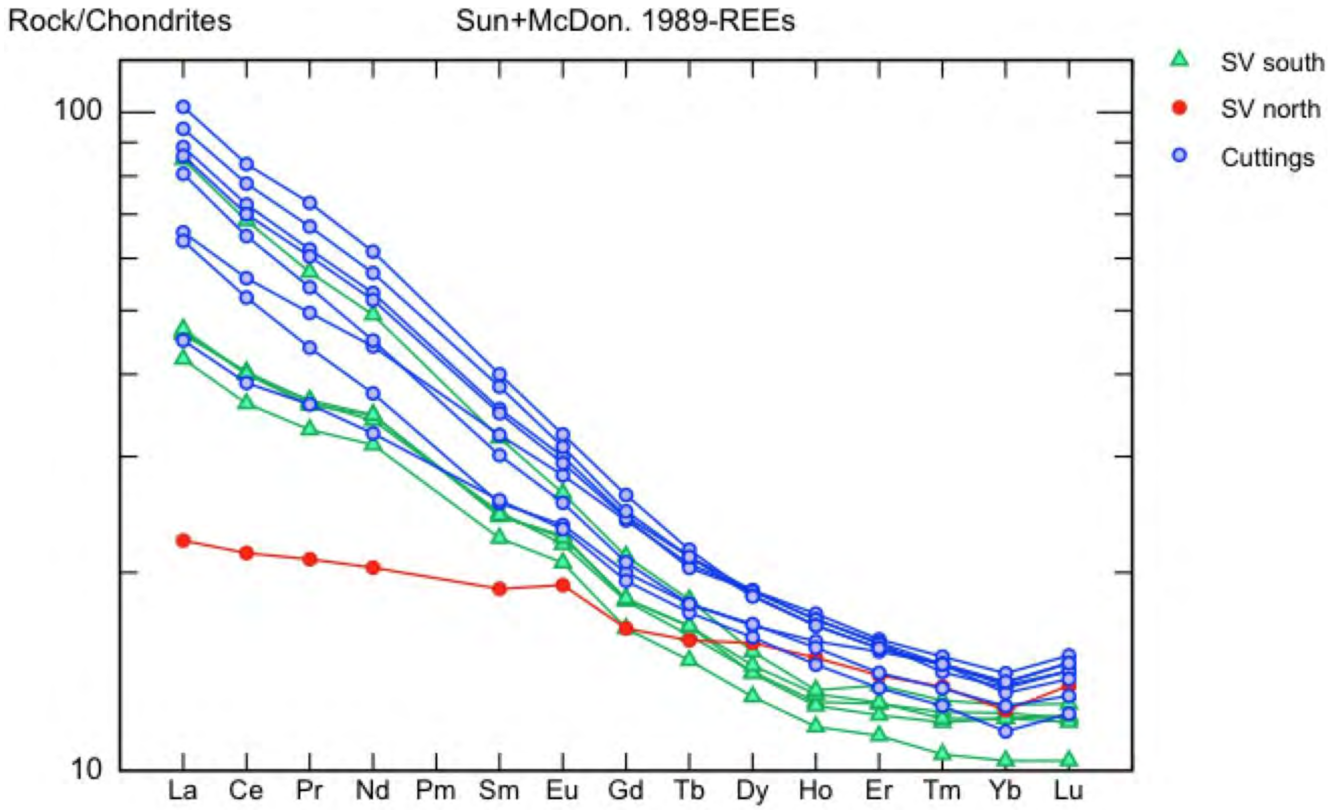

Rare Earth abundances (spider diagrams) that appear to confirm the affinity of drill hole basalts with the outcrops located to the south of Surprise Valley and the lack of affinity with the outcrops located to the north of Surprise Valley. This indicates that the outcrop located to the south of Surprise Valley and cuttings are from a different source than the outcrops located to the north of Surprise Valley. Abundances are normalized to Chondrite abundance.

2.2 Shallow Subsurface Geological Exploration

2.2.1 2-meter Soil Temperature Probe Survey

From May to October 2015, WME had installed 123 soil temperature probes in the study area. Sixteen sites were surveyed in May; fifty-nine sites were surveyed in June; twenty-eight sites were surveyed in September and twenty sites were surveyed in October.

Figure 25 shows locations of SV- and WME-subsets of soil probes and the results of the survey in October 2015. The highest temperatures are observed to lie adjacent to the hot springs. The warmest temperatures (80+ °F) trend northeast while the heat anomaly in the 70 °F range also extends in the same direction to the west of the 80 °F anomaly (Figure 26). These anomalies are consistent with the data obtained from aeromagnetic survey (Ponce et al., 2009) and field observations of basalt outcrops that altogether support a model where basalts and associated faulting, provide conduits for geothermal fluids.

Figure 25: Map showing 2M soil temperature probe locations surveyed in October 2015.

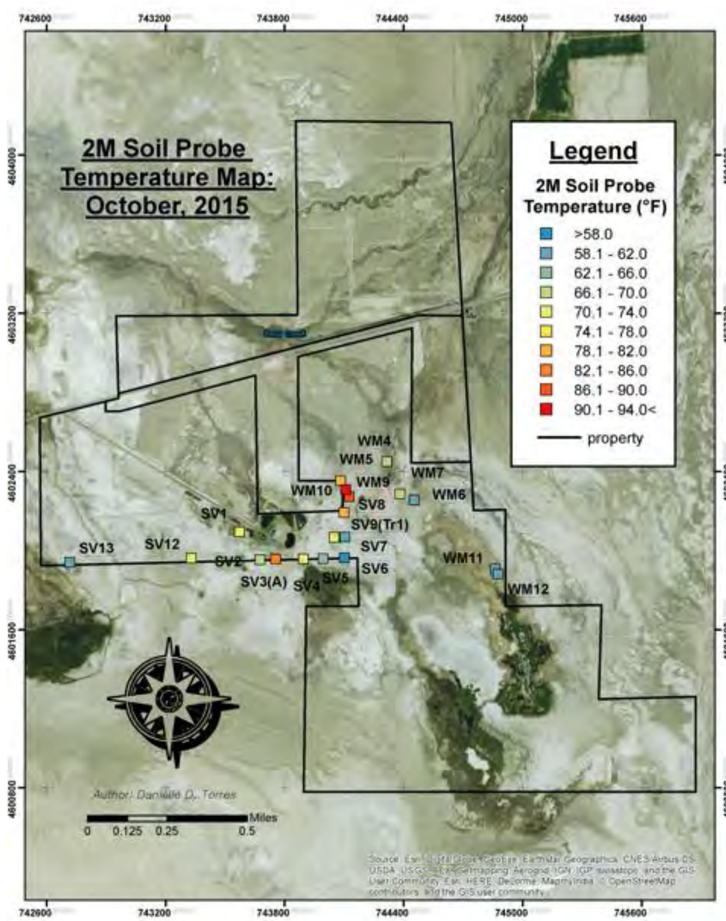

"Property" in the legend refers to project boundaries.

Figure 26: 2M soil probe temperature zone model.

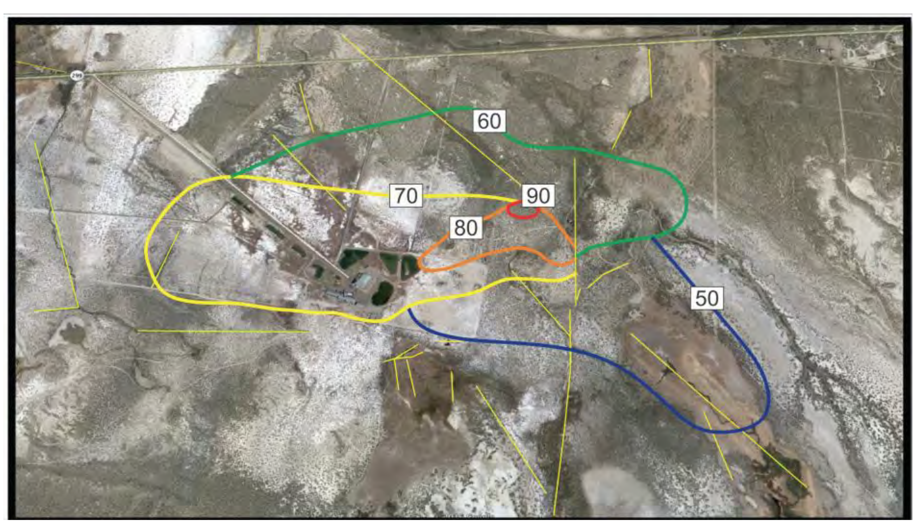

Colors and respective numbers represent boundaries of the areas with the same average soil probe temperature (°F).

2.2.2 Shallow Auger Holes

Seven shallow auger holes (2-inch in diameter, TH1 to TH-7) were drilled by WME in October 2015 (Figure 27) to measure temperature gradient beyond the depth limitations of the 2-M soil temperature probes. The depths of the auger holes ranged from approximately 10 to 30 feet below ground surface. The inconsistency of depth is due to augering conditions and limitations at the auger locations.

The temperature gradients of TH2, TH3, and TH4 are 1.08 °F/foot, 0.1 °F/foot, and 2.96 °F/foot, respectively. Gradients of TH2 and TH4 are significant thermal signals while TH3 is a very low positive gradient. While the temperature gradients of TH1, TH5, and TH6 showed a decrease in gradient, gradient in TH7 decreased and then increased (Table 6).

Two of the locations drilled (TH2 and TH4) showing significant geothermal signals are approximately the same locations selected for the temperature gradient program DS-1 and DS-2. TH7 and TH3 coincide approximately with the alternative drilling sites DS-A4 and DS-A3. While the TH7 shows a decrease in temperature gradient, this location is important in that MT data suggests a clay cap where hotter fluids may exist at a greater depth. The remaining locations, TH1, TH5, and TH6 did not show increase in temperature gradient and were not considered as priority sites given consideration of results of the other exploratory methods.

Figure 27: Map showing locations of shallow auger holes in the study area.

Table 6: Shallow auger hole survey results.

DEPTH (ft.)	TH1 (˚F)	TH2 (˚F)	TH3 (˚F)	TH4 (˚F)	TH5 (˚F)	TH6 (˚F)	TH7 (˚F)
0	72.0	57.8	58.3	46.3	65.9	59.4	59.7
5	70.2	-	-	-	-	-	-
10	60.2	68.6	60.7	75.9	63.3	58.8	59.3
15	60.0	-	-	-	-	-	-
20	-	-	58.4	-	60.5	58.2	56.2
25	-	-	-	-	-	-	-
30	-	-	61.2	-	58.2	56.4	54.6
33	-	-	-	-	58.7	-	55.8

2.2.3 Soil Gas Surveys

Forty-two soil gas chambers were placed adjacent to a subset of 2-m soil temperature probe sites and measured after 24 hours during June 2015.

The meter used for this survey was an RKI-brand instrument, model Eagle2-6 Monitor. This instrument is capable of measuring percent carbon dioxide, methane, hydrogen sulfide and oxygen. Results of this survey are shown in Figure 28.

Measurements are obtained as a percent volume of gas detected. Gas detected during this survey was primarily carbon dioxide. Two sites showed presence of methane gas. Hydrogen sulfide was not detected. For carbon dioxide, the gas measurements ranged from 0.02 to 0.6 percent. The presence of carbon dioxide in soil gas results, is in part, from the oxidation of organic matter in the subsurface. Carbon dioxide originating from organic and inorganic sources is in the range of 0.2 to 5.0 percent for most soils. While it is likely that the concentrations observed are due to decay of organic matter, it should not be ruled out that the concentrations observed may be indicative of gases associated with a geothermal system. Given the results, there are two areas of interest where concentrations of gas were in the range of 0.25 – 0.6 percent.

One of the areas shows a trend along the previously discussed north-south lineation shown in Figure 28. It is questionable as to whether these soil gas concentrations correlate with a structural feature.

A second area of interest during the soil gas survey was identification of a ground fracture located 800 feet due east of the hot springs (Figure 29). The fracture occurs along a water channel for approximately 180 feet, trending northeast. Water flowing in this channel suddenly disappears as it reaches the fracture. Measurements of soil gas chambers placed at two locations in the fracture showed repeated concentrations of 0.28-0.3 percent respectively, on two consecutive days.

One site showing presence of methane gas is located in the wetland area to the south; the second methane gas site is within approximately 300 feet of one of the SVHS geothermal wells.

Figure 28: Map showing locations and results of soil gas survey.

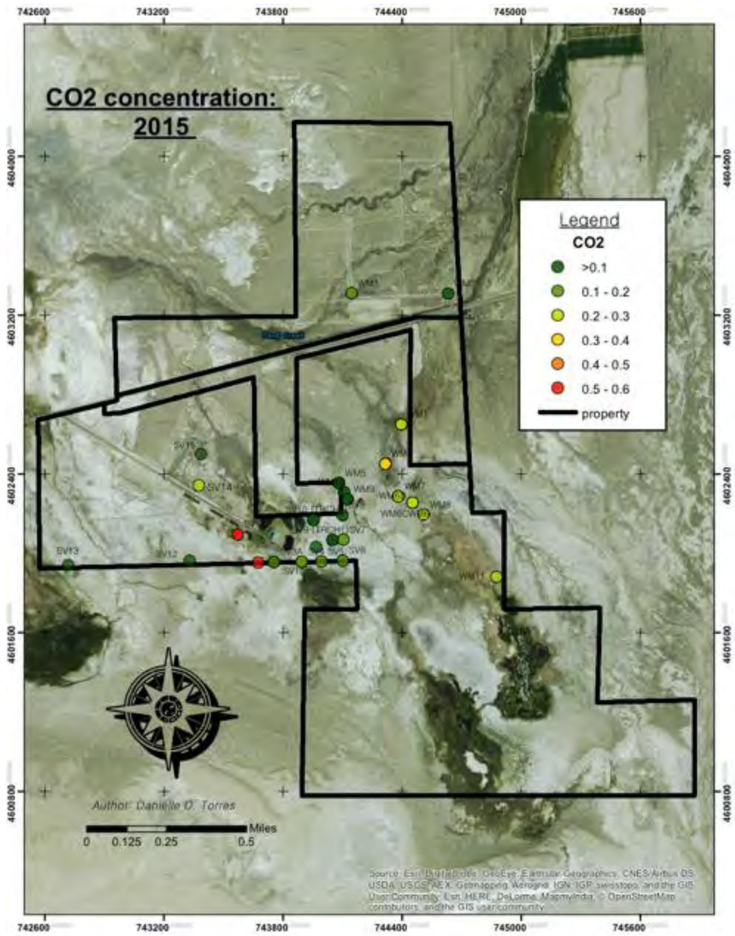

Figure 29: Ground fracture indicated by blue flags.

2.3 Temperature Gradient Well Drilling and Logging

2.3.1 Temperature Gradient Holes and Logs

Three temperature gradient holes were drilled in October 2016. Drilling was conducted by Welsco Drilling Corporation with drilling oversight and data evaluation provided by WME. These wells are referred to as WME-TG2, WME-TG3 and WME-TG4. Gradient drilling locations (Figure 30) were selected based on the geological studies completed as part of CEC GEO-14-003.

Following the completion of the drillings and allowing time for the gradient hole temperature to stabilize, the holes were logged using a HOBO brand, stainless-steel temperature data probe mounted on a reel. The probe was lowered at constant speed in the well and allowed to sit for two to three minutes at each depth interval. At the bottom of the hole, the probe was left to rest for a minimum of five minutes and then pulled up to the surface. Data were downloaded into a data logger software program and then exported to an Excel spreadsheet to correlate the temperature, time, and depth. A graph was produced from the data sheet.

Temperature gradient logging occurred as per the following timeline in Table 7.

Figure 30: Locations of temperature gradient drillings in the study area.

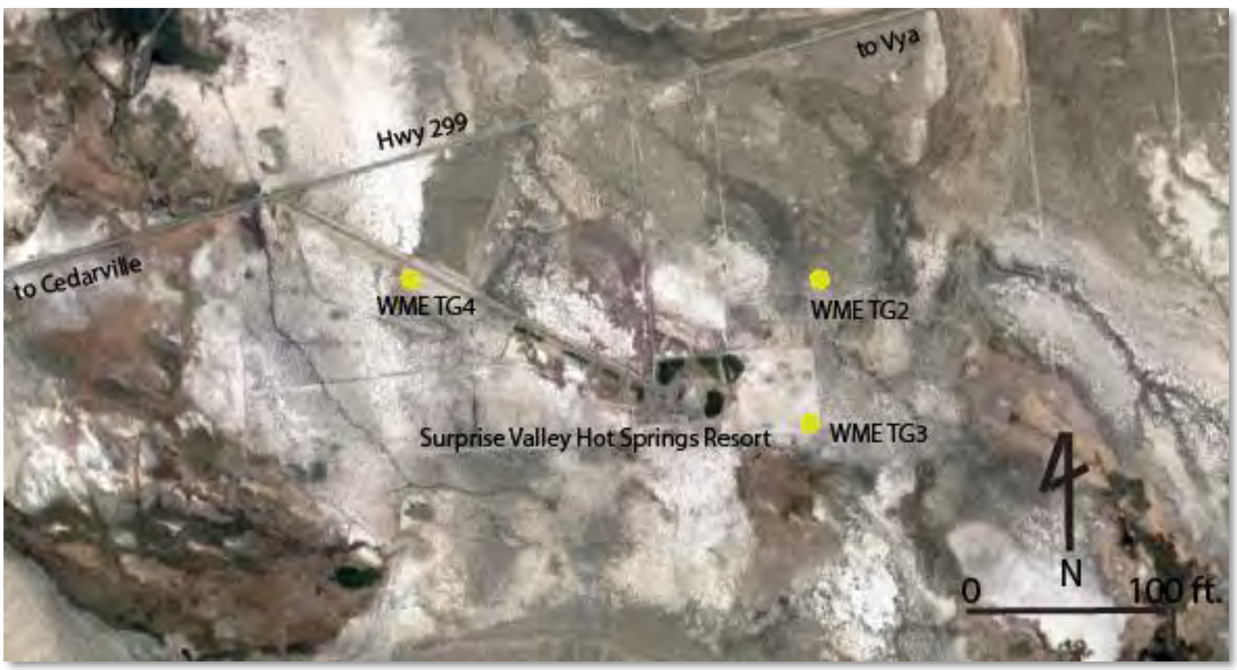

Table 7: Logging timeline.

Well Name	Date Completed	Date Logged	Fluid Equilibration Time
WME-TG2	Oct. 12, 2016	Oct. 31, 2016	19 days
WME-TG3	Oct. 18, 2016	Oct. 31, 2016	13 days
WME-TG4	Oct. 30, 2016	Nov. 8, 2016	9 days

2.3.1.1 WME-TG2

Drilling of WME-TG2 began on 10/7/16 and was completed on 10/12/16 to a depth of 929 feet. Drill cuttings show primarily basalt, cinders, white ash and sticky clay. Monitoring of drilling mud temperatures going in and coming out of the hole showed a temperature differential throughout the hole. However, starting at about 310 feet, temperature differential of mud in and mud out increased from about 10F° differential to 20-30F° differential. Mud in and out temperature is utilized as a guide for gauging downhole temperatures but is dependent on such factors as outside air temperature.

Figure 31 shows the location of the WME-TG 2 well plotted on MT profile EW-3, simplified lithology and alteration minerals. In examining the correlation of mineralogy with lithology in this figure, it is observed that the higher hydrothermal temperature minerals, chlorite and epidote, coincide with the presence of basalt. WME-TG2 was drilled into a zone of low resistivity (about 20 ohm-m). In this resistivity zone, increasing temperatures are observed ranging from 72 F° to 215 F°.

Figure 31: Log of WME-TG2 showing simplified lithological units and alteration mineral assemblages plotted on MT section.

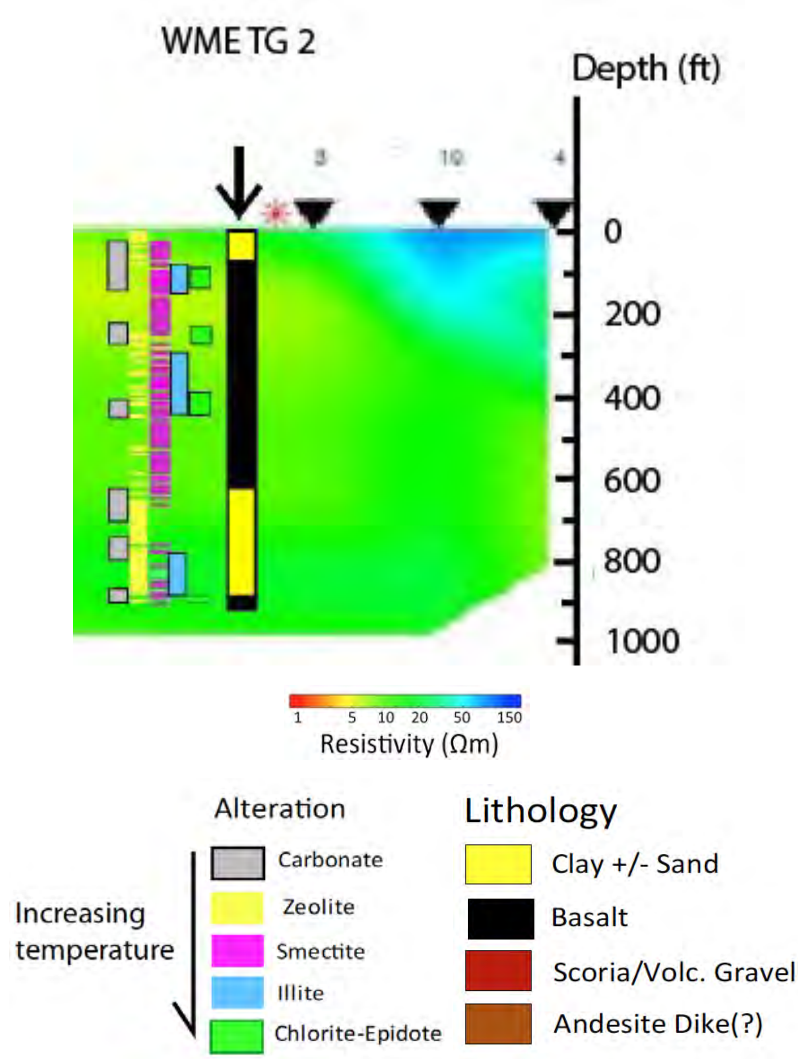

The clay layers observed in WME-TG 2 provides good insulation of geothermal fluids at depth. As observed in Figure 31, two distinct clay layers (smectite and illite) are present. Lost circulation of drilling cuttings occurred from 873 feet to bottom hole. Drilling was ceased at 929 feet due to lost circulation and increasing costs associated with attempting to gain circulation. Lost circulation in the hole indicates permeability in the subsurface and possibly a fault system or dike which allow for upwelling of geothermal fluids.

Temperature gradient logging (Figure 32) shows a rapid increase in gradient from 0-100 feet followed by what is likely a cooler water aquifer from 100-150 feet. This is followed by a somewhat isothermal zone from 200-616 feet. After about 616 feet, gradient then begins to increase again to total depth. From 616-919 feet, temperature gradient is 7.48°F/100 feet. The maximum temperature measured is 215°F at 919 feet below ground surface. Heat flow is observed in the low resistivity MT range of about 10-20 ohm-m. As a point of reference for comparison amongst the three gradient holes, the temperature at 700 feet in WME-TG2 is 201°F.

Figure 32: Temperature gradient log of WME-TG2 well.

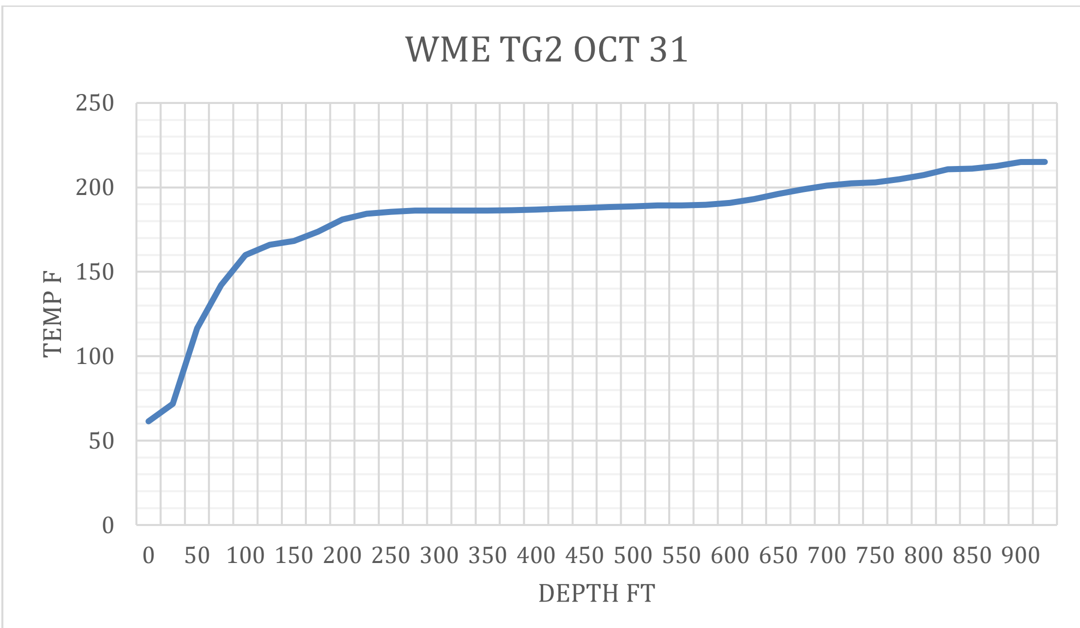

2.3.1.2 WME-TG3

Drilling of WME-TG 3 began on 10/14/16 and was completed on 10/18/16 to a depth of 750 feet. In this hole, approximately 70 feet of very sticky clay overlies about 250 feet of basalt and volcanic gravel. At 320 feet below ground surface, a 20-foot-thick layer of sticky clay is again encountered followed by basalt and mixed volcanic rocks to total depth. In WME-TG3, it is also observed that the higher temperature hydrothermal minerals (chlorite and epidote) are associated with the basalt and mixed volcanics. Minor lost circulation was observed at approximately 660 – 670 feet (Figure 33).

Temperature gradient in WME-TG3 shows a steady increase from 0-750 feet (Figure 34). Focusing on the interval from 650–724 feet, the temperature gradient is 12°F/100 feet. The maximum temperature observed is 183°F at bottom hole. Heat flow is observed in the low MT resistivity range of 10-20 ohm-m.

Figure 33: Log of WME-TG3 showing simplified lithological units and corresponding mineral assemblage plotted on MT section.

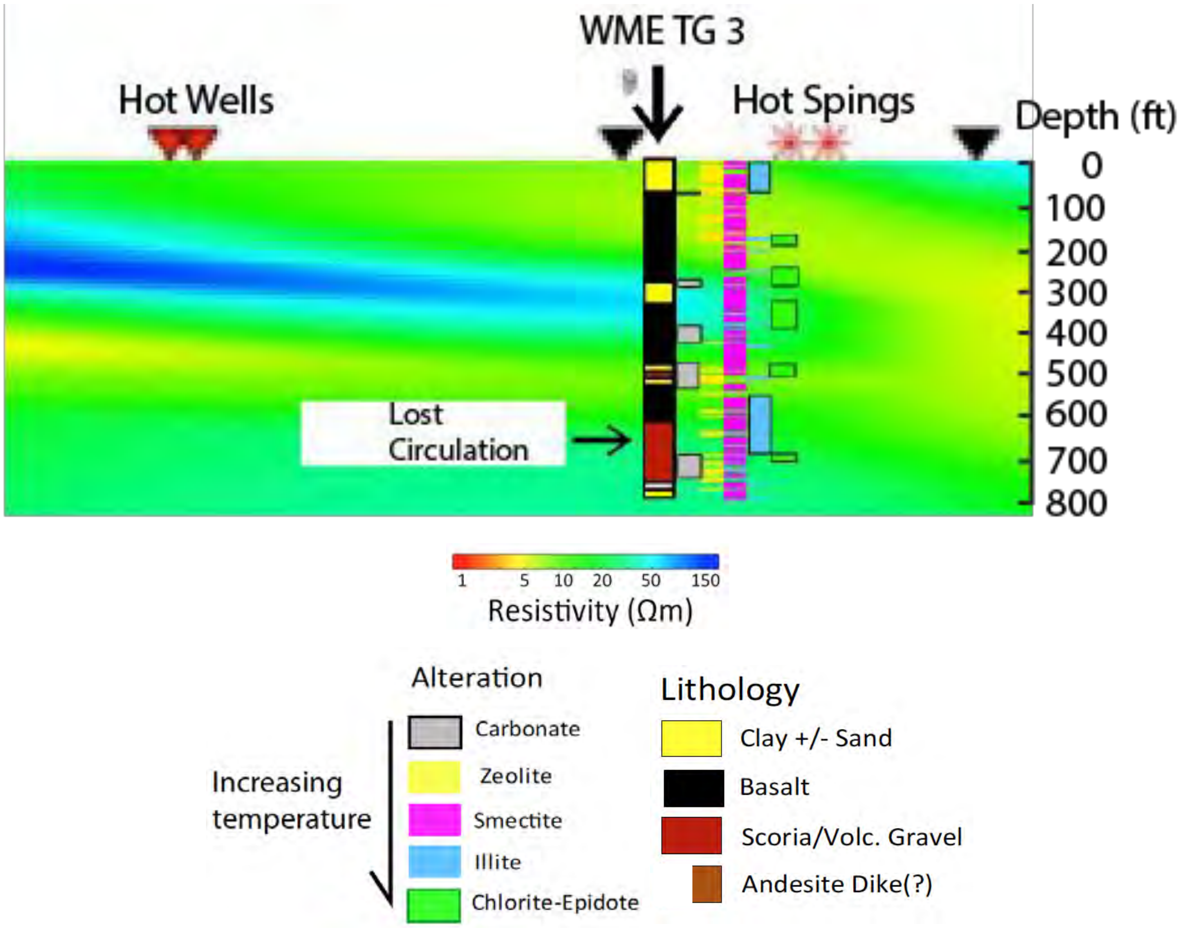

Figure 34: Temperature gradient log of WME-TG3 well.

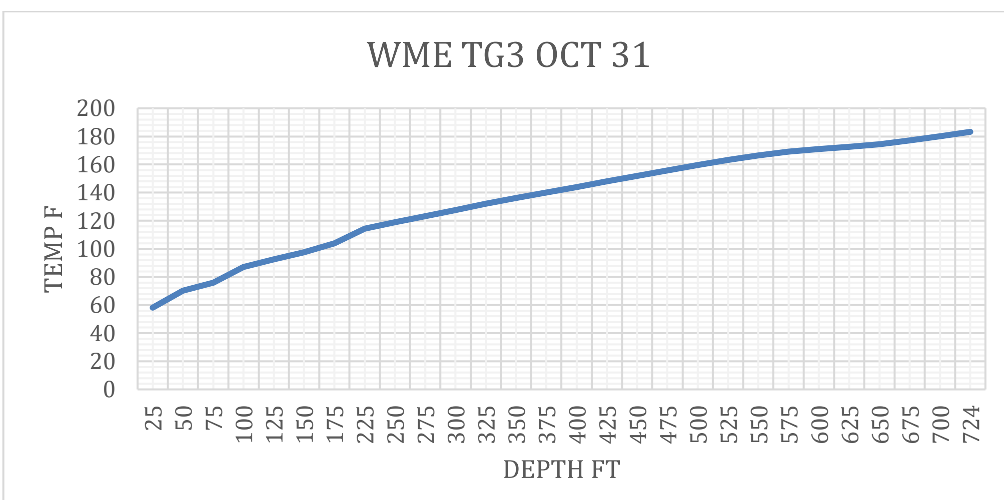

As a point of reference for comparison amongst the three gradient wells, the temperature at 700 feet in WME-TG3 is 181°F. WME-TG3 is 20°F cooler at 700 feet than WME-TG2 and WME-TG4.

2.3.1.3 WME-TG4

Drilling of WME-TG4 began on 10/24/16 and was completed on 10/30/16 at a depth of 1,416 feet. Approximately 500 feet of clay overlies basalt and mixed volcanic rocks to the total depth (**Figure 35**). Bivalve fossils were seen in the clay layer. Basalt was encountered deeper in WME-TG4 than in WME-TG2 and WME-TG3 and the clay cap at the WME-TG4 location is also thicker than at the WME-TG2 and WME-TG3 locations. There was no significant loss of circulation during the drilling of WME-TG4, indicating that a high permeability zone was not encountered to that depth.

Figure 35: Log of WME-TG4 showing simplified lithological units and alteration mineral assemblages plotted on MT section.

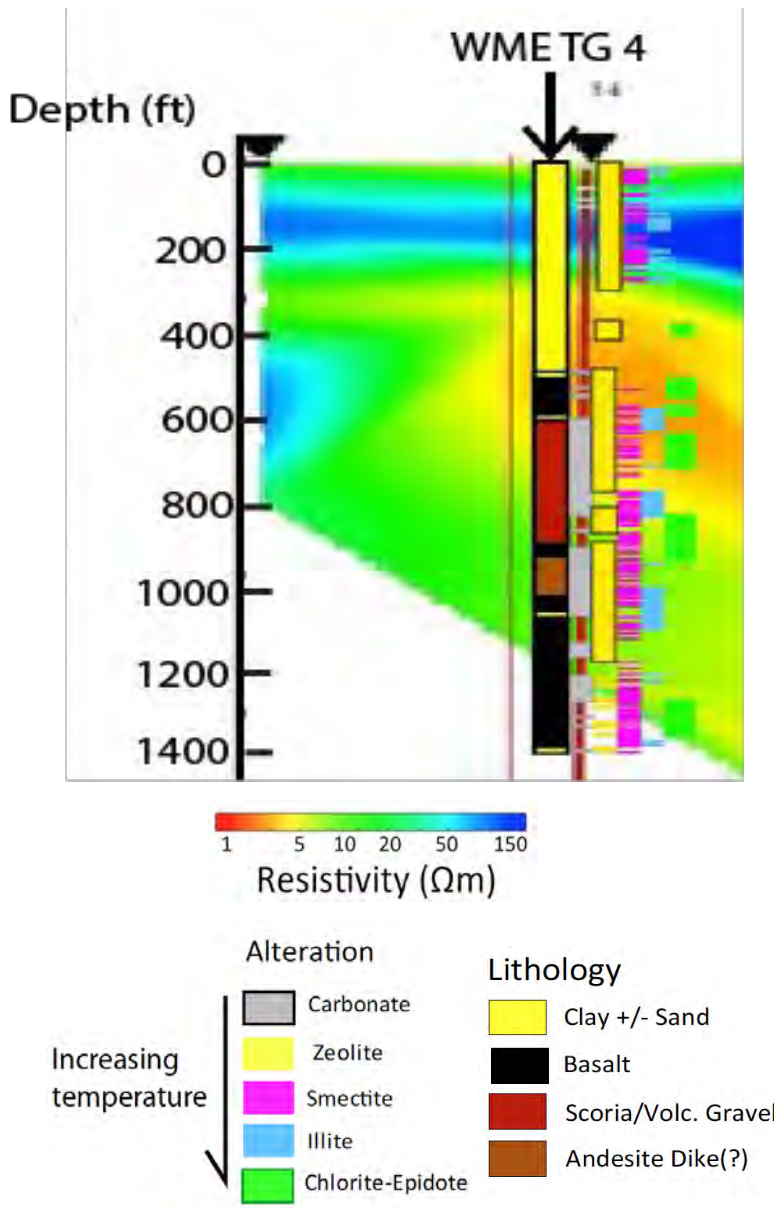

Temperature gradient shows three trends in WME-TG4 (Figure 36). Between the depth of 0-800 feet gradient is calculated to be 18.5°F/100 feet. On the other hand, between 800-1,400 feet, gradient is calculated to be 1.78°F/100 feet and between 1,400-1,415 feet, it is calculated to be 22.9°F/100 feet. The maximum temperature measured at the bottom of the well is 223°F in WME-TG4. As a point of reference for comparison amongst the three gradient wells, the temperature at 700 feet is 201°F.

Figure 36: Temperature gradient log of WME-TG4 well.

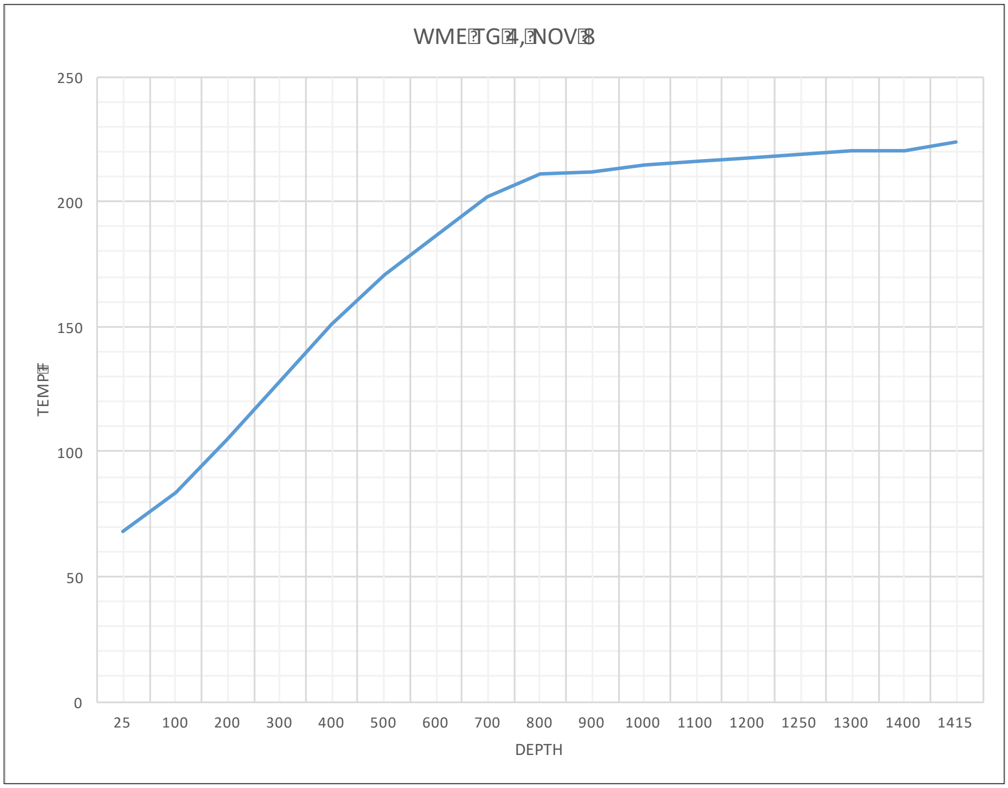

2.4 Temperature Gradient Well Abandonment

All three temperature gradient holes were abandoned per the California Division of Oil, Gas, and Geothermal Resources regulations. Abandonment documentation is through the Division. The abandonment procedure was performed as required by the State of California which included cementing the wells from the bottom to the surface. The state does not allow these holes to remain open.

CHAPTER 3:

Distributed Energy Resource (DER) Demonstration

3.1 Introduction

The goal of this task was to demonstrate the benefits of a small distributed electric energy resource utilizing low temperature and low flow thermal fluid using an existing geothermal resource.

Development of a hot spring resource discharging at 190˚F and flowing at about 150 gallons per minute located about 1400 feet east of the Surprise Valley Hot Springs resort in Cedarville was undertaken to facilitate the demonstration of a 20kW DER unit with plans to supply power to the grid through a net-metering agreement with Surprise Valley Electrification Corporation.

Infrastructure installed for the demonstration included hot and cold water closed loops, plumbing, cooling tower and heat exchanger, electrical, pad, and a DER unit building. The hot spring is located about 15 feet from the unit building.

The County of Modoc contracted with WME to supply the geothermal resource and site infrastructure and with Cornerstone Sustainable Energy doing business as PwrCor, Inc. to supply the DER unit. WME contracted with Sustainable Engineering to assist with designing the layout for the hot and cold loops and review engineering reports from PwrCor. WME contracted with local electrician, McCombs Electric, to install the electrical components necessary to facilitate connection of the DER to the grid. PwrCor, subcontracted with the Southwest Research Institute (SWRI) Laboratory to assist with designing, building, and demonstrating the DER unit.

This chapter discusses the activities associated with installation, commissioning, and operation of the DER unit at the Surprise Valley Hot Spring project site.

3.2 Site Description

The DER unit is placed on private land leased to WME situated adjacent to the Surprise Valley Hot Spring resort in Cedarville. The hot spring is naturally occurring where a 16-23 ft. pool forms at the point of discharge.

Figure 37 shows the location of the unit relative to the resort along with associated infrastructure and the hot spring, located by call-out “DER unit location”.

3.3 DER Unit Design Parameters

The design parameters for the DER unit provided to PwrCor by the County of Modoc specified a hot water supply at a temperature of 185˚F, with flows up to 20 gpm and a cold water supply at a temperature of 75˚F, flowing up to 25 gpm.

However, the parameters used at SWRI, contracted by PwrCor, to assist with building the DER unit were 190˚F at 80 gpm for the hot side and 45˚F at 80 gpm for the cold side.

Figure 37: DER unit location relative to Surprise Valley Hot Springs resort.

3.4 DER Unit Basic Operating Principle

The DER unit engine operates based on the thermal expansion or contraction of supercritical carbon dioxide [sCO_2 (s denotes that the CO_2 is in a supercritical state)]. When heat is added sCO_2 expands and when heat is removed sCO_2 contracts. The engine simultaneously adds and removes heat to the sCO_2 connected to each end of the piston cylinder device via two heat exchangers. The heat exchangers are connected to each working volume at the ends of the cylinder via stainless steel tubing. Each end of the cylinder has a piston that is displaced when the sCO_2 in the heat exchanger is heated or cooled. The two pistons are connected by a shaft fixed to each piston. The linear piston movement is therefore the same for both pistons. One end is heated while the other end is cooled. This cycle reverses based on the timing of valves.

This causes the sCO_2 in the cylinder to produce a net force in the axial direction. In between the two working volumes of the cylinder is another piston with a working volume on each side of the piston. This piston is fixed to the same shaft that connects the two other pistons controlling the sCO_2. The working fluid in the center is a regular hydraulic fluid and its purpose is to transfer the displacement energy of the sCO_2 into the hydraulic fluid. A single hydraulic piston acts back and forth and pumps the hydraulic fluid through a hydraulic motor to create shaft power. The hydraulic fluid is circulated to the pump, to a reservoir and back through the system. There is a complex system of fast acting valves that control the flow of water (hot and cold), CO2, and hydraulic fluid. These valves are coordinated to produce the maximum net energy. The heat engine operation requires that the heat source and cooling source be cyclically alternated through each heat exchanger.

In summary, one heat exchanger heats to expand the sCO_2 (Figure 38), while the other heat exchanger cools to contract the sCO_2. This simultaneous expansion and contraction causes a force differential and the pistons move axially from the hot side toward the cold side and causes flow in the coupled hydraulic circuit. Once the pistons reach the end of the stroke, the heating and cooling processes are reversed: e.g. the hot end of the cylinder now gets cooling and vice versa. The heating and cooling action is reversed by changing the flow of the heating water to the heat exchanger that was just in cooling and sending the flow of cooling water to the heat exchanger that was just in heating. By changing the flow of the water, the process at each end of the cylinder is reversed. The control of the heating and cooling water is by a system of valves and is coordinated with the control of the hydraulic fluid and sCO_2. The continuous switching of the heating and cooling flow in the heat exchangers is a hysteresis loss in the system and also creates a somewhat slow cycle rate compared to other piston cylinder engines.

Figure 38: Opposing piston operation.

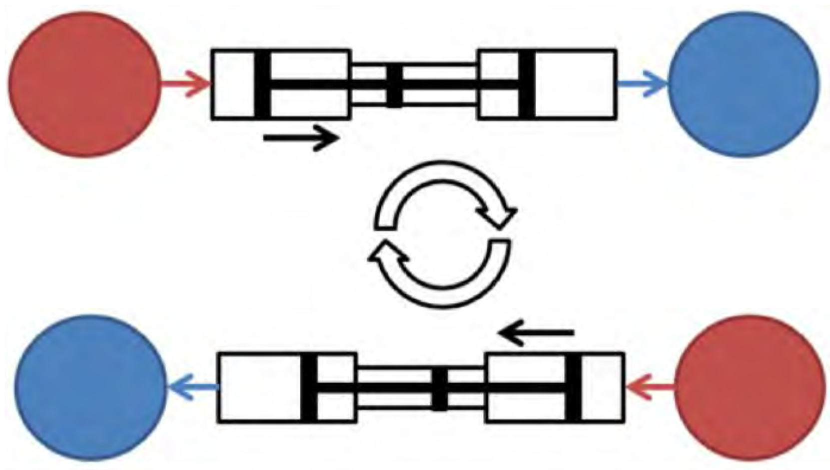

The hydraulic motor produces shaft power and is coupled to an electric generator to produce electric power. The electric generator is a permanent magnet type alternator. The generator does not require excitation current (it is synchronous type machine) but will not produce grid power. In fact, the output from the generator depends on the shaft speed of the hydraulic motor. The output from the generator is fed to rectifiers and then to inverters that are there to convert the raw electric energy into grid quality electrical energy.

This engine was tested at the lab with heating water temperatures from 130-200˚F and cold water temperatures of 40-80˚F with each flow at 80 gpm. The parasitic loads of the engine are two water pumps on the engine that drive the heating and cooling water, a Program Logic Controller (PLC), and the automatic valves located on the engine. The changes in density via heat addition/rejection to CO_2 near the critical point allow the heat engine to produce power in the temperature ranges given. The control unit (PLC) provides the capability of the engine to be operated remotely via an internet connection and has a user interface panel for on-site control.

Figure 39 shows side views of the heat engine with major components identified and indicates the direction of the hot and cold water flow through the heat engine. One hot water pump and one cold water pump provide the water flow. Both pumps are centrifugal pumps that are driven by electric motors. One pump is for the hot water and one is for the cold water. Four solenoid valves control the flow into the heat exchangers and four solenoid valves control the flow out of the heat exchanger.

Figure 39: Side views of DER unit.

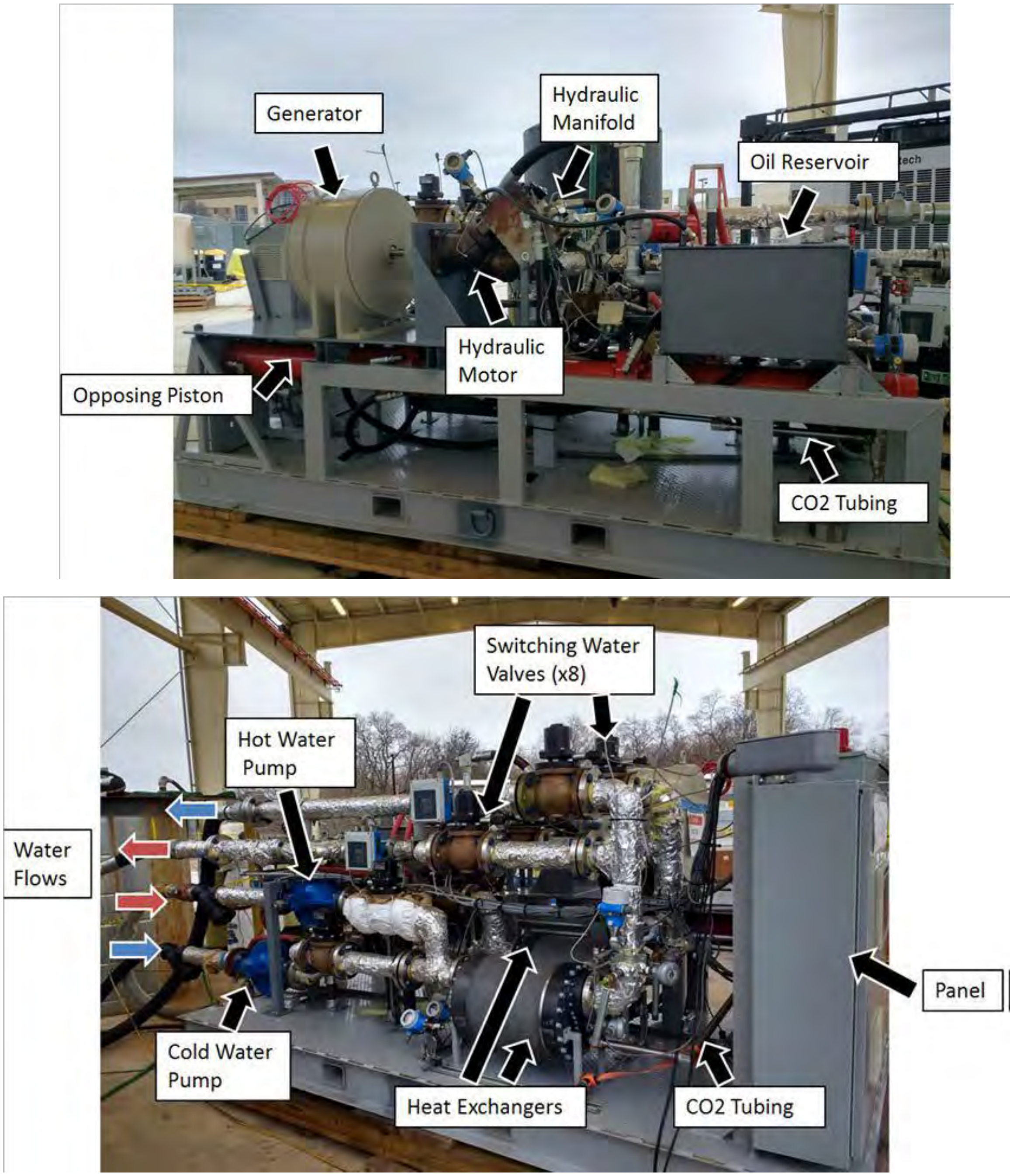

3.5 Expected DER Unit Output and Laboratory Testing

PwrCor agreed to supply a DER unit capable of producing 20kW at flows of 20 GPM of hot water (185˚F) and cold water at 25 GPM (75˚F). However, laboratory testing indicated the unit was only going to supply about 11kW at flows of 80 GPM hot water (190˚F) and cold water at 80 GPM (75˚F). The 11kW reported by the lab was an average of the output and not a steady state number. The power output surged from zero (no output) to the peak value which is approximately three times the average value. SWRI stated that the 11 kW of power output was a computed number based on the measured sCO_2 values and represents a relationship between CO_2 pressures and hydraulic fluid pressures. WME personnel requested the lab demonstrate electric output by connecting the generator and measuring electric output values. When the SWRI laboratory connected the output of the generator, the unit was demonstrated to produce an average electric output at 6.1 kW. WME representatives on site during the laboratory test noted that the measured output was not steady, varying from zero to 31 kW in a cycle time of approximately 26 seconds. This output was also unsteady with the surging as the computed output. SWRI and PwrCor stated that the load bank used was not appropriate because the measured electric output was not representative of the machines capability. A different load bank was installed with the same results. It is also noted that the machine was not tested for more than a few minutes (several cycles).

3.6 Installation

3.6.1 Site Preparation and Configuration

WME developed the site for placement of the DER unit including supplying a building to house the DER unit. Activities consisted of road access, gravel pad, gates, security fence, electrical, plumbing, hot and cold water closed-loop supplies, geothermal heating inside of the building, and insulation on the hot spring.

Deionized water tanks were also supplied by WME to charge the lines and DER unit with water.

Figure 40 shows the components of the DER demonstration unit site installed by WME.

3.6.1.1 Building for DER Unit

WME developed an access road and gravel pad on which to place a 12x16 foot insulated and painted building (inside and out) for the DER unit (*1. Hot Spring, 2. Inner fence around the hot spring, 3. Outer fence around the hot spring, engine building, and gravel pad, 4. DER unit building, 5. Gate, 6. Culvert, 7. Gravel road, 8. Gate, 9. Trench that contains pipes for supply and return cooling pipes, electric and control cable, 10. Manifold for cooling pipes. "A" is the continuation of the trench with only the electric and control cable to the electric interface between the resort and Surprise Valley Electrification Corporation.*

Figure 41). A window for viewing the unit is included and a roll-up door provided for access. The floor is painted, waterproofed, and reinforced with steel plates to accommodate the excess weight of the power unit beyond that which was initially specified by PwrCor. The building is intended for the public to be able to view the DER demonstration unit. A security fence is placed around the building and a locked gate for access. The building is pad-locked, and a security camera is inside of the building for continuous and remote monitoring of the unit. The building is heated geothermally.

Outside of the building, stands a project sign that includes information about the California Energy Commission funding source and cost-share partners.

Figure 40: Site configuration.

1. Hot Spring, 2. Inner fence around the hot spring, 3. Outer fence around the hot spring, engine building, and gravel pad, 4. DER unit building, 5. Gate, 6. Culvert, 7. Gravel road, 8. Gate, 9. Trench that contains pipes for supply and return cooling pipes, electric and control cable, 10. Manifold for cooling pipes. "A" is the continuation of the trench with only the electric and control cable to the electric interface between the resort and Surprise Valley Electrification Corporation.

Figure 41: Building housing the DER unit.

3.6.1.2 Electrical

Preparation for electrical work includes 1,680 feet of electrical conduit from the Surprise Valley Hot Springs resort electrical system to the DER unit building. Electrical work included:

- Installation of a main breaker and brackets in distribution cabinet.
- Installation of a transformer at main distribution cabinet stepping voltage to 480 single phase.
- Installation of underground wire from the transformer to the DER unit location.
- Installation of second transformer to get voltage back to 120/240.
- Installation of 100 amperage disconnect switch back to back with 100 amperage automatic transfer switch.

The electrical connections installed after the DER unit allow for connection to a net meter to the grid.

3.5.1.3 Plumbing

Water supply lines include 1,900 feet of buried 3-inch supply and return water lines for the cold water loop between the pond and DER unit building for heat exchange. Hot water plumbing includes two 11 outlet manifolds plumbed to the supply return of the DER machine and buried 3/4 inch pex piping from the DER building to the hot spring (average length of the pex piping is 80 feet per circuit).

Plumbing inside of the building includes four automated ball valves and piping for connecting the DER unit to the heat exchanger manifold system (both hot and cold systems) and to the plate and frame heat exchanger and cooling tower.

3.6.1.4 Hot and Cold Water Heat Exchange/Rejection System

Eleven closed-loop supply lines were installed for each hot and cold water side of the system. The closed-loop system consists of eleven 100-foot coils of 3/4" copper tubing attached to 3/4" pex piping. Each 100 feet of copper tubing is attached to about 40 feet of pex on each open end of the tubing to create one loop. The copper tubing serves as heat exchangers between the DER water and the hot spring or cooling pond. Eleven coils are placed in the hot spring and fed into the building and eleven coils are placed in a cold water pond and fed into the building. The cold system is connected via the 3-inch supply and return lines. The hot system, immediately adjacent to the power building, is directly connected to the hot manifolds (supply and return) in the power building. The cold water loops are attached to a PVC pipe manifold system, equipped with two valves for each circuit. The PVC manifold is located near the cooling pond and buried in an insulated utility box to prevent freezing. See

Figure 42 through Figure 47.

Figure 42: Copper tubing used for heat exchange attached to pex piping.

Figure 43: Hot water loops.

Figure 44: Hot and cold water manifolds inside of building.

Figure 45: Cold water manifolds.

Figure 46: Installation of cold water loops.

Figure 47: Hot water flow system.

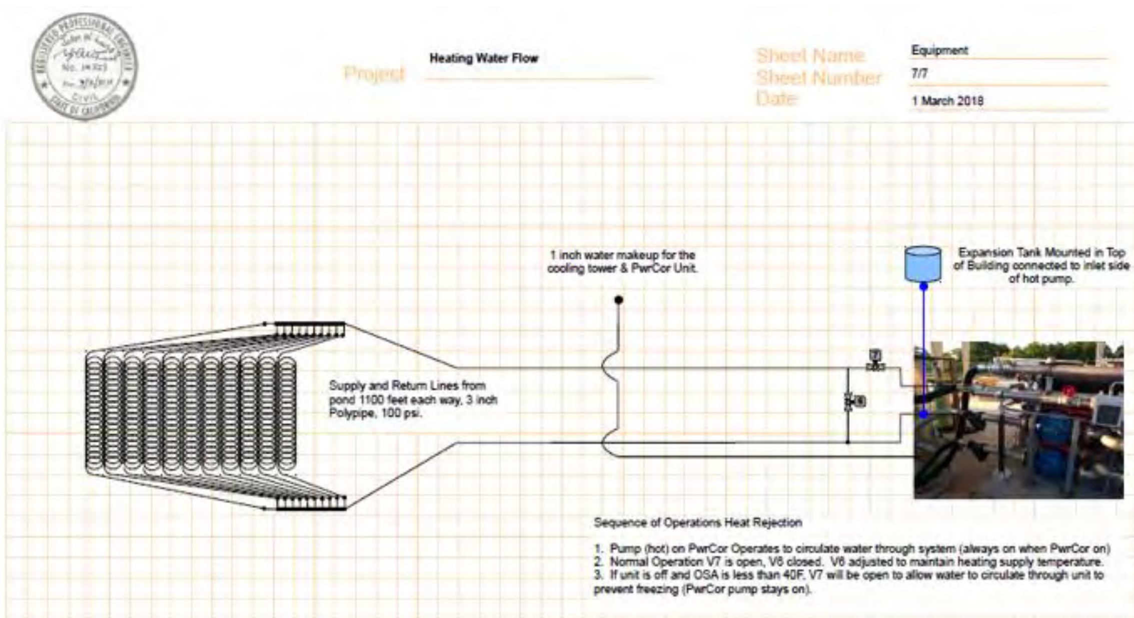

A separate two-inch line is attached to an alternate cooling system, a cooling tower with a plate and frame HX for use in the summer months when the pond does not supply sufficient cooling temperatures. Four valves allow the transfer of cooling water from the pond piping system to the cooling tower. The plate and frame heat exchanger isolates the open cooling tower from the PwrCor cooling circuit and prevents mixing of the two sources of water to keep the PwrCor treated water separate.

Figure 48 shows the configuration of the cooling tower relative to the supply and return lines to the cooling pond.

Figure 48: Cooling water flow.

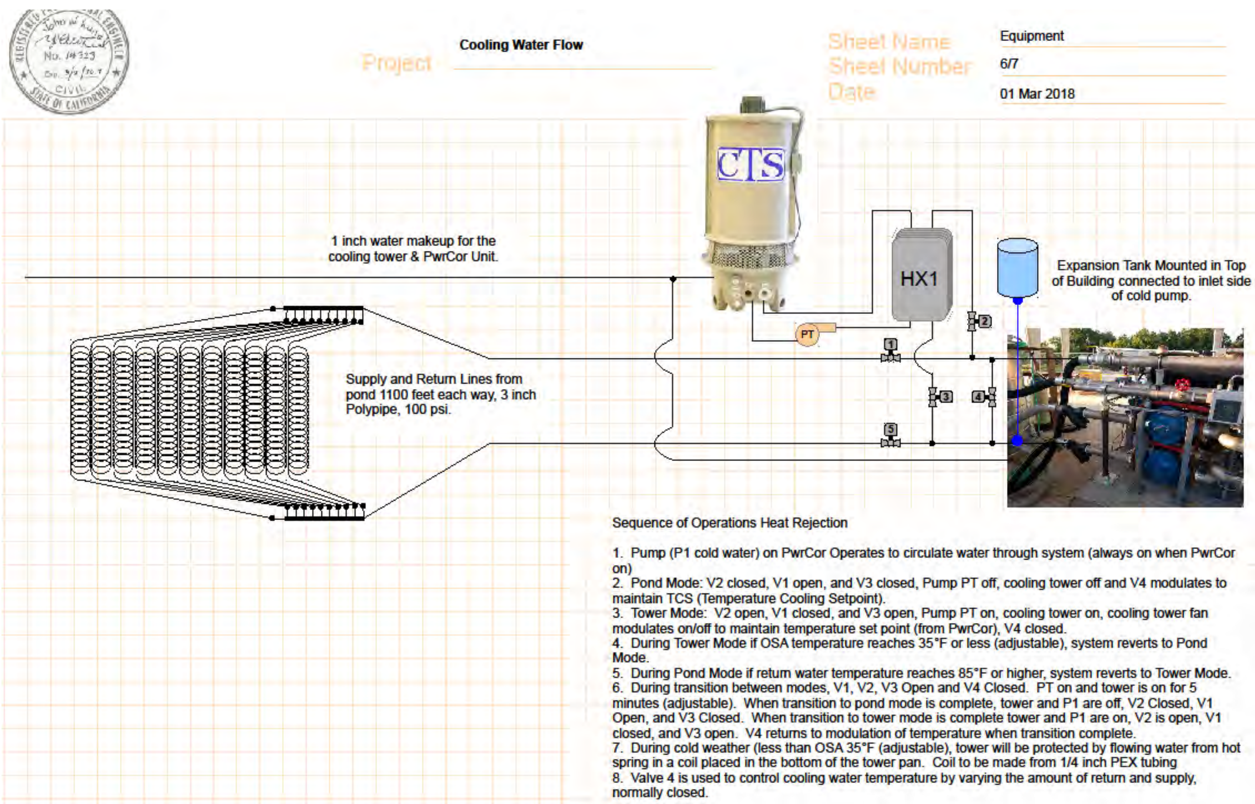

3.6.1.5 Geothermal Heating Inside of Building

The building is geothermally heated by a pex coil submerged in the hot spring. The spring heated water is circulated by a 1/3 horsepower pump, then passes through a radiant fin tube wall heater and back to the hot spring to pick up more heat (Figure 49).

Figure 49: Geothermal heating system inside the building.

3.6.1.6 Insulation on Hot Spring

Dense foam insulation panels topped (Figure 50) by a 60 ml rubber tarp (Figure 51) cover the hot spring which increased the temperature of the outflow of the hot spring from 190˚F to approximately 203˚F. It is noted that the 203˚F is near the boiling temperature of 204˚F at the altitude of the site.

Figure 50: Insulation of hot spring.

Figure 51: Rubber tarp for second layer of insulation.

3.7 Commissioning of DER Unit

3.7.1 Delivery and Placement of DER Unit

The DER unit arrived on site Thursday, February 22, 2018 from San Antonio, Texas. WME facilitated off-loading of the unit using a specialized forklift to unload the DER unit which weighs approximately 11,000 pounds. (PwrCor's original weight estimate was 5,000 pounds.)

The unit was delicately placed inside of the building once off-loaded from the transport vehicle

Figure 52 and Figure 53).

Figure 52: Off-loading and placing DER unit inside building.

Figure 53: DER unit inside of building.

3.7.8 Commissioning Activities

Once the unit was positioned inside the building, the plumbing and electric connections were made to allow for heat addition, heat rejection and electric output. Plumbing and electric installation could not be completed until the unit arrived since design specifications for the unit were not provided.

3.7.9 Commissioning Process Overall Plan

The commissioning process consisted of the following steps in the overall plan:

- Install infrastructure on site
- Validate machine performance at SWRI Laboratory in San Antonio, Texas
- Authorize shipment once validated and administrative items are complete
- Deliver machine on site
- Start-up procedures for machine
- Train WME on machine operation
- Begin operations

3.7.10 Actual Process

Commissioning of the DER unit began on March 1, 2018 upon arrival of a representative of the SWRI Laboratory, Jordan Nielson, who worked in conjunction with the PwrCor representative.

The process for start-up of the unit included the following steps, as narrated in-person by Jordan Nielson on March 6, 2018 to Lisa Safford of WME with Daniel Hand, Sustainable Engineering being present. The following steps and narrative were verified by Jordan Nielson.

- Hook up DER unit to hot and cold water supplies.
- Fill system with water and bleed air.
- Run pumps to demonstrate pumps can run continuously.
- Hot side was pumping up to 90 gpm the first day at 189˚F.
- Cold side pumped up to 65 gpm at 50˚F.
- This was initial testing.

- Running hot and cold loops independently.
- Charge system with CO_2.
- Move piston back and forth manually to verify getting heat into the CO2.
- Check to see if all valves are working.
- Run low pressure test under hydraulic load (2,000 psi) to verify software is running and engine is working. During this test, pump was running at 50 gpm on both hot and cold. Cold side was 60-65˚F cold and about 185˚F on hot side. Ran this for about 15-20 minutes. After that time, machine was shut down. The machine ran as expected under low pressure conditions. Not getting full kW at that time because not running at full capacity. This was being monitored via computer hard-wired to the digital computer unit mounted on the machine.
- Do low electric load test to confirm that generator is working.
- Need to do high pressure release under mechanical load to see if any more adjustments needed. Will then run at 2,400 psi.
- Upon satisfactory completion of the above steps, the DER unit would be fully tested with CO_2 pistons running.

3.7.11 Issues During Commissioning

There was some difficulty in bleeding all of the air out of the system. The best way to purge the air was to keep the make-up water on and moving while running either the hot or cold loop circulating pumps. Air was removed through opened valves with garden hoses attached. The machine did not come with air purge locations other than the bleeders that came pre-manufactured on each circulation pump. An air purge valve was installed on site at the highest point of the water system located on the cold loop line. This was found to work well but was a slow process. The hot and cold loops were purged separately using make up water to replace the air that was removed. The only pumps for purging the system of air are the PwrCor pumps. This created an issue since WME did not have control of the pumps and PwrCor did not stay with the equipment during the connecting and air purging. Detailed drawings of the plumbing and electrical systems prior to delivery would have been beneficial in overall site readiness.

The machine came with in-line filters, one on each hot and cold closed loop in order to capture fine particles that could damage the heat exchangers and the entire system. The machine's design did not include isolation valves on each side of the filter housings. Isolation valves allow for a section of the system to have flow isolated from the rest of the system. This is important when addressing plumbing issues. As a result, each time a filter was checked or changed, 3-4 gallons of water would escape and thus allow air back into the system upon each filter change. This required the air purging process to be started all over again every time there was a filter change. Upon initial start-up there were roughly 10 to 15 filter changes until all the particulates from the newly installed pipelines were removed. Upon continuous iterations of the machine's filter being clogged, WME supplied sediment filtration on the inlet and outlet of the deionized water tank.

- The machine was shipped void of fluids for safety reasons including the potential danger of shipping components under high-pressure and the fact the designated site location was experiencing below freezing temperatures in February 2018.

- The machine eventually was purged of all its air and had a series of successful tests and CO_2 balances, one of which the public was able to view and was recorded by the local newspaper.
- Charging of CO_2 into the system was very slow and then it appeared that only one charge could happen per day. WME was informed this was because the machine's component temperature had to cool down prior to additional cooling. WME never received any data on the engine's temperature nor the parameters during the cooling and CO_2 charging process nor was this topic covered in the O&M manual.
- Complete and total balancing of CO_2 was never completed as PwrCor had safety concerns surrounding the machine.

There were leaks in the system and the PwrCor unit that allowed air to be reintroduced into the system when makeup water was not continuously connected. Purging was a learning process but was successfully completed using the purging ports that WME provided on its cold and hot water loops.

Data during any testing procedure could only be recorded for 45 minutes at a time and had to be downloaded manually to a thumb drive, according to PwrCor.

3.7.12 Electric Output Test

The electric output from the generator was tested on a temporary load bank of ten 100- watt incandescent light bulbs for 6 minutes and 25 seconds.

During the load test, the lighting from the bulbs surged from completely off-to-on and the cycle rate from off-to-on occurred about 2-3 times per minute. After the start of the demonstration, 1 minute and 40 seconds elapsed before the first light began to glow. Below is a record of times based on a video after the first 1 minute 40 seconds to the end of demonstration.

Power Bursts	Lights On (Seconds)	Lights Off (Seconds)
1	4	20
2	6	1 min 09
3	5	07
4	5	05
5	4	09
6	5	05
7	4	08
8	6	03
9	5	08
10	5	04
11	5	08

12	5	05
13	5	08
14	5	05
15	5	07
16	6	05
17	5	08
18	5	

3.8 Conclusions of DER Unit Test

3.8.1 Successes

a) DER Unit

The unit demonstrated the use of supercritical carbon dioxide (sCO_2) based on the fundamental thermal expansion properties of sCO_2.

The unit demonstrated that electricity can be created at very low temperatures and flows (190˚F at 80 gpm and at 50˚F at 65 gpm), albeit for a very short period of time with a non-steady output unsuitable for grid connection.

A test was performed using ten 100-watt light bulbs and ran for 6 minutes, 25 seconds after which time the test was terminated.

b) Geothermal Resource

The flows in the hot and cold water loops were greater than contractual requirements by PwrCor, which is a favorable condition. Flows in the cold loop were reported at 65 gpm at 50˚F and the hot loop flowed up to 100 gpm at 198˚F. Heat exchange capability on the cold and hot water loops was exceeded by a factor of three.

An existing geothermal resource (hot spring) was proven effective to supply a steady heat supply and was used in conjunction with an existing cold water supply for heat addition/rejection.

The outflow temperature of the hot spring was increased from 190˚F to 202˚F by using insulating materials to reduce evaporation and heat loss.

c) Installed Infrastructure

An infrastructure of hot and cold heat exchange/rejection system is effectively installed and can deliver flows and accommodate heat exchanges higher than anticipated.

Based on the availability of an operational DER unit, WME has the electrical connections in place to be able to connect to the grid.

Powerhouse is installed, wired, lighted, heated and ready for installation of a small power unit that can use the heat and cooling sources to produce useful electric energy.

d) Economic and Employment Benefits

Short-term economic benefits were created for Modoc County. WME used local contractors for electrical work, plumbing work, building construction, materials, and supplies.

Contractors in the community of Modoc County provided the services required to develop the infrastructure at the site; contractors made themselves available evenings and weekends and worked as strong team players in order to come to the point of commissioning.

e) Public Outreach

Several public outreach events occurred to bring awareness to the public on the potential of California geothermal resources. Newspaper articles were published and members of the public were on site during the initial demonstration of the capability of the unit to produce electricity (

Figure 54). All of these activities have contributed to the public outreach goal of increasing awareness of California's renewable energy potential in a rural community.

Figure 54: DER unit demonstration event (Modoc Record).

3.8.2 Requirements for Connecting to Grid - Surprise Valley Electrification Corporation

Given an operational machine, Surprise Valley Electrification Corporation requires the following for connection to the grid.

Net-metering service is available to Surprise Valley Electrification Corporation Members who own and operate a net metering generating facility and enter into a Net Metering Agreement with the Cooperative, subject to the following conditions:

- The facility uses solar, wind, fuel cell, hydroelectric power, landfill gas, digester gas, waste, dedicated energy crops available on a renewable basis, low emission non-toxic biomass based on solid organic fuels from wood, forest or field residues, geothermal energy, to generate electrical power in the Cooperative's service territory.
- Nameplate generating capacity limits: OR & NV - not more than twenty-five (25) kilowatts. CA - not more than 1 MW.
- The project must be located on the Members' premises (owned, leased, or rented). Interconnects and operates in parallel with the Cooperative's existing transmission and distribution system.
- The project must be intended to offset part or all of the Members' own electrical requirements. Net-metering service is not available to those Members that have installed net metering facilities with a nameplate capacity that is greater than the expected electrical requirements of the Member.

- Cooperative Program Cap: OR & NV – 0.5 percent of the utility's historic single-hour peak load. CA – 5 percent of peak load.

Surprise Valley Electrification Corporation also requires the new customer to attest that they have received system warranty information and operations manual and have been instructed regarding the proper operation of the net metering facility and associated equipment.

3.8.3 Shortfalls

The PwrCor unit is generating DC power demonstrated on-site with power surging from zero to a maximum of 1 kW; testing at the SWRO lab resulted in an average of 6.1 kW with similar surging from 0 to 31 kW. The final power output will not be definitive until the unit can produce continuous steady power without surging. As it now exists, the unit pulses from being on for 4 to 6 seconds and off for 4 to 9 seconds as the piston reverses and gains pressure. The goal for this project was to provide measurable electrical power capable of connecting to the Surprise Valley Electric Cooperative grid.

The capability of the machine to produce electric power suitable to connect to the grid has not been proven.

3.8.4 Opportunities to Meet Interest of Project

Continue to Market the Resource for Demonstration

Modoc County and WME plan to continue to market the existing resource and infrastructure for potential demonstration projects. Universities, private laboratories, national laboratories, and private developers are all viable opportunities to continue to demonstrate the potential of this site.

Potential Modification to the DER Unit

Two factors seem critical to make piston system continuous. One engineering suggestion is to put a bypass on the hydraulic system so the hydraulic motor will continue to operate spinning the generator. This may still have power surges but could allow continuous electrical generation.

The other concept discussed by WME engineers would be having the heat exchanger dedicated to a hot cycle and the other to a cold cycle. The system now has the exchanges switch from hot-to-cold-to-hot to feed the piston system. A significant amount of energy goes to continuously heating and cooling the metal parts of the heat exchanger and does not contribute to the amount of energy available for conversion to electric energy.

A governing unit on the machine to control speed would be beneficial if made to operate continuously.

Air vents need to be mounted on the machine to vent trapped air. A vent system exists on the cold and hot water loops but not on the machine. They were not needed at the lab because the lab employed open systems where the WME system is a closed loop, which was always part of the plan.

There needs to be valves on both sides of the filter to minimize the drainage of water and introduction of air into the system when cleaning the filter. An air bleed valve as part of the air filter is also recommended so that air can be immediately drained from the filter when the filter is replaced. It is important to now allow air to enter the lines as it may cause performance issues.

It is thought the engine can produce usable power. One potential way of producing steady power is to use an accumulator device (which was part of PwrCor's original design) that stores the power surges and allows these power surges to be released on a steady basis to turn the generator without the pulsing. SWRI lab briefed that the accumulator significantly compromised the power output so it was abandoned, however the DER unit delivered had an accumulator on board. This issue should be revisited.

The points above are the initial observations by WME engineers without adequate design/construct diagrams of the power unit. PwrCor would not provide design/construct diagrams to Modoc County or WME.

Continue to Showcase Infrastructure Design and Transfer Model

Education on the concept of a DER system can continue to occur without the machine running. The design and operation of the hot and cold loops can be explained and how it relates to a geothermal source for the DER unit. The model for the infrastructure design and function can be transferred to other projects.

CHAPTER 4:

Economic Feasibility of Additional Geothermal Opportunities

4.1 Purpose and Scope

The purpose of this chapter is to identify and quantify development of other geothermal resource opportunities at the project site.

4.2 Basis of Feasibility

Based on the geoscientific data acquired as part of this study, the following assumptions are made regarding the resource:

Drilling Depth: to 3,000 feet

Flow per well: 2,500 GPM

Temperature: 285˚F.

The drilling depth to obtain 285˚F is estimated from the temperature gradient graph of WME-TG2 (Figure 55). The best estimate came from the deepest part of the well, from the extrapolated part of the gradient line. The extension of the gradient is shown in red and is projected based on the linear interpolation from the 600 to 900-foot interval. Geothermal wells that intercept a fracture typically have large flow rates. Since the target depth of 3,000 feet is assumed to have intercepted fractures, flow rate is taken as 2,500 GPM. The resource temperature of 28˚F was estimated by using geothermometry data.

Figure 55: Temperature gradient graphic of WME-TG2 well.

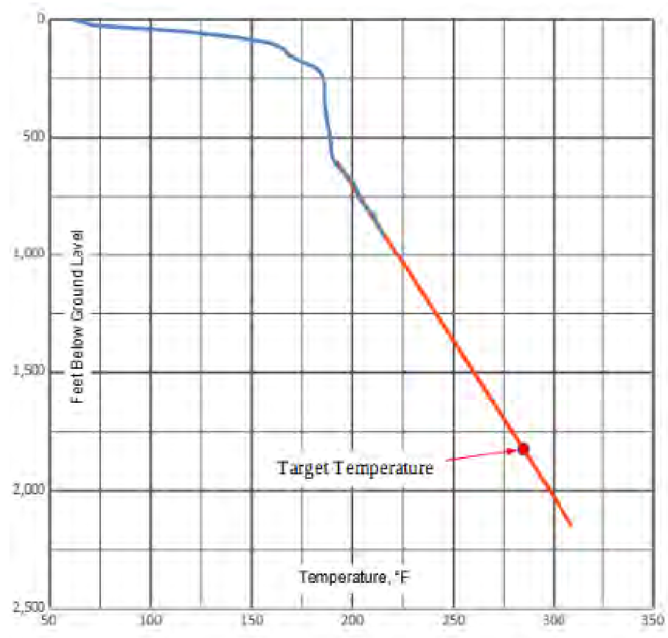

4.3 Key Goals and Strategy

The following were the key goals and strategies of the project:

- Develop the geothermal resource to its economic and sustainable potential
- Create sustainable economic activity for Modoc County
- Test new uses of geothermal equipment and applications
- Provide a model for development of small geothermal resources
- Develop information that assists with geothermal development

Modoc County sought to acquire information about the geothermal resource; technical information about the size, scope and development parameters of the resource and information about what can be developed. The data will assist in assessing funding opportunities for further investigation. Funding entities require validated data and quantified development opportunities.

4.4 Climate

The area is characterized by hot summers, cold winters, and low rainfall (12.49 inches per year of average precipitation). The data in

Table 8 is from the Agrimet network weather station located in Cedarville covering statistics from 2010 to 2016. It is located at an altitude of 4,599 feet and 8 miles northwest of the study area. The data was used to model the weather conditions in the study area.

The minimum low temperatures are extreme at -19 °F while the summers are hot with temperatures approaching 100 °F. Winds peak to more than 60 mph. This type of weather requires any facility to be built to function in extreme conditions both for heating and cooling. The high desert climate also has an intense amount of sunshine (measured in Langley's) as shown in

Table 8. Table 9 shows monthly distribution of precipitation around Cedarville between the years 1894 and 2010. Precipitation is low and slight snow cover is observed about two months within the year. This is a general weather pattern for an average year.

From a climate point of view, it is important to have adequate protection from freezing and high winds for any proposed project at this site. Although it does not rain often, the silty alkaline lakebed soil does not support vehicle traffic because it becomes very sticky and slippery. Any facility located in the area will need all weather roads for access. The minimum road improvement requires placing and compacting gravel. Highway 299 provides all weather transportation into the site and to Highway 395 to the east. The Cedar Pass between Cedarville and Highway 395 is open year- round with only temporary snow removal closings.

Table 8: Average monthly weather data.

Cedarville, CA Monthly Weather Statistics (Jan 210 to Dec 2016)									
Month	Min Daily Air Temp, °F	Max Daily Air Temp, °F	Mean Daily Air Temp, °F	Average Daily Global Solar Radiation (Langleys)	Average Daily Relative Humidity (%)	A Daily Dew Point, °F	Daily Peak Wind Gust, mph	Daily Average Wind Speed, mph	Daily Average Wind Azimuth, ° (Direction Wind is Coming From)
Jan	-17.6	58.9	32.3	187.6	71.6	23.4	58.1	3.8	277.6
Feb	-1.1	67.4	36.9	279.5	63.3	24.2	57.0	4.8	274.6
Mar	8.4	74.6	41.8	370.7	56.0	25.3	54.4	6.0	258.3
Apr	18.4	84.0	46.1	510.6	52.4	27.2	59.6	5.0	276.9
May	20.4	84.3	52.7	579.9	53.0	33.5	42.5	4.3	294.0
Jun	29.5	100.6	63.3	664.3	43.2	37.4	39.2	4.3	298.9
Jul	37.8	99.6	72.0	680.7	35.0	39.5	39.9	4.1	296.9
Aug	35.3	97.5	69.9	599.0	34.4	37.3	50.2	3.9	295.1
Sep	28.6	93.5	62.6	478.0	38.6	33.6	45.4	3.8	285.4
Oct	20.2	91.5	51.0	322.4	51.2	31.0	56.8	4.1	271.4
Nov	-0.1	73.6	38.4	209.1	64.1	25.8	53.5	4.4	272.8
Dec	-19.0	60.9	31.0	154.2	72.7	22.7	61.2	4.8	271.3

Weather data from the time period 2010 to 2016, showing minimum and maximum values over the 6-year period as well as average values. Credit: *Agrimet Weather USDA Cedarville Station*.

Table 9: Average weather data for Cedarville, CA (1894 to 2010).

Month	Average Max. Temperature, °F	Average Min. Temperature, °F	Average Total Precipitation, in	Average Total SnowFall, in	Average Snow Depth, in
Jan	40.2	20.3	1.7	10.5	1.0
Feb	44.6	24.2	1.4	6.1	0.0
Mar	50.9	27.9	1.3	6.2	0.0
Apr	59.3	33.3	1.0	2.8	0.0
May	67.9	39.9	1.0	0.8	0.0
Jun	77.3	47.1	0.8	0.0	0.0
Jul	88.3	54.5	0.3	0.0	0.0
Aug	86.9	52.1	0.3	0.0	0.0
Sep	78.1	43.9	0.5	0.0	0.0
Oct	65.6	35.0	1.0	0.6	0.0
Nov	50.4	27.1	1.6	3.5	0.0
Dec	41.1	21.2	1.7	6.8	1.0
Annual	62.5	35.5	12.5	37.3	0

Average weather data including precipitation. Credit: Western Regional Climate Center, wrcc@dri.edu

4.4 Potential Outputs and Products

4.4.1 Geothermal Resource Potential

The geothermal resource in Surprise Valley is known to be present in most of the valley. There are numerous surface flows of hot water to the north and south of the project site. Existing wells validate a geothermal resource at depth.

For the purposes of this study, the focus is on the amount of the resource that is technically and economically available for use. If one assumes a well separation distance of 0.8 to 1.0 mile, it would be possible to locate up to 8-12 wells on the site. Well location is determined based on the geology of the area rather than the surface separation distance; yet, most geothermal sites tend to separate wells by distances of a half to a full mile or more. Therefore, this nominal distance is used here as a starting point for estimating the amount of resource one could reasonably produce. Using the surface separation distance, it is reasonable to locate four production wells with suitable injection wells on the property. If each production well produced 2,500 GPM, a production yield of 10,000 GPM could be reached at the projected temperature of 285 ˚F. Table 10 summarizes the overall thermal energy available from a deep resource assuming flow rates up to 10,000 GPM.

Additionally, there are three hot springs on the property that have a combined flow of approximately 250 GPM. The thermal energy from these hot springs could be captured without any drilling by diverting the flow through a heat exchanger and then discharging the flow back into the existing outflow stream. A resource estimate of the thermal energy in the Mineral Springs is shown in Table 11.

Table 10: Deep geothermal resource value as compared to propane.

Flow Rate, gpm	$MW_{thermal}$	Annual Thermal Energy Available, Therms	Value of the Thermal Energy at the Existing Price of Propane in the Area
1,000	30.0	8,835,336	$8,941,892
2,000	60.1	17,670,672	$17,883,783
3,000	90.1	26,506,008	$26,825,675
4,000	120.1	35,341,344	$35,767,567
5,000	150.1	44,176,680	$44,709,459
6,000	180.2	53,012,016	$53,651,350
7,000	210.2	61,847,352	$62,593,242
8,000	240.2	70,682,688	$71,535,134
9,000	270.3	79,518,024	$80,477,026
10,000	300.3	88,353,360	$89,418,917

Table 11: Potential value of the hot spring.

Flow Rate (GPM)	$MW_{thermal}$	Annual Thermal Energy Available (Therms)	Value of the Thermal Energy at the Existing Price of Propane in the Area
250	4.3	1,271,426	$1,286,760

4.4.2 Geothermal Comparison to Fossil Fuels

Table 12 shows a list of parameters used to compute the thermal energy and the value of energy in Mineral Springs and in deeper resource. The amount of thermal energy was computed by finding the difference between the temperature of the spring or resource and an exit temperature of 80°F.

Table 12: Parameters for computing thermal energy value.

Deep Resource Production Temperature (˚F)	285
Hot Springs Flowing Temperature (˚F)	198
Injection temperature (˚F)	80
US Wholesale Propane Price / Gallon, Average Oct. 2013 to March 2017 ($)	0.92
Resulting Price per Therm of Energy ($)	1.01

The value of a gallon of propane is the average wholesale price of propane. It is clear that the price of propane has plummeted from a peak ($3.50) to an average price of just under a dollar a gallon in the winter of 2014 (Figure 56). The geothermal value is sensitive to both the temperature of the geothermal resource and the price of the propane. While it is not expected that the geothermal temperature will change over time, the price of propane is likely to change, perhaps significantly.

Figure 56 shows a weekly plot of wholesale propane prices from October 2013 to March 2017. The price of propane spiked more than three times its current price in 2006. Since the price of fossil fuel, in general, is at a relative low point, it is expected that the values shown here could increase by a factor of 2-3 in the near future. The value computation using propane provides an upper value estimate on this resource. Table 10 and Table 11 indicate that the value could exceed $89 million for the deeper resource and $1.2 million for the Mineral Springs resource. If the price of propane increases to its peak value, exceeding its value in 2014 ($3.50/Gallon), the value of the geothermal energy would likewise increase. It is noted that this value will fluctuate with the price of other forms of energy available in the market.

A rising cost of energy elevates the value of all energy resources. Since geothermal energy is not as portable as propane, natural gas or other fossil fuels it must be used on site or converted into an energy product that is transportable (electricity, for example). Although geothermal flow can be piped long distances, the piping adds a significant capital cost. The pipe can be insulated to minimize the energy loss; however, the insulation adds cost to the pipe, increasing the initial capital cost. The use and value of geothermal energy is very dependent on location. The closer the resource is to its intended use, the lower the development cost and the more the value of geothermal resource.

The value can be considered on a volume basis. A gallon of propane for example, has about 91,000 BTUs of energy whereas a gallon of geothermal flow (high temperature water) has only about 1,700 BTUs (assuming 285˚F source temperature and 80˚F rejection temperature).

Therefore, the energy density (energy per unit of volume of mass) of geothermal energy is small compared to equivalent amounts of fossil fuels.

Figure 56: Weekly wholesale price of propane.

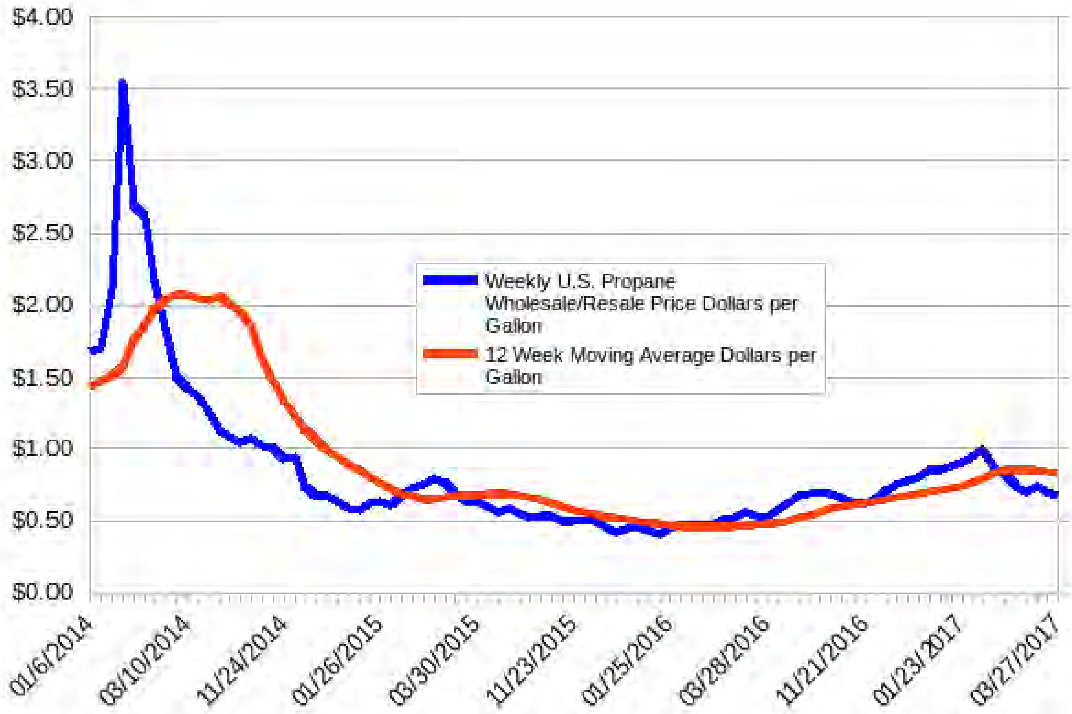

Source: US Energy Information Administration

4.4.3 Geothermal Compared to Other Fossil Fuel Power Plants

Although the energy content of a geothermal resource is immense and seemingly endless, the energy is not very transportable, and that restricts both the usefulness and ultimately the value. In short, the use of geothermal energy reaches a peak value when the businesses it supports are co-located with the resource and the supported businesses can use the geothermal energy at an efficiency on par with other forms of available energy.

For example, if one builds a thermal electric power plant at the resource location, the geothermal energy could replace the thermal energy from fossil fuels and cause the fuel bill to completely vanish. A fossil fuel electric power plant, however, operates at a much higher temperature than the geothermal resource and delivers a thermal efficiency that ranges from 30 to 45 percent, whereas geothermal power plants have a thermal efficiency of 8 to 15 percent. This means that consuming the same amount of input energy, the geothermal energy produces only one-third of the power than a fossil fuel plant does.

The power industry uses the term “heat rate” to express this difference. A heat rate for a 45 percent thermal efficient plant is 7,500 BTU/kWH, whereas a power plant at a thermal efficiency of 15 percent would have a heat rate of 22,500 BTU/kWH. The higher heat rate indicates three times the energy use for the geothermal plant compared to the 45 percent efficient power plant. The fossil fuel plant is also less expensive to build by about one-half to two-thirds compared to the cost of building a geothermal power plant. For these reasons, it is difficult for a geothermal power plant to economically compete with a fossil fuel thermal power plant, especially when fossil fuel is inexpensive.

4.4.5 Use of Geothermal for Direct Use Applications Compared to Fossil Fuels

If one considers using the geothermal energy for a direct heating application such as a greenhouse, aquaculture, manufacturing, or space heating, the value comparison to other forms of energy is very different than for electric energy. In direct use applications, the geothermal energy normally offsets a unit of heating energy for every unit that is used; in other words, if geothermal resource supplies 10 therms of heat for a greenhouse, then the fossil fuel or electric alternative would have to supply an equal amount, 10 therms. So, unlike the thermal electric power plant, the value of the geothermal energy is not diminished because its temperature and thermal efficiency are lower.

Co-locating is important for the direct heating applications because it lowers the installation cost (less connecting pipe). The most promising economic applications for geothermal energy are when the geothermal energy use is local and the application of this resource offsets a high cost form of energy on a one to one basis.

External factors that impact the value of geothermal energy include the price of other sources energy, including fossil fuel, solar energy, wind energy, and other forms of energy.

The WME geothermal resource at 89 million therms per year (Table 10) is a large resource and represents a large development opportunity. The challenge is to identify a niche opportunity where geothermal energy can easily replace other forms of thermal energy and thereby create a market advantage.

4.4.6 Electric Production Potential

To estimate the electric production potential, a single producer/injector pair of wells were assumed at a flow of 2,500 GPM at a temperature of 285˚F. Typical binary power plant technology is used to estimate the available electric power. Temperature of the tail-water coming from the geothermal power plant is assumed to be 140˚F. Typical numbers are used for pumping power, heat injection, and other parasitic losses. The amount of electric energy that can be produced is listed in Table 13 and

Table 14.

The single producer/injector pair of wells yields a production of 39,424 MWhs per year and a plant nominal size of 6.4 MWs. Nominal size and other parameters of the power plant are shown for a typical geothermal power plant (Table 13 and

Table 14). A single production /injection pair of wells is used as a first estimate because it is the minimum size that would first be developed. This basic unit could be increased in multiples of whatever flow rate and temperature is discovered during the well field development when more information is available.

One must complete at least one MWh pair of wells for a power plant (this is the smallest economic unit). If the full flow of 10,000 GPM at 285 ˚F is developed, a power plant of approximately 22 MWs is possible.

Table 13: Geothermal electric production parameters 1.

Rejection Temperature (˚F)	60
Maximum (Carnot) Efficiency	30.2 percent
Turbine Isentropic Efficiency	80.0 percent
Geothermal Brine Exit Temperature (˚F)	140.0
Gross Thermal Efficiency	121.1 percent
Net Thermal Efficiency (Parasitic Loads Included)	10.4 percent
Transmission Losses	1.0 percent
Annual MWhs Produced	39,424

Table 14: Geothermal electric production parameters 2.

Plant Net Output (kW)	Percent Online	Plant Nominal Size (kW)	Parasitic Load, Production Well Pump (kW)	Parasitic Load, Cooling Tower (kW)	Total Parasitic Load, CT and PW (kW)	Temp. (˚F)	Geothermal Flow (GPM)
5,530	95.0 percent	6,418	292	595	887.6	285	2,500

It is noted that the tail water is at 140˚F and at this temperature the thermal energy in the water could still be used for uses such as heating a greenhouse, aquaculture, building heating or spa facilities.

Flow from the Mineral Springs could also be used to make a small amount of power. If the full flow were diverted through a heat exchanger with an exit temperature of 120˚F, it is possible to produce approximately 50 to 100 kW of power using today's technology. This could be used to support a small business or use it on site; but is too small to export for sale in the electric market. The exit temperature could be lower for this plant than the larger plant because the Total Dissolved Solids (TDS) in the flow could precipitate out of the flow without fear of plugging up an injection well since the outflow would return to the existing surface stream.

Capturing the energy in this hot spring would be the cheapest way to develop an electric energy resource, although the net amount of energy would be small. It could be adequate to support several businesses. At the approximate rate of \$0.07/kWH (local rate) a 100-kW net plant would generate approximately \$56,000 worth of electric energy per year (806,000 kWH). A plant of this small size would be more expensive than a larger, higher temperature plant on a cost per kW basis. This amount of electric energy would allow a small development to be completely independent of the local grid.

The cost of a power plant using existing technology would be approximately \$0.8 million to \$1.0 million.

4.4.4 Agricultural Production Potential

The use of geothermal energy to provide heating for a greenhouse is common and many greenhouses that are heated with geothermal energy were developed because the geothermal energy keeps the heating costs low and makes the greenhouse operation economic. This is especially true in regions of the country where significant heating is needed to operate the greenhouse during the winter (e.g. Cedarville). There are several greenhouse operations in the Klamath Falls area that are heated by geothermal water and are nearby (within 90 miles) examples of how geothermal heat makes the greenhouse competitive with other producers.

The geothermal heating system does not need the high temperature required for agricultural production. Temperatures at 140 ˚F or higher are very suitable. Temperatures even as low as 90˚F can be used. For the greenhouse operation it has been assumed that the Mineral Springs at the site will be used instead of drilling wells. This significantly reduces the first cost as no well drilling is required. The hot spring water is intercepted at the spring and sent through a heat exchanger and then placed back into the existing outflow. Since the water is of good quality, no injection well or cleanup is required.

The total flow from the three active springs is estimated to be 250 GPM (150 for the largest spring and 50 GPM each for the two smaller springs). During testing of the larger hot spring in September 2017, the spring was partially covered to increase the temperature. The slight barrier the tarp provided between the air and spring surface eliminated most of the convective heat transfer and was adequate to get a measurable increase in the spring temperature from 190 ˚F to 202 ˚F.

To compute the peak heating required for a greenhouse, weather data of Cedarville (

Table 8 and Table 9) was used. The heating system is sized so as to maintain the temperature in the greenhouse at 72 ˚F. The greenhouse is modeled as Nexus Vail type (Figure 57). It has 14-foot sidewalls, a pitch roof to 24.5 feet, a grow area of 2.5 acres and a processing warehouse area of 0.6 acres. The greenhouse used in the estimate is manufactured in standard units of 42' x 300' and assembled on site under one contiguous roof (common gutters), with a single perimeter wall. The model used here has 9 42'x300' units. The warehouse unit is slightly larger at 42'x324'. The metal-framed greenhouse is covered with Solar Soft 8 mm polycarbonate panels while the warehouse is covered with metal panels with insulation. The R value for the Solar Soft 8 mm Polycarbonate is 1.72 (Hr. Ft^2. ˚F)/BTU.

The heating design temperature was selected from the weather data (

Table 8). On average, there are 38 days the low temperature for the day reaches 20˚F or lower each year but only 9 days the average temperature for the day is 20˚F or below. For Only 0.7 days does the minimum temperature reach -10˚F and there are no days when the average daily temperature is -10˚F or below. The heating system has to be able to maintain the worst condition; therefore -10˚F was selected as the design point of the heating system.

Using the greenhouse as stated above with the Cedarville weather and heating, the greenhouse at 72˚F requires approximately 8.4 million BTUs per hour at peak conditions and about 14,844 million BTUs annually. It is noted that most commercial greenhouses will have a similar thermal performance and 8.4 million BTUs per hour peak for a 2.5-acre greenhouse could be used as a planning figure for most commercial greenhouses. The solar soft skin thermal performance is very close to the 6-mm polyethylene double layer skin often used for the skin cover.

Figure 57: Nexus Vail-style greenhouse.

The greenhouse could be heated with either water from the existing three hot springs or water from new wells to be drilled on the site. Since the greenhouse does not require high temperature water that the electric production requires, the water from the springs is considered in the economic analysis.

If, on the other hand, deeper wells were drilled, the greenhouse could use the tail water from electric production or from the springs.

The amount of acreage that could be heated with either resource (new well or springs) is given in the

Table 15 and Table 16. A well at 2,500 GPM and 285˚F could support 70 acres of greenhouse. This large size of the greenhouse would exceed the market in the region. This demonstrates the point that there is a significant amount of thermal energy to provide heating to greenhouse operations.

The Mineral Springs can provide adequate flow for the size of greenhouse considered in this report (3.1 acres including the warehouse).

The tail water from the greenhouse is still adequately hot to support aquaculture, facility heating, or spa facilities. Cascading will be considered later.

Table 15: New well greenhouse heating potential.

Pumped Flow (GPM)	2,500
Pumped Temperature (˚F)	285
Assumed Tail Water Temperature (˚F)	110
Max. Peak Heating Available from Flow (MMBTU/Hr)	218.7
Max. Peak Heating Available from Flow (MW_1)	64.1
# of Acres Possible to Develop	70.9

Table 16: Mineral Springs greenhouse heating potential.

Pumped Flow (GPM)	250
Pumped Temperature (°F)	198
Assumed Tail Water Temperature (°F)	110
Max. Peak Heating Available from Flow (MMBTU/Hr)	11.0
Max. peak Heating Available from Flow (MW_1)	3.2
# of Acres Possible to Develop	3.6

4.4.5 Aquaculture Production Potential

Aquaculture is environmentally-controlled commercial farming and husbandry of freshwater and marine species for predominantly food and secondarily for hobby/ornamental purposes. Species include fin-fish, shrimp, craw-fish, clams, and tropical fish. Leading food aquaculture species include catfish, striped bass, trout, tilapia, and shrimp.

Aquaculture is a fast-growing agricultural sector, as commercial marine fisheries worldwide are showing depletion and consumer demands are adding significant fish and shrimp consumption to a predominantly beef, pork, and chicken diet of people located far from coastal areas. Catfish, shrimp, and tilapia are popular fish that are suitable to geothermal aquaculture. In areas with low winter temperature such as Cedarville, geothermal aquaculture is gaining importance as viable where agriculture endeavors with outdoor ponds are not possible for year-round fish production on a commercial basis. Aquaculture coupled with geothermal heat shows that several warm water species have important marketability and profitability.

To estimate the potential of geothermal energy to support a warm water fish operation, the same geothermal resource and weather information as used in the electricity and greenhouse production potential is used. As in the case of greenhouse operation, the hot spring water is sufficiently hot and plentiful to support a large warm water fish operation. A tank water temperature of 85 ˚F for the fish will be used and the tanks will be placed in a culture barn. The culture barn will provide some thermal protection but still needs to be heated as well as heating the aquaculture water. Although it may be suitable to use the water directly, it is assumed a plate and frame heat exchanger is used to add heat to the fish water. The fish water will be cleaned and recycled and it will need only make up water lost to evaporation or otherwise required (not a flow through operation).

In order to estimate the size of aquaculture that could be supported by the resource, a basic operation that uses two nursery tanks and nine grow out tanks are taken into consideration. The nursery tanks are 8'x16' and the grow tanks are 8'x32', with all tanks being 3-4 feet deep. The tanks are re-circulation tanks where the water is constantly cleaned, conditioned, and injected with oxygen to create the optimum environment for aquaculture. It is also assumed that the tanks are placed in a warehouse (metal prefab building). Dimensions of the warehouse is 50'x120'x15', allowing room for maneuvering in it and for potential expansion. Heating for the warehouse is included in the estimate. The size of the system is designed to provide the capability to raise approximately 100,000 pounds of fish a year. Table 17 shows the heating requirements for the base unit (fish pens only) of aquaculture with and without the warehouse. The warehouse is a good investment because it reduces the initial cost of the heating system and allows for a much larger fish operation. The warehouse also reduces the convective heat losses and the overall water use.

Table 17: Heating requirement - fish pans with and without warehouse.

	Heat Loss Outside Pens	Heat Loss Inside Warehouse Pens	percent of Original Energy Consumption Using Warehouse
Wind Velocity (MPH)	10	3	
Design Temperature (˚F)		65	
Convective Heat Loss (BTU/Hr.)	481,536	30,413	6.3 percent
Conductive Heat Loss (BTU/Hr.)	230,544	14,544	6.3 percent
Radiation Heat Loss (BTU/Hr.)	195,603	50,766	26.0 percent
Evaporative Heat Loss (BTU/Hr.)	681,054	205,524	30.2 percent
Building Overall Heat Loss (BTU/Hr.)		88,125	

Total Heat Loss (BTU/Hr.)	1,588,737	389,372	24.5 percent
Water Loss (lbs/Hr.)	648.62	195.74	
Water Loss (GPM)	1.30	0.39	
Altitude (Ft)	4,599	4,599	

The water evaporation from the pond reduces approximately 649 lbs/hr. (65.8 GPM) to ≈196 lbs/hr. (23.5 GPM) when the pens are inside a warehouse versus being outside. In addition to isolating and protecting the fish pens from potential predators, the warehouses provide protection from the weather and reduce the overall cost of operation.

The heating losses for the warehouse are computed and shown in Table 18. Heating requirements both with and without insulation are shown. The heating losses for the fish pens and warehouses are combined in Table 19. The GPM flow shown in Table 19 is that required to maintain the temperature of the warehouse and the fish water.

Table 18: Peak heating losses - fish warehouse.

Area	Peak Heat Load with Insulation (BTU/Hr.)	Peak Heat Load without Insulation (BTU/Hr.)
Roof Area	33,843	590,592
Walls	16,042	261,243
Leakage	29,203	43,805
Total Requirement	79,089	895,640

Table 19: Peak heating losses - fish pens and warehouse.

	Fish Pens	Warehouse	Total
Peak Heating Losses (BTU/Hr)	389,372	79,089	468,461
Resultant Water Flow (GPM)	39.0	7.9	46.9

Table 20 shows that approximately 2.85 million pounds of fish could be supported with the use of the geothermal energy in the Mineral Springs. If only tail water at 110˚F from the Mineral Springs was available, an aquaculture operation of approximately 524,000 pounds. could be supported. If the larger resource were used to support aquaculture, an operation of over 50 million pounds. of fish could be supported. Obviously, there is more than adequate geothermal to support aquaculture and the limitation for how large an operation will be more market limited than resource limited, similar to the conclusion for the greenhouse operations.

4.4.6 District Heating Potential

Use of the resource for district heating has already been implemented at the site. The existing resort heating system is a mixture of fin tube, coil heat exchange and direct use (use in spa). The resource used is likely connected in some way underground to the deeper resource and to the Mineral Springs. The direct heating use system taps into the resource with two wells located at the resort (Figure 58).

Table 20: Maximum size fish operations.

	Units (Two Nursery Pens, Nine Grow-out Pens)	Pounds of fish annually
# of units (Two nursery, nine grow-out pens) potentially heated with full spring flow (250 GPM) and temperature (197 °F)	29	2,853,952
# of units potentially heated with tail water at 110 °F and full spring flow (250 GPM)	5	533,449
# of units potentially heated with full deep flow at 285 °F and 2500 GPM	520	52,011,278

The two shallow wells tap into a self-flowing system that geysers boiling water out of the well and is diverted by the well cap (Figure 59) into the surrounding tank. The boiling water is temporarily held in a large open circular masonry tank and flows out to a series of cooling ponds by gravity head. During the time the boiling water is in the tank, it heats the water that is circulated in pipes.

Figure 58: Surprise Valley Hot Springs resort facilities.

These pipes are not visible in Figure 59, but they are looped around the tank perimeter near the bottom of the tank. Non-geothermal water is circulated inside the pipes and the hot geothermal water on the outside of the pipes heats the non-geothermal water, which is used for building heating and other purposes. A portion of the geothermal water is directly tapped for use in individual spas attached to each guest room.

Excluding the uses already in process at the site, the Mineral Springs and a deeper source as previously discussed could be used for building heating. In this climate a nominal value of 15 to 20 BTU/(SF-Hr) for peak heating is reasonable for determining the size of facility the geothermal resource could heat.

Figure 59: Artesian geothermal well at Surprise Valley Hot Springs resort.

The resource, if devoted to direct heating, could provide heating for 47 million square feet of conditioned space or in terms of homes, approximately 19,000, with an average of 2,500 square feet each. If tail-water from a power plant were used at 140 °F approximately 4,500 homes could be heated.

The advantage of using geothermal energy would be to offset the use of other means of heating (fossil fuel and electric) (

Table 21). When the price of fossil fuel starts to increase, it becomes a big advantage and requires pursuing the businesses that would want to locate in Surprise Valley.

Although there is not a large commercial laundry business in Modoc County, if the hospital continues its expansion, a laundry business could be a near term possibility.

Table 21: Potential district heating square footage.

Resource	Flow Rate (GPM)	Source Temp. (°F)	Return Temp. (°F)	Thermal Energy Available (Therms/Year)	Square Feet of Facility Possible to Heat (ft^2)	# of Homes that the Geothermal Resource Could Heat at 2,500 SF per Home

Deep Resource	10,000	285	95	83,186,712	47,481,000	18,992
Deep Resource	10,000	140	95	19,702,116	11,245,500	4,498
Hot Spring	250	197	95	1,116,453	637,245	255

CHAPTER 5:

Market Feasibility

5.1 General

Market feasibility is evaluated by first determining the cost of each development opportunity (such as electric generation, greenhouse and aquaculture operations). Determining the development cost provides a start for determining the profitability of the opportunity (Bartok, 2012). There are obviously many different ways to develop the resource; the mission here is not to consider every development contingency but rather to identify reasonable costs for each development. Each opportunity can then be modified as desired to evaluate the merits of development. Given the cost of each opportunity, one can assess the economic merits of pursuing the development, for example, whether the market provides sufficient income or not to merit development. Lastly, the market comparison is followed by a discussion of the most sensitive variables, both for the development and the market.

5.2 Production Tax Incentives

Taxes are an important consideration because they can have a detrimental impact on the profits of a business venture, although taxes may provide some local benefits to the community. The 2018 tax rules were used to compute taxes in this study. Because this impact is so significant, and tax rules are subject to change, tax implications should always be considered in any business venture with property tax rates This study does not take into consideration any tax credits because currently none exist for the development opportunities discussed in this chapter.

5.3 Electric Power Developing Opportunities

5.3.1 Cost of Developing Electric Power and Type of Power Plant

The base plant considered is a binary Organic Rankine Cycle (ORC) 5.5 MW net plant with a nameplate capacity of 6.4 MW. This plant uses standard binary equipment, an evaporator (or boiler), a refrigerant pump, a wet cooling tower, a turbine and water pumps.

Binary power plants are available from several manufacturers. The capital cost per MW is $4.0 million which is in line with average cost data as published by the California Energy Commission in 2014 (CEC, 2014). The capital cost includes well field development. This base plant is assumed to use a single pair of producer/injector wells and is typically the smallest power plant that could be economically viable. The estimated cost of developing electric power at the WME site is listed in (Table 22).

Output from the 5.5 MW net plant was simulated using local weather conditions in Cedarville region for a typical year and is listed in Table 23. The table takes into account the local weather and assumes a 95 percent availability rate. Note the output from the plant decreases during the hottest months.

Table 22: Cost estimate - traditional turbine expander.

Major Item	Cost ($)	Comments
Exploration cost – geologist effort including during drilling	105,750	Data analysis, testing, drilling oversight
Field development, well drilling and completion	1,879,820	Cost to drill two wells ≈ 3,000 feet deep or less
Well pump (1), 2,500 GPM, with 400 feet of casing, line shaft and fabricated well head	225,000	One production well including electric connection
Electric motor for pump (1) @ 400 HP each	55,177	Electric motor only
Flow testing, requires a test pump, generator, diesel fuel, instruments	170,507	Labor/fuel/equipment rental for a 20-day test @ 2,500 GPM, assumes test pumps will be used for production
Transmission/electrical (substation, transformers controls, see attachment)	429,000	This is cost of connection which includes the regulatory requirements, right of way, load study, etc.
Plant		
Site work	214,176	Grading, concrete, fencing, road improvement
Pipe system	1,100,000	Pipe connecting wells, 5000' 14-inch pipe, assumes one producer and one injector
Power cycle equipment	16,044,046	Estimate, site connected, skid mounted
Permitting, water rights	125,000	Construction permitting and water rights
Construction labor/site assembly	4,011,012	Four-month site assembly
Site engineering	175,509	8 percent of well pump, transmission, piping, site work, pipe system, electric motor, drilling
Project management	827,709	4 percent of all except power plant, 3 percent power plant
Environmental regulation	200,000	Project on privately owned property
Connection negotiation/contract with power purchaser	250,000	Includes transmission
Total Cost	$25,812,706	

Table 23: Power plant output.

Month	Average Dew Point Temp (˚F)	Plant Nominal Size (kW)	Plant Output (kWH)	Transmission Losses (kWH)	Net Power Online (kWH)	Percentage Change (percent)
Jan	23.4	4,911	3,471,354	34,714	3,436,641	7
Feb	24.2	4,896	3,125,723	31,257	3,094,465	6
Mar	25.3	4,876	3,446,258	34,463	3,411,795	6
Apr	27.2	4,841	3,311,045	33,110	3,277,935	6
May	33.5	4,722	3,337,238	33,372	3,303,866	2
Jun	37.4	4,648	3,178,981	31,790	3,147,191	1
Jul	39.5	4,608	3,257,188	32,572	3,224,616	0
Aug	37.3	4,650	3,286,351	32,864	3,253,487	1
Sep	33.6	4,720	3,228,152	32,282	3,195,871	2
Oct	31.0	4,770	3,371,084	33,711	3,337,374	3
Nov	25.8	4,865	3,327,970	33,280	3,294,691	6
Dec	22.7	4,925	3,481,171	34,812	3,446,359	7
Annual	Totals		39,822,515		39,434,290	

By combining the plant output and cost of operation, a break-even point can be computed for the cost at which power can be sold to make the plant profitable. It has been assumed that a 20-year loan would be procured at an interest rate of 5 percent. When the model is run using the loan term listed, it requires a Power Purchase Agreement (PPA) of $107/MWh to break even. This would mean an investor would make only 5 percent of the investment. A higher PPA would mean more profit or a higher interest rate. Currently, the only incentive for developing this power is a tax incentive, where the Federal accelerated depreciation allows a tax credit of approximately $981,000 a year for the first five years. On the 6th year the facility is fully depreciated at the federal level and the tax benefit of 981,000 is replaced with a tax bill of $1.03 million. This causes the net cash flow to decrease from $2.56 million to $772k in year 6. As a basis for comparison to other uses of geothermal energy, Table 24 lists the overall cost of building the plant, the expected revenue generated, and the simple payback. This listing does not consider depreciation, interest and taxes. The sale price of electricity at $62/MWh is the maximum price one could expect in the market. The current avoided cost schedule of PacifiCorp reflects a cost of $24/MWh, significantly less than the starting price listed in Table 24. Operating parameters of the plant are given in Table 25. It should be noted that the net thermal efficiency is 10.4 percent which is typical of geothermal power plants using source water at 250-300 ˚F.

Table 24: Economic summary - geothermal electric production.

First year electricity cost avoidance price ($/kWh)	$0.062
Quantity of electricity exported (kWh)	38,597,292
Electric revenue generated first year	$2,393,032
O&M annual cost including transmission	$424,076
Net electric revenue before interest, depreciation & tax	$1,968,956
Installed plant cost	$25,812,706
Simple payback years	13.1

Table 25: Geothermal electric production - operating parameters.

Rejection temperature (˚F)	60
Maximum (Carnot) efficiency	30.2 percent
Turbine isentropic efficiency	80.0 percent
Geothermal brine exit temperature (˚F)	140.0
Gross thermal efficiency	12.1 percent
Net thermal efficiency (parasitic loads included)	10.4 percent
Transmission losses	1.0 percent
Annual MWhs produced	38,597

Geothermal plant operating parameters, efficiency, transmission losses, annual MWhs.

The low thermal efficiency puts geothermal power plants at a disadvantage compared to fossil fuel plants with much higher efficiencies (30-45 percent).

Table 26 lists the geothermal flow and plant net output factors including the loads of the pumping and cooling tower.

Table 26: Geothermal electric production - input/output parameters.

Plant Net Output (kW)	Percent online	Plant Nominal Size (kW)	Parasitic Load, Production Well Pump (kW)	Parasitic Load, Cooling Tower	Parasitic Load, CT and PW (kW)	Temp (˚F)	Geothermal Flow (GPM)
5,530	95.0 percent	6,418	292	595	887.6	285	2,500

5.3.2 Market Assessment of Electric Power

The electric market for renewable energy was evaluated in the 2017 Padilla Report "Cost and Savings for the California Renewable Portfolio Standard in 2016" (CEC, 2016). The report finds that California utilities are meeting their Renewables Portfolio Standard (RPS) while saving money based on the Market Price Referent (MPR) for electric energy (MPR of $105/MWh in 2016). The MPR is the life cycle cost of generating electric power by using a combined cycle gas turbine fueled with natural gas. The price of procuring renewable energy decreased from an average price of $94/MWh to $62/MWh from 2003 to 2016. Since power contracts are typically long-term deals up to 25 years, the high cost of acquiring power during earlier years has caused the average procurement price of renewable electric energy to remain relatively high, even though the current contracts are averaging $62/MWh. The current market for new renewable power is going down in price.

Table 27 is extracted from the Padilla Report (CEC, 2016) and reflects this downward trend. The Padilla Report is an analysis of the prices being paid for renewable electricity and clearly shows the downward price for renewable electricity. Note that only one contract for geothermal electricity was procured by California utilities in 2016. There are several reasons for the cost of power being less expensive. Utilities have been able to meet their RPS requirements and the cost of solar and wind energy is decreasing due to more acceptance and widespread development in the market.

Another indication of the cost of electricity is the existing short-term California "Independent System Operator" (CAISO) pricing. The existing next day price for electric power is $28 to $32 as shown in Table 28. It is noted that the day ahead pricing is less than the prices reported in the Padilla Report.

Table 27: Padilla Report - California renewable savings.

	PG&E	SCE	SDG&E	Total
Biogas				
+3-20 MW		Only 1 Contract		Only 1 Contract
Biogas Total		**Only 1 Contract**		**Only 1 Contract**
Biomass				
+3-20 MW		Only 1 Contract		Only 1 Contract
+20-50 MW		Only 2 Contracts	Only 1 Contract	0.1205
Biomass Total		**0.1202**	**Only 1 Contract**	**0.1198**
Geothermal				
+20-50 MW		Only 1 Contract		Only 1 Contract
Geothermal Total		**Only 1 Contract**		**Only 1 Contract**
Solar PV				
+3-20 MW	0.0593	0.0708		0.0692
+50-200 MW		0.0545		0.0545
Solar PV Total	**0.0593**	**0.0601**		**0.0600**
Solar Thermal				
+20-50 MW		0.0644		0.0644
Solar Thermal Total		**0.0644**		**0.0644**
Wind				
+50-200 MW		0.0523		0.0523
+200 MW				
Wind Total		**0.0517**		**0.0517**
Average of All Contracts	**0.0593**	**0.0610**	**Only 1 Contract**	**0.0620**

Source: Padilla Report, Cost and Savings for the California Renewable Portfolio Standard in 2016 (CEC, 2016).

Table 28: CAISO pricing electric power.

Investor Owned Utility	Day Ahead Market Price (Cents/kWh)
PG&E	2.98
SCE	2.79
SDG&E	3.18

Source: CAISO next day pricing for electric power in California.

Table 29 in Section 5.4.1 Cost of a Greenhouse shows the average cost of securing wind and solar energy is in the range of $0.05 to 0.07/kWh. A utility, under regulated rules, would be hard pressed to justify paying more for geothermal energy when solar and wind energies are cheaper and can be used to satisfy the RPS.

5.3.3 Discussion

The current average price for renewable electricity is lower than the cost of developing geothermal power by a significant margin. The analysis shows a life cycle cost for geothermal electricity is approximately $107/MWh whereas the market for renewable electricity is currently at about $62/MWh. The most expensive item in geothermal development is not the drilling, but the power plant. The drilling, however, is the riskiest part of the investment and although not the most expensive, it is still expensive. The area with the most opportunity for cost improvement is the actual power plant construction. If the power plant cost could be reduced by 25 percent (approximately 4 million dollars), the life cycle cost would be reduced to $90/MWh. This still exceeds the existing market price for electricity. Pursuing a traditional PPA does not appear to be the best economic use of a geothermal resource.

Another potential avenue to make the power plant economically feasible is to seek out a unique or niche market opportunity to get a higher price for electric energy. For example, a large private company or university. Over time, as the price of fossil fuel increases, the electric price in the market will also increase. Therefore, it may be possible to negotiate a higher rate that is currently fixed to a potential buyer who is betting on the price increasing significantly in the future. Some large purchasers of electricity (major manufacturers, large computer companies) are looking at negotiating directly with independent service providers of electric energy. This is especially true for companies who value a green image. These contracts are similar to a traditional PPA, except the consumer of the electricity is replacing the role of the power company as purchaser of the electricity. The power companies as well as transmission companies will still be involved in the transaction as they own and operate most of the connecting infrastructure that would transport the power from the point of entry to the grid to the point where it is used.

California is one of the states that allow what is called a virtual PPA. A virtual PPA is essentially where the energy contracted in the PPA is not necessarily used at the site of the purchaser. In other words, the purchaser might continue to use power supplied by the local utility and the local utility has a compensating agreement that addresses where the power is actually used. This agreement can involve multiple entities and it is obviously more complex than the arrangement where the purchaser directly uses the power produced by the seller (plant operator/owner). The objective is to open the markets as much as possible.

A simple version of a deal with an independent purchaser would be to convince a business, for example, a call center, to locate in Cedarville near the project site. The power plant could be located so that it directly serves the call center. This would be a more typical PPA. A virtual PPA would be to convince the business owners to purchase electricity but be located somewhere not in the immediate area (even far away). The virtual PPA would require negotiating exchanges of energy with other users of the transmission system between the purchaser's location and Surprise Valley so that everyone is made whole. This might be a couple users or many users. Obviously the virtual PPA does open up other ways to get the electricity to market but a virtual PPA can get very complicated.

Although the virtual PPA opens up other opportunities, the economics of developing geothermal electric power are not encouraging in the existing market.

5.3.4 Path to Market

The electric service provider to the local community is the Surprise Valley Electrification Corporation (SVEC). Any power transmitted from a development at the site would most likely be transmitted through SVEC to PacifiCorp (the balancing authority) or the Bonneville Power Administration (BPA), to which SVEC is also connected. SVEC is an electric service cooperative and a direct service customer of the BPA. Although SVEC is organized as a California organization, it is not connected to CAISO; whereas BPA and PacifiCorp have connections to CAISO. While it is possible to connect to distant markets electrically, it would involve several connections. This generally is not done; and when it is done, it is normally for a PPA in the 10s of MWs in size.

It is possible that any client connected to SVEC, PacifiCorp, or BPA could potentially arrange for a purchase of electricity generated; however, this type of deal is not normal and would require extensive negotiation and likely need to be of a size at least in the tens of MWs. It would also require agreements of transmission with whatever utilities are impacted by the transfer. This could potentially be attractive to a major client who wants to purchase green electricity and is willing to put in the effort to negotiate a deal for the energy purchase and transmission rights to get the power from the site to a mutually agreeable delivery point. The delivery point might not be at the physical location of purchaser of the energy, but some other location where a swap has been negotiated with another client. This process can be very involved; yet it is mentioned because some large clients (Google, Microsoft, for example) are negotiating separate deals with independent electric producers for their power.

The potential to get electric power to a wider market is very limited and will necessarily involve the local utility and PacifiCorp.

5.4 Agriculture Operation Opportunities

Geothermal energy has long been used to heat greenhouses. There are many existing businesses that are made more competitive through the use of geothermal heat to offset the otherwise high cost of heating. The geothermal energy allows for continuous operation of the greenhouse with a very small cost of heating once the geothermal resource and heating system have been installed. Considering the current low cost of electricity in the area, buying from the local provider is more economical.

5.4.1 Cost of a Greenhouse

To estimate the cost of a commercial greenhouse, it has been assumed that it will be a metal-framed greenhouse with polycarbonate 8-mm twin wall covering. The greenhouse complex is comprised of 9 units (42 ft x 300 ft) built together with an open interior, connected gutters, and a single exterior wall covered with the 8-mm twin wall polycarbonate. The walls are 14 feet high at the eave and 24 feet at the apex of the roof. The greenhouse has a grow area of 2.5 acres with 18 separate grow lines. The grow lines are elevated to about one meter and approximately 1/3 of the greenhouse is illuminated with high pressure sodium (HPS) lighting to provide the plants with approximately 15 micro-mole of light per day during periods of limited sunlight. The greenhouse is heated with a combination of pex pipe floor heat and fin tube heating system mounted along the walls in the greenhouse, above the plants. The heating water for the pex and fin tubes is heated with a plate and frame heat exchanger that separates the geothermal water from the heating water inside the greenhouse. The grow system selected for the base greenhouse is an automated hydroponic system using the Nutrient Film Technique (NFT). The NFT system is basically a plumbing system where the nutrient solution is mixed, checked, distributed to the plants (flows by the plant roots suspended in rock wool or peat moss), returned, recycled with nutrients being adjusted as required and sent back to the plants. The plants are raised in a plastic container (a trough) about 3 ft. x 3 ft. x 19 in. The plastic trough is lined with peat moss or rock wool and seeded prior to being placed in the germination area. The trough handling, seeding process and placement in the germination area is automated by a system specifically designed to automate and perfect these tasks. The automated system improves the output and reduces the amount of manpower required to operate the greenhouse. The automation essentially eliminates the repetitive tasks and gives a degree of precision in performing these tasks hard to replicate with hired labor. The fully automated greenhouse allows the greenhouse grower to accurately administer the nutrient solution and optimize greenhouse production. It is noted that this greenhouse has the capability of producing a quality product that once "dialed in" can be produced without fail over and over. The greenhouse is expensive as compared to a traditional more labor-intensive greenhouse. Table 29 captures in a summary form the major category capital expense for the greenhouse.

The "Project Management" line item includes the cost of the professionals that will manage the process of building the greenhouse, starting the business and securing the market (the intent is to hire a team that builds and starts the business, both making the facility operational and securing the market). The "Hires and Fixed Cost" line item assumes that greenhouse operational personnel will be brought online about halfway through construction and these personnel would operate the greenhouse long term. At $67 per square foot, this greenhouse is about twice the traditional cost of a greenhouse. The two primary sources of the increased cost are the automation system and the hydroponic grow system. In Table 29 this is captured as the automated growing system for $3.26 million and the automated packaging (install and equipment) for $0.685 million which is more than half the $7.32 million of the greenhouse grow facility cost.

Table 29: Fully automated greenhouse - major cost categories.

Area of Budget	Budgeted Amount ($)	percent Cap X
Project management	454,542	4.29
Hires & fixed costs	197,875	1.87
Total labor/admin/overhead	852,417	6.15
Site & infrastructure	1,329,170	12.54
Greenhouse & warehouse buildings turnkey including freight	1,826,754	17.23
Installation labor	409,248	3.86
Automated growing system	3,255,154	30.70
Lighting system	461,295	4.35
Automation installation labor	168,320	1.59
Automated packaging system	517,000	4.88
System controls & software	80,648	0.76
Warehouse internal build	601,613	5.67
Total grow facility construction units	7,320,032	69.05
Subtotal without working capital	9,301,619	87.74

Working capital	1,300,000	12.26
Total capital expenditure	10,601,619	100.00
Cost per square foot	67.61	

The automated hydroponic greenhouse is capable of producing approximately 1.26 million pounds of leafy greens per year. This level of production is possible because of the automation equipment, the hydroponic feeding system for the plants, the ability to create the best environment for the plants to grow, and a crew of personnel that maintain and optimize the system (Kaiser and Ernst, 2012). The small amount of waste generated is packaged and sold as a garden supplement. Table 30 is a summary of the Revenue, O&M cost, and projected net profit before depreciation and taxes. This opportunity produces a 3.5-year simple payback and is very attractive from a rate of return perspective.

The wholesale sell price used here for leafy greens is approximately 35 percent of the price they fetch in the best retail markets (COOP, 2017). A typical box of leafy greens sells for about $3.99 per 4.5 oz. box or $14/lb. Although the greenhouse price seems very high, part of the value of the automated greenhouse is the complete packaging of the product in a ready to sell container which makes the product more valuable to the grocer or retailer. Less automated greenhouses normally sell product in bulk and this forfeits some of the value to either the grocer or a middle entity that provides the packaging. There are two-line items in the capital cost (Table 29) that address the automated packaging totaling about $685,000.

Table 30: Major cost categories - greenhouse.

First year amount (lbs) of leafy greens produced (5 percent waste included)	1,256,270.52
Value of leafy greens (wholesale $/lb)	5.07
Greenhouse revenue generated first year ($)	6,370,305
O&M annual cost including plants, production and personnel ($)	3,381,209
Net greenhouse profit before interest, depreciation & taxes	2,989,096
Greenhouse installed cost ($)	10,601,619
Simple payback years	3.5

5.4.2 Market Assessment of a Greenhouse

Unlike the electric market, the agriculture market does not provide a single entity that purchases all of the product and the agriculture market is nimbler than the power market. Much of the value added to an agriculture product is done after it leaves the farm (Pena, 2005). The more this processing can be done "at the farm" the more valuable the product. Leafy greens have been used in the analysis because they currently sell for a high price in the market and make an agriculture business much more possible. In order to estimate the market size, two separate sources of data were used: 1) population of major metropolitan areas as collected by the US Census Bureau, and 2) the rate of salad consumption per capita as published by the Produce for Better Health Foundation. The consumption rate is 69 salads per year per individual at a wholesale cost of $1/salad. The Better Health Foundation study also finds that there is an increase in the use of pre-packaged salads like the one used in this greenhouse analysis. Consumers want a product that is nutritious yet simple and quick to prepare. Data for the market of packaged leafy greens is shown in Table 31 with the distance to each market from WME.

The size of the total market within a given radius of the project site is shown in Table 32.

Salad market size within radius of project site, computed using the Better Health Foundation (BHS, 2015) of 69 salads per year per individual and a wholesale $1/salad.

While the market size within a 200-mile radius exceeds the ability of the greenhouse to produce product, $14.6 versus $6.4 million in product, this would be a larger percent of the market (43.7 percent) and one would not expect to command that much of the market. As the radius served extends to 500 miles the greenhouse production falls from 43.6 to 1.8 percent of the market share (Table 33). In short, most of the salads will need to be transported by refrigerated truck to distant markets. Buyers of the product will supply transportation.

Percent computed by using estimated WME production of salads divided by the market size within the radius listed.

Table 31: Leafy green market data by nearby metropolitan areas.

Market, Metropolitan Area	Road Miles from WME to Market (miles)	Driving Time at 50 mph Average Speed (hours)	Metropolitan Area Population, US Census Data	Potential Market Size, Wholesale Dollars ($/salad and 69 salads per year)
Redding – Red Bluff, CA	170	3.4	63,463	1,373,658
Reno-Carson City-Fernley, NV	199	4.0	613,608	13,281,558
Medford, OR metropolitan area	200	4.0	208,545	4,513,961
Bend, OR metropolitan area	245	4.9	165,954	3,592,078
Eugene, OR metropolitan area	299	6.0	160,561	3,475,346
Sacramento-Roseville, CA	330	6.6	2,567,451	55,572,532
Coos Bay and Roseburg, OR	359	7.2	63,761	1,380,108
The Dalles, OR	373	7.5	25,213	545,736
Hood River, OR	386	7.7	22,346	483,680

Boise-Nampa-M. Home-Ontario, ID	395	7.9	697,535	15,098,160
Portland-Salem, OR, Vancouver, WA	406	8.1	2,921,408	63,233,939
San Jose-San Francisco-Oakland, CA	416	8.3	8,751,807	189,433,052
Kennewick-Pasco-Richland, WA	469	9.4	253,340	5,483,550
Ellensburg, WA	497	9.9	41,672	901,991
Moses Lake-Othello, WA	543	10.9	107,848	2,334,372
Seattle-Tacoma-Olympia-WA	570	11.4	4,199,312	90,894,199

Source: Data from Census Bureau and Produce for Better Nutrition Foundation.

Table 32: Salad market within given radius of WME location.

Market Radius	Metropolitan Area Population, US Census Data	Potential Market Size, Wholesale Dollars ($/salad and 69 salads per year)
Market value within 200 miles of WME location	677,071	14,655,216
Market value within 300 miles of WME location	1,212,131	26,236,602
Market value within 400 miles of WME location	4,588,437	99,316,818
Market value within 500 miles of WME location	16,556,664	358,369,351

Table 33: Salad production as a percent of market sale.

Radius Surrounding Site	Salad Production as a Percent of Salad Market Size
200 miles	43.70 percent
300 miles	24.40 percent
400 miles	6.40 percent
500 miles	1.80 percent

5.4.3 Discussion

This greenhouse analysis suggests a greenhouse could be very profitable with a simple payback of 3.5 years. The greenhouse in the analysis is a hydroponic automated greenhouse with value adding packaging equipment, which give the greenhouse several advantages over traditional greenhouse operations. Hydroponics has proven to be much more efficient than traditional farming or farming plants planted in soil, even in a greenhouse. The primary reason for the hydroponic efficiency is that the plants are supplied with the nutrient mix that optimizes production. The second reason this greenhouse is more productive has to do with the automation system. The automation works throughout all stages of plant production, from planting to harvesting and packaging. The automation system performs repetitive tasks that can be easily done by machines. For example, planting the seeds can be done very precisely (depth and spacing), which cuts down on waste while increasing productivity. An extensive system of conveyor belts transports the trays in which the leafy greens are grown. The trays automatically move from washing, to seeding, to germination, to growing, to harvesting, to washing. This saves labor and essentially removes labor from the grow area. Labor is still required to operate the machines (keep them maintained and full of seed/fertilizer/etc.). An important aspect of the automation is that it frees up grow area and instead of a space utilization factor of 67 to 93 percent the fully automated system has a space utilization factor of 105 percent. This is because the grow line is elevated and a germination area is beneath the grow line. Table 34 lists the space utilization factor of traditional greenhouse grow arrangements.

Using a high utilization factor of 93 percent would give a 12 percent advantage to the automated system on space alone. The transportable benches also require more labor than the automated system and create downtime for grow operations during the move, whereas the fully automated system makes continuous use of the space.

In short, the advantage of the automated system not only reduces labor but also increases production by increasing the grow space, decreasing down time, improving the precision of the seeding, fertilizing, positioning, harvesting and packing of the product. Its main disadvantage is the cost.

The cost of the automated grow system is approximately $3.9 million (includes labor to install, the system and the packaging equipment). Assuming the system increases the grow space by 12 percent and improves production by 5 percent, it would indicate an overall increase in production of 17 percent without compounding. The labor cost of operating the automated plant is $1.14 million per year. Assuming additional low skilled labor would be required, e.g. increasing the greenhouse staff and processing employees from 8 to 16, the labor budget would increase by $420,000. The revenue would reduce from $6.3 to $5.2 million and the cost of labor would increase by $420,000. The impact on the overall economics is shown in Table 35. Although this is a significantly lower capital cost (about $4 million cheaper), the simple payback grows at a rate of about one year to 4.5 years.

Table 34: Space utilization percent for greenhouses.

Space Utilization for Various Benching Schemes	
Longitudinal benches	67 percent
Peninsula benches	74 percent
Movable longitudinal benches	82 percent
Movable peninsula benches	86 percent
Transportable benches	93 percent
Floor system	90-92 percent

Source: http:/ depts.washington.edu/propplnt/Chapters/Greenhouse_benches.htm

Table 35: WME summary economics - greenhouse without automation.

First year amount (lbs) of leafy greens produced (5 percent waste included)	1,042,705
Value of leafy greens (wholesale $/lb)	5.07
Greenhouse revenue generated first year ($)	5,287,353
O&M annual cost including plants, production and personnel ($)	3,801,209
Net greenhouse profit before interest, depreciation & taxes	1,486,144
Greenhouse installed cost ($)	6,661,145
Simple payback years	4.5

5.4.4 Path to Market

The path to market is by refrigerated trucks using Highway 299 to connect with Highway 395 and then move north or south to the appropriate market. The market within 500 miles is more than adequate to support a greenhouse of this size. This automated greenhouse is projected to produce about 2 percent of the market within 500 miles.

Since the marketing of perishable product is time - sensitive, this makes the marketing of produce require somewhat more effort than marketing electricity under a PPA agreement where both the market and the path are outside the concerns of the business. Although there is a clear path (roads) to many markets, maintaining the market relationships will require a sustained effort.

5.5 Aquaculture Operation Opportunities

Geothermal energy is especially useful in the raising of warm water fish. Although not native to the United States, tilapia is a popular species of fish to raise and is raised in many states of the United States. Since this project is in California, it will be necessary to get an exception to existing California law which prohibits the raising of tilapia in all but four southern counties. Tilapia is allowed in southern California, in counties located south of the Tehachapi mountain range that separates southern California from the Great Central Valley. There is one tilapia operation in Modoc County that raises tilapia and has been granted an exception to California law. The California Department of Fish and Wildlife (CDFW, 2012) acknowledges that exceptions are possible. Another option for a warm water fish is catfish, which requires about the same water temperature as tilapia. (Wurts, 2014). Note that it is unlawful to import any live catfish or bullheads (including adults, fingerlings, or eggs) into California due to the danger of introducing channel catfish virus (pers. comm. with Randy Lowell). This California law creates a competitive advantage for live catfish, e.g. they must be raised within the state, essentially eliminating out of state competition for live catfish.

5.5.1 Cost of an Aquaculture Operation

As a basis for cost estimating, the same base unit which was used to estimate the size of warm water fish operation is used here. The base unit includes 2 nursery tanks and 9 grow-out tanks. The nursery tanks are 8 ft x 16 ft and the grow-out tanks are 8 ft x 32 ft, with both tanks being 3-4 feet deep. The tanks are re-circulation tanks where the water is constantly cleaned, conditioned and injected with oxygen to create the optimum environment for aquaculture. It is also assumed that the tanks are placed in a warehouse (metal prefab building). Heating for the warehouse is included in the estimate. The base system is designed to provide the capability to raise approximately 100,000 pounds of fish a year. Table 36 and Table 37 list the cost for the base unit of aquaculture, including the warehouse and provide basic economic data. Table 38 provides an economic overview including the cost of fry, feed, electricity, labor and administrative costs. Table 38 lists also the equipment in summary form. Table 39 lists the equipment costs in more detail including site infrastructure costs. It is noted that the heating costs are listed as zero, which assumes the geothermal energy is harnessed to provide heating and hence no ongoing costs associated with a fuel cost for heating.

The incentive from the USDA REAP (Rural Energy for America Program)is 25 percent of the renewable energy costs or $500,000, whichever is smaller. Only the geothermal portion of the project applies(the heating system), which fixes the REAP incentive (a grant after the project is finished and in operation) of approximately $21,800. The renewable equipment is the heating system driven by the Mineral Springs.

The cost and revenue of the base warm water fish operation is estimated in Table 38.

At simple payback of 6.5 years to develop aquaculture is less attractive than a greenhouse but significantly more attractive than electric energy. It is also possible to start a warm water fish operation for significantly less first cost than either the automated greenhouse or electric energy production.

Table 36: Aquaculture - major cost categories.

Category		Unit	Unit Price	Quantity	Total ($)
Gross Revenue	Tilapia	lb.	$3.00	108,000	324,000
	Fry	each	0.14	85,000	11,499
	Feed	ton	983.90	84	82,648
	Electricity	kwh	0.07	90,000	6,300
	Heating (geothermal)	gal	0.00	3,000	-
	Labor	hr	25.00	3,000	75,000
	Maintenance				
	Miscellaneous				
	Chemicals				
Total Costs	**Variable**				200,447
Fixed Costs	General and administrative				16,603
Total FC					16,603
Total Costs					217,050
Net Returns					106,950
Investment (First Costs)	Metal prefab building (50’x120’x10’)				210,000
	Infrastructure preparation				43,400
	Recirculating equipment				
	Piping, pumps, HX to and from Hot Springs, heating equipment (qualifies for USDA REAP grant)				308,434
	Other support equipment				47,134
Total	**Investment**				696,163
	USDA grant renewable energy				21,799
Total Net Investment					674,364

Table 37: Aquaculture basic site infrastructure and equipment summary.

Item	Price ($)	Quantity	Total ($)
Site Infrastructure			
Clear site & road (21,650 SF, 10 days of equipment time)	1,000.00	10	10,000.00
Gravel	40.00	460	18,400.00
Electric service	15,000.00	1	15,000.00
Total Site Infrastructure			**43,000.00**
Recirculation Equipment:			
9 Growout systems	30,052	9	270,468
2 Nursery systems	18,983	2	37,966
Total System Cost			**308,434**
Support Equipment:			
Piping, pumps, HX to and from Hot Springs	38,000	1	38,000
Geothermal and emergency heating equip.	49,125	1	49,195
Water storage	922	3	2,767
Generator	14,758	1	14,758
Purge tanks	3,075	2	6,149
Agitators	492	8	3,936
Blowers	1,168	2	2,337
Booster pumps	307	1	307
Monitoring equipment	922	1	922
Feeding equipment	922	1	922
Water quality equipment	1,845	1	1,845
Fish handling equipment	1,230	1	1,230
Feed storage	3,075	1	3,075
Tank plywood	34	258	8,885
Total Support Equipment			**134,329**
Total Equipment Cost			**486,163**

Table 38: Aquaculture basic economic parameters.

First year lbs of fish	108,000
Value of fish (wholesale $/lb)	$3
Aquaculture revenue generated first year	$324,000
O&M cost fish	$217,050
Net aquaculture profit before interest, depreciation & taxes	$106,950
Aquaculture installed cost	$696,163
Simple payback years	6.5

Basic economic parameters including pounds of fish produced, annual revenue, O&M cost, net profit, and simple payback.

5.5.2 Market Assessment of Aquaculture

To estimate the market size a process similar to that for leafy greens is used. Two separate sources of data were used: 1) population of major metropolitan areas (Table 39) and, 2) the rate of fish consumption per capita as published by the USDA. The rate varies between 0.5 to 1.5 pounds per capita per year with tilapia being the more popular fish. Hence for this analysis tilapia is used to project economics.

Table 40 shows a significant market potential for tilapia within a 500-mile radius. The 100,000 pounds could easily be absorbed in the market with significant room for growth. Table 41 shows tilapia production as a percent of the market size within a given radius.

Fish, like agriculture products, have a perishable life and time is of the essence when getting them to market. The species of fish will have a large impact on price. There are several warm water species of fish that might be grown including channel catfish and tilapia. Tilapia would require an exemption from California law. The following table provides a snapshot of the overall economics before taxes, depreciation and interest.

5.5.3 Discussion

Table 42 and Table 43 list aquaculture cost by category of expense from two different sources. The point of the Table 41 and

Table 42 is to show that heating is not a major cost category for raising tilapia or catfish. Tilapia and catfish produce optimum growth when the water is 83-86˚F.

At the project site, a mixture of hot and cold water would be used to reach the optimum fish production temperature range. Geothermal resources at the project site provide a substantial cost savings advantage.

It is likely that these tables were from businesses somewhere in the southern US where heating is not required. The main advantage one gains from inexpensive heating is to be nearer markets without a significant transportation cost.

Table 39: Aquaculture market characteristics for tilapia.

Market Metropolitan Area	Road Miles from WME to Market (miles)	Driving Time at 50 mph Average Speed (hour)	Metropolitan Area Population, US Census Data	Potential Market Size, Wholesale Dollars (Tilapia $3/lb. and 1.50 lbs /person - year)
Redding – Red Bluff, CA	170	3.4	63,463	285,584
Reno-Carson City-Fernley, NV	199	4.0	613,608	2,761,236
Medford, OR metropolitan area	200	4.0	208,545	938,453
Bend, OR metropolitan area	245	4.9	165,954	746,793
Eugene, OR metropolitan area	299	6.0	160,561	722,525
Sacramento-Roseville, CA	330	6.6	2,567,451	11,553,530
Coos Bay and Roseburg, OR	359	7.2	63,761	286,925
The Dalles, OR	373	7.5	25,213	113,459
Hood River, OR	386	7.7	22,346	199,557
Boise-Nampa-M. Home-Ontario, ID	395	7.9	697,535	3,138,908
Portland-Salem, OR Vancouver, WA	406	8.1	2,921,408	13,146,336
San Jose-San Francisco-Oakland, CA	416	8.3	8,751,807	39,383,132
Kennewick-Pasco-Richland, WA	469	9.4	253,340	1,140,030

Ellensburg, WA	497	9.9	41,672	187,524
Moses Lake-Othello, WA	543	10.9	107,848	485,316
Seattle-Tacoma-Olympia-WA	570	11.4	4,199,312	18,896,904

Table 40: Tilapia market size estimate.

Market Radius	Metropolitan Area Population, US Census Data	Potential Market Size, Wholesale Dollars, Tilapia
Market value within 200 miles of WME location	677,071	3,046,620
Market value within 300 miles of WME location	1,212,131	5,454,590
Market value within 400 miles of WME location	4,588,437	20,647,967
Market value within 500 miles of WME location	16,556,664	74,504,988

Table 41: Tilapia production as a percent of the market size within a given radius.

Market	Percent of Tilapia Market Based on Production
Within 200 Miles	10.63 percent
Within 300 Miles	5.94 percent
Within 400 Miles	1.57 percent
Within 500 Miles	0.43 percent

Table 42: Variable operation costs for tilapia recirculating systems.

Direct Operating Expenses Category	AMI New System		AMI Old System		Lasorda System	
	percent of cost	$/lb. of tilapia	percent of cost	$/lb. of tilapia	percent of cost	$/lb. of tilapia
Feed	0.4	0.3	0.3	0.26	0.2	0.261
Electricity	0.1	0.08	0.2	0.2	0.2	0.168
Heating	0.0	0.01	0.0	0.015	0.0	0.033
Liquid Oxygen	0.0	0	0.0	0	0.0	0
Labor	0.1	0.05	0.1	0.05	0.2	0.169
Fry	0.1	0.11	0.1	0.1	0.1	0.096
Depreciation	0.2	0.15	0.2	0.15	0.2	0.182
Maintenance	0.1	0.05	0.1	0.05	0.1	0.094
Miscellaneous	0.1	0.05	0.1	0.05	0.1	0.1
Total cost per lb.		0.80		0.88		1.10

Table 43: Variable operating costs for tilapia and catfish systems.

Direct Operating Expenses Category	Catfish-1989		Tilapia-1991	
	percent of cost	$/lb.	percent of cost	$/lb.
Feed	32.30	0.307	20.58	0.261
Labor	7.90	0.075	13.33	0.169
Recirculation	3.10	0.030	0.00	0.000
Heating	15.00	0.143	2.60	0.033
Oxygen	2.70	0.026	0.00	0.000
Aeration	0.00		5.68	0.072
Pumping	0.00		5.44	0.069
RBC energy	0.00		2.34	0.017
Electric demand	0.00		0.79	0.010
New water	0.00		0.08	0.001
Fingerlings	6.80	0.065	7.57	0.096

Depreciation	9.30	0.088	24.35	0.182
Maintenance	7.90	0.075	7.41	0.094
Operating	2.00	0.019	1.18	0.015
Cost of borrowed capital	7.20	0.068	10.96	0.139
Cost of equity	5.70	0.054	8.68	0.110
Total Cost per lb.		0.950		1.270

5.5.4 Path to Market

The path to market for aquaculture is the same as for produce products. The mode of transport will either be refrigerated truck or a truck capable of hauling live fish.

5.6 Direct Heating Opportunities

Currently, there is no market for direct heating in the local area since the area is rural and not densely populated.

5.7 Conclusions

5.7.1 Comparative Table of Uses

The following table (Table 44), by listing the use and economic factors, compares the economic performance of the three options analyzed. Two new economic factors are listed. The first factor is the amount of gross profit per therm of geothermal energy used while the second factor is the gross profit generated per dollar of investment. These two factors are dimensional numbers that can be used to compare the opportunities where the impact of size has been eliminated.

The automated greenhouse operation provides the highest profit per dollar of capital cost at $0.27/dollar invested, followed by aquaculture at $0.15 and electric generation at $0.12. This simply means that the automated greenhouse creates more profit per dollar invested.

The column of gross profit per therm of energy used is a measure of the value created by each therm consumed. Clearly, the automated greenhouse creates the highest value per therm consumed. Electricity is at a disadvantage since a relatively fixed amount of geothermal energy is used for each unit of electricity produced, whereas the aquaculture and greenhouse do not need heat in the warmer periods of the year, yet fish and produce are produced. This tends to make electric generation look particularly unfavorable. It also shows that there are more productive uses of geothermal energy than producing electricity.

The amount of geothermal energy used is an important factor to consider and, in this category, electric production clearly uses the highest amount of geothermal energy. One way to look at this factor is that it takes a lot of geothermal energy to make a unit of electricity. This subject was discussed earlier in the electric generation section but under the notion of thermal efficiency. It is the low geothermal efficiency that causes the high use of geothermal energy. Fish and greenhouse operations do not require as much geothermal energy because there are many more inputs to both fish and agriculture operations; thermal energy is only one of the many inputs. The non-electric uses also are mainly wintertime use and have an efficiency about the same as other competitive forms of heating.

The automated hydroponic greenhouse is clearly the best economic performer, generating much more gross profit per unit of geothermal energy used and more gross profit per unit of capital cost.

5.7.2 Discussion

The three businesses listed all require a dedicated group of professionals to build, operate and maintain. Of the three businesses, electric generation is the easiest to operate from a management perspective. With geothermal energy being used to produce electricity, operating and maintaining the power plant is relatively straightforward. The market and path to market are also well defined. In other words, geothermal electric generation does not require adapting continuously to market conditions. The other two businesses require much more involvement in terms of management, equipment, and market. Greenhouse and aquaculture operations are by their very nature labor-intensive and require a lot of inputs as compared to geothermal electric energy generation. Both the greenhouse and the aquaculture business are food businesses and there is more certainty that these markets will continue to grow. Currently the electricity market is not creating demand for geothermal energy and secondly there are significant economic advantages to other forms of electric generation. Geothermal electric generation is less efficient than fossil fuel electric generation and currently the fossil fuel is cheap enough that its life cycle cost is lower than geothermal electric generation. The greenhouse and aquaculture also have the ability to change or adjust to the market (such as growing a different crop or raising a different fish), whereas an electric generation business has only one product and one market.

Of course, the optimum solution would be to cascade the geothermal fluid through the businesses (electric to greenhouse to aquaculture). This could be done in phases in a way that is mutually supportive.

5.7.3 Recommendations

According to the analyses in this report, the most economic application is to start an automated hydroponic greenhouse business, followed by aquaculture and then geothermal electric production. While many factors were considered, it may be beneficial to conduct a more detailed economic study to ensure all costs and revenues are accounted for in determining next steps for geothermal-related business development. Any of the businesses could be developed and they might be developed in a smaller or larger footprint than presented in this report.

Table 44: Comparative table of geothermal uses.

Business	Amount of geothermal energy used (therms)	End use product	End use product units	Produced amount	End use product value ($)	O&M cost ($)	Gross profit ($)	Capital cost ($)	Gross profit dollars per therm of geothermal energy used ($/therm)	Gross profit dollars per dollar of capital cost
Raising Tilapia	43,065	Fish	lbs	108,000	324,000	217,050	106,950	696,163	2.48	0.15
Automated Hydroponic Greenhouse	148,439	Salad mix	lbs	1,322,390	6,370,305	3,381,209	2,989,096	11,273,396	20,14	0.27
Electric Generation	15,871,149	Electricity	kWh	39,424,290	3,426,365	428,211	2,998,154	25,812,706	0.19	0.12

CHAPTER 6: Public Outreach Activities

A public outreach and communication plan were prepared to address the following goals as part of the project to:

- Keep the public and project stakeholders informed of the project activities and geothermal development progress at specific project sites and Modoc County in general.
- Help create a synergistic environment of community economic development supported by geothermal energy use and development.

The public outreach and communication plan strategies that have been developed to implement the plan included organizing special events, activities and other outreach efforts to engage and educate the public and project stakeholders and other interested parties such as local and state government officials and school administrators and students. Strategies included educational outreach, project updates, public gatherings and spontaneous activities. Spontaneous strategies can be in the form of events/activities such as meetings, magazine and newspaper articles, scientific presentations, conferences or other similar forms.

Throughout the project period, approximately ten outreach activities were conducted and approximately nine spontaneous activities occurred.

Public outreach activities were well attended, well received, and much interest from the public was expressed. Public outreach activities were very effective in educating the public on geothermal resources, geology, study results, and potential use of the resource.

Appendix C shows photographs and newspaper articles associated with some of the public outreach events.

CHAPTER 7: Conclusions

Project Goals

The goals of this project were to conduct geologic exploration with the long-term goal of marketing Modoc County's large-scale geothermal potential, to generate a market and economic feasibility report regarding resource potential, to demonstrate the feasibility of a distributed energy resource, and to bring awareness to the public on geothermal resources and development potential.

Contribution to California's Geothermal Energy – Planning, Research Impacts and Development

A project deliverable was to help work toward achieving California's RPS goals. These deliverables include geologic exploration activities and marketing and economic feasibility. When the project began in 2014, the RPS was 33 percent by 2020. With the signing of SB 350 in October 2015, the RPS is now 50 percent by 2030.

The results of geologic exploration further prove the geothermal resource potential on the eastern side of Surprise Valley. Market and economic feasibility studies provide detailed information on the viability of developing the resource given many scenarios and conditions.

The results of this project facilitated refined planning, documentation and processes for economic development using geothermal resources. There is more information on the geothermal resource, at depth, which shows steadily increasing and favorable temperature gradients and temperatures. Results provide preliminary feasibility on development costs and needs and feasibility and opportunities and options.

The economic and market feasibility analyses facilitate transition of the utilization of the geothermal resource to future phases and provides quantitative information for investors.

Research impacts include a contribution to the State's knowledge of geothermal resource potential. MT and seismic data collected, temperature gradient and geochemistry data all will help to better understand the source and flow of geothermal fluids. Prior to this project, knowledge of these data about the eastern side of Surprise Valley were not well known.

While currently not very economical for electrical generation, verification of the resource on the eastern side of the valley helps to support the potential need for transmission studies and development of transmission capabilities from Northern California to the southern part of the state, if and when the economics change. Stakeholder discussions have included utility companies and large geothermal developers with interest in the valley.

While the DER unit commissioning was not completed, the DER demonstration site facilities serve as a transferrable model and example for other communities to implement a distributed energy resource and/or direct use application. Design of the infrastructure temperature and flow parameters exceeded expectations by a factor of three. Results of this project include the design of the infrastructure, costs, resource requirements, services required, electric grid requirements, equipment requirements, and supplies needed given the use of hot fluids and freezing temperatures.

Non-Economic Benefits

Non-economic benefits resulting from the project involve community outreach successes, support of continued research, academic training, and expansion of regional geologic information.

Community outreach activities created a synergistic effect and provided a positive vision of opportunities for the community, which is essential for the County given the economic conditions of rural California. Throughout the project period, approximately ten outreach activities were conducted and approximately nine spontaneous activities occurred. Many newspaper articles were published throughout the project. Public outreach activities were well attended, well received and much interest from the public was expressed. Public outreach activities were very effective in educating the public on geothermal resources, geology, study results and potential use of the resource.

In working with the UCD on-going research of Surprise Valley geothermal resources, not only were there benefits to understanding the geothermal resource potential in the State of California but in understanding geothermal resources more generally in support of the global geothermal community. The Energy Commission has previously supported UCD research in Surprise Valley. In addition, this exploration contributes to knowledge of the Basin and Range province which contributes to projects not only in California but also in Nevada, Idaho and Utah.

Academic and hands-on training opportunities were provided over multiple field excursions for more than a dozen university students. Students were able to work alongside professionals involved in private industry. At least one result was employment for two of the UCD students in the geothermal field in private industry.

This project has been brought to the attention of the global geothermal community. Several inquiries have been fielded from interested developers with a track record of accomplishing geothermal development projects. Two abstracts have been submitted to the Annual Geothermal Resources Council meeting in 2018, a presentation was given to the American Geophysical Union and a paper published in Applied Geochemistry.

Benefits to the Local Community

The results of this study provided economic and market feasibility information on the types of projects that would be possible given the geographical location, market demand and resource characteristics using Modoc's geothermal resource. This can lead to job opportunities and economic development.

This project has helped to build community pride by bringing together various stakeholders showing progress toward economic development. This is evidenced by public gatherings, the responsiveness by local contractors in supplying services to the project, support and enthusiasm with the Modoc Board of Supervisors through meetings and site visits. In addition, there were discussions with various developers interested in a distributed energy project as well as long-term electric power development.

Cumulatively, this project has been successful in increasing economic development opportunities in Modoc County.

Payback and Cost Effectiveness

The foundation for long and short-term economic benefits of implementing this project has been laid in terms of planning for development of electric power resources and collection of detailed information for implementation of direct use projects.

Multiplier effects during implementation of this project includes goods and services supplied during the project, short-term employment for services and economic activity in the local community resulting from re-spending of wages. Examples of recipients of economic beneficiaries of this project included but are not limited to: Hardware stores, electrical contractors, building manufacturer, gravel supplier, hotels, restaurants, grocery store, gas stations, equipment rentals and equipment manufacturers.

Moving Forward

The project team has championed the efforts to move forward with geothermal development. The team is strong with diverse knowledge, skills and backgrounds that are essential for development. The team's backgrounds include but are not limited to: power plant development, geothermal science, State and Federal regulations, engineering design, construction, PPA development and negotiation, County administration relationships, economic incentive opportunities, investor relations, a wide network in global geothermal community, hands-on experience with all aspects of geothermal development.

Plans for the next phase of exploration include drilling a deep exploratory well at the drilling location showing the most favorable temperature gradient.

The team will work together to make strides toward commissioning the DER unit.

GLOSSARY

acoustic magnetotelluric	Geophysical procedure mapping underground geology
aeromagnetic	Measurement of earth's magnetic field using airborne instruments
air bleed valve	Mechanism to release air from the system
alluvial scarp	Small offset on ground surface where one side of a fault has moved
alluvium	A deposit of clay, silt, sand, and gravel left by flowing stream
alteration minerals	Natural processes that alter a mineral's composition
anisotropy	Rock whose engineering properties vary with direction
basement rocks	More resistant rock beneath younger layers of rock
breccia	Rock consisting of angular fragments cemented together
cation	Positive charged ion
convective heat loss	Transfer of heat from a body to moving molecules such as air or liquid
dextral slip	Right lateral fault in which the block moves to the right
distributed energy unit	Power unit for small scale electrical generation
ephemeral lake	Lake that is usually dry but fills briefly during and after precipitation
evaporites	A natural salt or mineral deposit left after evaporation of body of water
excitation current	Excites or energizes an electrical apparatus
geophone	Instrument used to record seismic waves
geothermometry	Used to estimate reservoir temperature
graben	Narrow block moved between two faults
heterogeneities	Quality of variation in rock properties
horsts	Elongated block bounded by parallel faults
inter-fingering horsts	Digital base slope sediments commonly grade to alluvial fills
isothermal	Involving or possessing a constant temperature
linear interpolation	Method of curve fitting using linear polynomials
lithology	Study of general physical characteristics of rocks
mafic dike	Sheet of rock that is formed in a fracture in a 45 - 52% SIO2
normal slip	Fault in which the block moves downward
peak load	The maximum of electrical power demand
petrographic	Chemical and physical features of rock
photo lineaments	Linear feature expressed by underlying geological structure
quarternary fault	Active fault which has evidenced at the surface and moved in the last 1.6 million years
R value	Measures how well certain building insulation materials can resist heat
rectifiers	Electrical device that converts AC to DC
refraction analysis	Used to characterize subsurface geologic conditions
resistivity	Measure of resistance to electrical conduction
seismogram	A record produced by a seismograph
space utilization factor	Refers to how often a space is used, who uses it and why it is being used
splay	Surface making an oblique angle with another
spur	Lateral ridge of land descending from a hill

step overs	Structural features along strike slip faults
stratigraphy	The study of rock layers and layering.
surface outcrops	Often show at the surface
tectonic transition	Located between the lower mantle and the upper mantle of earth
tomographic	Imaging subsurface with seismic waves
transverse antithetic accommodation zone	Zones across which strata have opposite tilt direction
tuff	Light, porous rock formed by consolidation of volcanic ash
utilization factor	The utilization factor or use factor is the ratio of the time that a piece of equipment is in use to the total time that it could be in use.

acoustic magnetotelluric	Geophysical procedure mapping underground geology
aeromagnetic	Measurement of earth's magnetic field using airborne instruments
air bleed valve	Mechanism to release air from the system
alluvial scarp	Small offset on ground surface where one side of a fault has moved
alluvium	A deposit of clay, silt, sand, and gravel left by flowing stream
alteration minerals	Natural processes that alter a mineral's composition
anisotropy	Rock whose engineering properties vary with direction
basement rocks	More resistant rock beneath younger layers of rock
breccia	Rock consisting of angular fragments cemented together
cation	Positive charged ion
convective heat loss	Transfer of heat from a body to moving molecules such as air or liquid
dextral slip	Right lateral fault in which the block moves to the right
distributed energy unit	Power unit for small scale electrical generation
ephemeral lake	Lake that is usually dry but fills briefly during and after precipitation
evaporites	A natural salt or mineral deposit left after evaporation of body of water
excitation current	Excites or energizes an electrical apparatus
geophone	Instrument used to record seismic waves
geothermometry	Used to estimate reservoir temperature
graben	Narrow block moved between two faults
heterogeneities	Quality of variation in rock properties
horsts	Elongated block bounded by parallel faults
inter-fingering horsts	Digital base slope sediments commonly grade to alluvial fills
isothermal	Involving or possessing a constant temperature
linear interpolation	Method of curve fitting using linear polynomials
lithology	Study of general physical characteristics of rocks
mafic dike	Sheet of rock that is formed in a fracture in a 45 - 52% SIO2
normal slip	Fault in which the block moves downward
peak load	The maximum of electrical power demand
petrographic	Chemical and physical features of rock
photo lineaments	Linear feature expressed by underlying geological structure
quarternary fault	Active fault which has evidenced at the surface and moved in the last 1.6 million years
R value	Measures how well certain building insulation materials can resist heat
rectifiers	Electrical device that converts AC to DC
refraction analysis	Used to characterize subsurface geologic conditions
resistivity	Measure of resistance to electrical conduction
seismogram	A record produced by a seismograph
space utilization factor	Refers to how often a space is used, who uses it and why it is being used
splay	Surface making an oblique angle with another
spur	Lateral ridge of land descending from a hill
step overs	Structural features along strike slip faults

stratigraphy	The study of rock layers and layering.
surface outcrops	Often show at the surface
tectonic transition	Located between the lower mantle and the upper mantle of earth
tomographic	Imaging subsurface with seismic waves
transverse antithetic accommodation zone	Zones across which strata have opposite tilt direction
tuff	Light, porous rock formed by consolidation of volcanic ash
utilization factor	The utilization factor or use factor is the ratio of the time that a piece of equipment is in use to the total time that it could be in use.

REFERENCES

Athens, N. D. (2011). ATV magnetometer systems for efficient ground magnetic surveying. *The Leading Edge , 30*, 394-398.

Bartok, J. W., 2012. Greenhouse Management, Tech Solutions: "Finding More Room.", http://www.greenhousemag.com/article/gm0312-increase-production-space-tips/

Blackwell, D. D. and Richards, M., (2004). Geothermal map of the North America. *American Association of Petroleum Geologists, 1 sheet, scale: 1: 6,500,000.*

Better Health Foundation (BHP), 2015. "State of the Plate" http://www.pbhfoundation.org/ pdfs/about/res/pbh_res/State_of_the_Plate_2015.

California Department of Fish and Game (CDFW), 2012, "Farm Fish Pond Management in California," Inland Fisheries – Informational Leaflet No. 23, July 1988, Sacramento, CA. Southern California Public Power Authority, "Request for Proposals for Renewable Energy Projects," Response Deadline: November 30, 2012, 225 S. Lake Avenue, Suite 1250, Pasadena, California.

California Energy Commission (CEC), 2014. "Estimated Cost of New Renewable and Fossil Generation in California", May 2014, CEC-2 – 2014-003-SD, Sacramento, CA.

California Energy Commission (CEC), 2016. "The Padilla Report: Costs and Savings for the Renewable Portfolio Standard in 2016 (Pursuant to Public Utilities Code Section 913,3)", May 2017, Sacramento, CA.

Cantwell, C.A., and A.P.G. Fowler, 2014. Fluid Geochemistry of the Surprise Valley Geothermal System. PROCEEDINGS, 39th Workshop on Geothermal Reservoir Engineering, Stanford University, Stanford, California, SGP-TR-202.

COOP, 2017. Produce Price List, https://www.foodcoop.com/go.php?page=produce, Park Slope Food COOP.

Duffield, W. A. and Fournier, R. O., (1974). Reconnaissance study of the geothermal resources of Modoc County, California. *US Geological Survey Open-File Report no. 74-1024*, 21

Egger, A. E. and Miller, E. L., 2011. Evolution of the northwestern margin of the basin and range: The geology and extensional history of the Warner Range and environs, northeastern California. Geosphere, 7, 3, 756-773.

Egger, A. E., Glen, J. M. G., and Ponce, D. A., 2010. The northwestern margin of the Basin and range province: Part 2: Structural setting of a developing basin from seismic and potential field data. Tectonophysics, 488, 1-4, 150-161.

Egger, A.E., J.M.G. Glen, and D.K. McPhee, 2014. Structural controls on geothermal circulation in Surprise Valley, California: A re-evaluation of the Lake City fault zone. Geological Society of America Bulletin, doi:10.1130/B30785.1.

Faulds, J. E., Coolbaugh, M., Blewitt, G., Henry, C. D., (2004). Why is Nevada in hot water? Structural controls and tectonic model of geothermal systems in the northwestern Great Basin. *Transactions, GRC Annual Meeting, 2004/08/29, Indian Wells, CA, Davis.* , 649-654.

Fontiveros, V. C., 2010, 2-D high-resolution seismic imaging of small-scale intra-basin faulting in Surprise Valley, California (MS thesis. Stanford University).

Fraser, D. C. and Hoover, D.B. (1983). Airborne electromagnetic surveys of the Cascade *Geological Survey Miscellaneous Field Study Map, MF-1299.*

Glen, J. M. G., Egger, A. E., Ponce, D. A. (2008). Structures controlling geothermal circulation identified through gravity and magnetic transects, Surprise Valley, California, Northwestern Great Basin. *GRC Transactions , 32*, 279-283.

Glen, J. M., Egger, A. E., Ippolito, C. and Athens, N. (2013). Correlation of geothermal springs with sub-surface fault terminations revealed by high-resolution, UAV-acquired magnetic data. *Proceedings, 38. Workshop on Geothermal Reservoir Engineering. Stanford University, Stanford, California, February 11-13, 2013.*

Hedel, C. W. (1980). Late Quaternary faulting in western Surprise Valley, Modoc County, California. *Master's Thesis, San Jose State University, San Jose, California*.

Hedel, C. W. (1981). Map showing geothermal resources of the Lake City - Surprise Valley Known Geothermal Resource Area, Modoc County, California. *US Geological Survey Miscellaneous Field Study Map, MF-1299.*

Hedel, C. W. (1984). Map showing geomorphic and geologic evidence for late Quaternary displacement along the Surprise Valley and associate faults, Modoc County, California. *U.S. Geological Survey Miscellaneous Field Studies Map. MF-1299.*

Kaiser, C and Ernst M., 2012. "Hydroponic Lettuce". University of Kentucky College of Agriculture, Lexington, KY. Oregon Department of Energy, “Summary of Oregon's Renewable Portfolio Standard,” July 2012, www.oregon-rps.org, Salem, OR.

Lerch, D. W., Klemperer, S. L., Egger, A. E., Colgan, J. P., and Miller, E. L., (2010). The northwestern margin of the Basin and Range Province, part 1: Reflection profiling of the moderate angle (app. 30 degrees): Surprise Valley Fault. *Tectonophysics , 488*, 143-149.

O'Connell, J. F. and Ericson, A., (1974). Earth lodges to wickiups: a long sequence of domestic structures from the northern Great Basin. *Nevada Archaeological Survey Research Paper No: 5*, 43-61.

Pena, J. G., 2005. “Greenhouse Vegetable Production Economic Considerations, Marketing, and Financing,” Texas Cooperative Extension, http://aggie-horticulture.tamu.edu/greenhouse/hydroponics/economics.html

Ponce, D. A., Glen, J. M. G., Egger, A. E., Bouligand, C., Watt, J. T., and Morin, R. L., (2009). Geophysical studies in the vicinity of Warner Mountains and Surprise Valley, northeast California. *USGS Open-File Report No. 2009-1157.*

Reed, M. J. (1975). Chemistry of thermal water in selected geothermal areas of California. *Caifornia Div. of Oil and Gas, Sacramento (USA)*.

Roberts, C. W. and Jachens, R. C., (1999). Preliminary aeromagnetic anomaly map of California. *USGS Open-File Report no. 99-440*, 14.

White, D. E. (1955). Violent mud-volcanoe eruption of Lake City Hot Springs, northeast California. *Geological Society of America Bulletin, 66* (9), 1109-1130.

Wurts, W. A., 2014. “Guidelines for Producing Food Size Channel Catfish,” Kentucky State University Cooperative Extension Program, Princeton, KY.

APPENDICES

APPENDIX A: History of Geothermal Activity in Surprise Valley, Previous Studies and Regional Geology

APPENDIX B: Geological Map of the Warner Range and Surrounding Region

APPENDIX C: Photographs and Newspaper Articles Associated with Some of the Public Outreach Events

APPENDIX A:

History of Geothermal Activity in Surprise Valley, Previous Studies and Regional Geology

A1. History of Geothermal Activity in Surprise Valley

Geothermal activity in Surprise Valley has long been known. Archaeologists have found that the first known human inhabitants of the valley constructed dwellings selectively in hot spring areas 5000 to 6000 years ago (O'Connell and Ericson, 1974). In the early 1900s, spas flourished at Leonards Hot Springs, Menlo Baths, and Surprise Valley Mineral Wells, and the operators claimed therapeutic benefits to those who bathed in the pools filled with mineralized water from thermal springs. However, Surprise Valley was not considered to be an attractive target for geothermal prospecting until 1951 when a spectacular phreatic eruption of mud volcanoes (White, 1955) occurred at an isolated group of hot springs near Lake City. This eruption propelled rocks, clots of mud, steam, and gases upward as much as 1600 m from six vents ranging from 18 m to 61 m in diameter. Immediately after the explosive eruption, springs at the site discharged water at or near boiling temperatures. Subsequent investigations have shown this group of hot springs to be among the most important geothermal resources in Surprise Valley.

In accordance with the provisions of the Federal Geothermal Steam Act of 1970, 150 km^2 (37,160 acres) in the vicinity of Lake City were designated as potentially valuable for production of geothermal energy and were classified as a “Known Geothermal Resource Area” (KGRA) by the USGS. In 1974, an additional 145 km^2 (35,780 acres) were so classified, bringing the total area of the KGRA to 295 km^2 (72,940 acres).

A2. Previous Studies

Since the designation of the KGRA by the USGS remarkable scientific research and studies were carried out in Surprise Valley.

Duffield and Fournier (1974) collected water samples from the hot springs in Modoc County and studied their chemistry. The authors estimated the sub-surface temperature by various geochemical methods.

Reed (1975) studied chemistry of thermal waters in selected geothermal areas in California including Surprise Valley. Using silica, sodium, potassium and calcium concentrations, the author estimated sub-surface temperatures to be less than 150 °C, probably a result of mixing with near-surface cold water.

Under the light of plate tectonics and new geological concepts, a new stage of geological studies aiming to understand the geothermal potential of the area was started at the beginning of 1980s. Hedel (1980) studied the late Quaternary faulting in western Surprise Valley, and the next year he prepared a map that showed the geothermal resources around Lake City (Hedel, 1981). Finally, Hedel (1984) published the map showing geomorphic and geologic evidence for late Quaternary displacement along the Surprise Valley and associated faults.

In line with geologic studies several geophysical studies were also conducted in 1980s and 1990s. Fraser and Hoover (1983), Roberts and Jachens (1999) conducted regional airborne electromagnetic surveys in Cascade Ranges and in California, respectively. These pioneering studies were followed by more regional and problem-based studies in the following years.

Glen et al. (2008) identified the structures controlling geothermal circulation by gravity and magnetic transects.

Ponce et al. (2009) compiled the earlier gravity – magnetic works and collected new data as an aid to understand the geologic framework of the Surprise Valley geothermal area and in general, geothermal systems throughout the Great Basin.

Lerch et al. (2009) conducted a 16-km long 2D seismic reflection study across Surprise Valley and examined the slip geometry and evolution of the Surprise Valley fault. The authors stated that the Surprise Valley fault is a low angle fault at its present configuration and is cut by major intra-basin normal faults.

Egger and Miller (2011) studied the evolution of the northwestern margin of the Basin and Range and the extensional history of the Warner range. New geologic mapping, combined with geochemistry and geochronology of rocks in the Warner Range documented a history of volcanism and extension from the Eocene to the present that provided an insight into the evolution of this margin.

Egger et al. (2010) conducted a study in Surprise Valley using seismic velocity modeling and potential field maps and models. The authors tried to examine the structural setting of a developing extensional basin focusing on Lake City Fault and the other intra-basin faults.

Egger et al. (2014) studied the role of faults and fractures in the circulation of geothermal fluids in the crust based on the structural setting and state of stress. They concluded that the thermal fluid circulation is most likely controlled primarily by interactions between north-south-trending normal faults.

Glen et al. (2013) collected high-resolution magnetic data from the air using an unmanned aerial system (UAS) combined with ground-based data. A >35-km long magnetic high was detected using the data. Origin and segmentation of the magnetic high was discussed in this paper.

Cantwell and Fowler (2014) overviewed and modeled the geochemical data for thermal fluids in Surprise Valley in an attempt to understand the source and flow-path of geothermal waters in the valley. Their initial results support the theory that discrete recharge sources and mechanisms are operating throughout the valley.

A3. Regional Geology

Geologic units exposed in the Warner and Hays Ranges and Surprise Valley are approximately 4.5 km-thick and include a west-dipping sequence of Eocene to Upper Miocene sedimentary and volcanic rocks (Egger and Miller, 2011) (Appendix B). From bottom to top, these units can be summarized as follows:

A3.1 Late Eocene-Oligocene Volcaniclastic Sedimentary Rocks

The oldest rock exposed in the Warner Range consists of deeply weathered andesitic breccias, lahars, and debris flows with minor pyroxene- and hornblende-andesite lava flows. This unit, called the McCulley Ranch Formation (Tmrv) is only exposed in the central portion of the range near Cedarville.

The Oligocene sedimentary rocks in the region were grouped as Steamboat Formation (Tsbn, Tscc, and Tsu). The Steamboat Formation is a cliff-forming, coarse-grained alluvial sandstone and conglomeratic sequence that ranges from approximately 1500 m thick in its southernmost exposures to 200 m thick where it is encountered in a drill core. This change in thickness, paleo-current indicators, and detrital zircon ages indicate a proximal volcanic source to the SSW, most likely within 20 km.

The Deep Creek Formation (Tdc) consists primarily of tuffs and reworked tuffaceous sediments, and generally forms a tree-covered slope above the conglomeratic cliffs of the Steamboat Formation. These tuffs are silicified and slightly hydrothermally altered to a greenish tint.

The Lost Woods Formation (Tlw) consists of conspicuously red-weathering volcanic breccias, volcanoclastic sandstones and conglomerates, minor mafic tuff, and autobrecciated lava flows. This unit consists of more basalt than the underlying volcanic sequence and many of the breccias consist of homogenous vesicular basalt clasts. In finer-grained sedimentary layers, Tlw includes petrified logs up to 1 m in diameter, orientations of long axes of these logs indicate paleo-fluvial transport direction.

This entire sequence of Late Eocene-Oligocene volcaniclastic and sedimentary rocks was deposited in a continental basin within a system of active volcanoes-an intra-arc basin, as suggested by the presence of numerous ash layers, coarse volcanic breccias, highly variable thickness of units and the presence of occasional lava flows throughout the sequence.

A3.2 Oligocene Arc Volcanic Rocks

The Lake City basalts (Tovl), a sequence of basalt and basaltic andesite flows and mafic tuffs, are exposed in the northern Warner Range where they reach a thickness of more than 2 km. This sequence thins to the south and pinches out completely just north of Cedar Pass, indicating the flows likely represent part of a basaltic shield volcano. The cinder-rich mafic tuffs are thickest approximately 10 km north of the Cedar Pass, suggesting a vent area in this general area.

The Cedar Pass complex (Tovc) consists of primarily volcanic breccias, hornblende-rich andesite and basaltic andesite flows, and minor shallow dacite intrusions. A series of dikes of hornblende andesite that radiate out from a center approximately 5 km southwest of Cedar Pass in Dry Creek Basin and breccias that dip radially away from Dry Creek Basin suggest a vent location in this area.

Farther south of the vent area, breccias disappear and contemporaneous Oligocene volcanics (Tovu) consist mostly of more distal andesite flows and ignimbrites. Tovu is also exposed in the Hays Canyon Range to the east.

The Hays volcano (Tovh), exposed in the southern portion of the Hays Canyon Range, is a basaltic to basaltic andesitic shield volcano.

Major- and trace-element geochemistry of these Oligocene arc volcanic rocks reveals that they are similar to rocks of both modern and ancestral Cascade arc. The volcanic edifices exposed in the Warner and Hays Canyon Ranges may mark the easternmost extent of subduction-related arc volcanism during the Eocene and Oligocene.

A3.3 Early Miocene Tuffs and Sediments

Few rocks of early Miocene age are preserved in the Warner Range, suggesting a near cessation of proximal volcanic activity ca. 24 Ma. A thin unit of rhyolitic tuffs and sediments (Trt) crops out between Parker Creek and Emerson Peak. A new date on a reworked tuff suggests a hiatus in deposition, followed by a minor deposition of sediments and tuffs derived from distal, rhyolitic eruptions during the early Miocene.

A3.4 Mid-Miocene Basaltic Volcanic Rocks

Despite the decrease in volcanic activity, it appears that relatively little erosion took place during this time, as Oligocene features still acted as topographic barriers to subsequent, younger volcanic flows and breccias. In the southern Warner Range, more than 1 km of basalts and basaltic andesites (Tmbl and Tmbu) and tuffs (Tmt) were deposited from ca. 16 to 14 Ma. However, the map indicates that these lavas were blocked from flowing north because of topographic high formed by the Cedar Pass complex. A similar relationship is observed in the Hays Canyon Range, where mid-Miocene basalt flows bank into flanks of the Hays Volcano, as well as farther north in Oregon.

A3.5 Late Miocene to Pliocene Volcanic Rocks

Latest Miocene and Pliocene volcanic rocks in the region consist primarily of distinctive series of low-potassium, high-alumina olivine tholeiites (Tlb) erupted between 8 and 3 Ma. These basalts are interbedded with rhyolite domes (Tmr) and tuffs and tuffaceous sediments (Tts). Geochemically, the compositions of the basalt flows show little variability. Individual flows are thin, reaching only a few meters in thickness at most, and are interbedded with tuffs, tuffaceous sediments, and lacustrine deposits (Tts). The flows crop out extensively throughout the region, on both west and east sides of the Warner Range and Surprise Valley fault. Despite their broad distribution, the map indicates that these flows were limited by pre-existing topography of both the Hays Canyon and warner ranges. On the east side of the

Surprise Valley, a 3 Ma flow banks into the Oligocene tuffs of Hays Canyon Range; on the west side, horizontal flows directly overlie Oligocene rocks west of the range. On the southwest side of the Warner Ranges, they appear to have flowed across pre-existing normal faults, which may also have controlled the vent locations. Unlike the earlier Oligocene and Miocene volcanism, this magmatic event did not generate significant volcanic edifices, and what are likely volcanic vents appear as small, low- relief shields and plugs. Vents are located just north of the road between Vya and Cedarville, on the Devil's garden Plateau, and on the west flank of the Warner Range.

A3.6 Pleistocene Lake Deposits

Pleistocene and younger deposits are dominated by sedimentary deposits from pluvial Lake Surprise, which reached a high stand of 1533.6 m, filling the valley with water to a depth of approximately 156 m. Along the western side of the valley, the remains of several Gilbert-type fan deltas stand up to 30 m above the surrounding valley floor. Numerous shorelines are visible, particularly at the southern end of the valley, where tufa deposits have cemented Pleistocene beach gravels.

APPENDIX B:

Geological Map of the Warner Range and Surrounding Region

Credit: Egger and Miller, 2011.

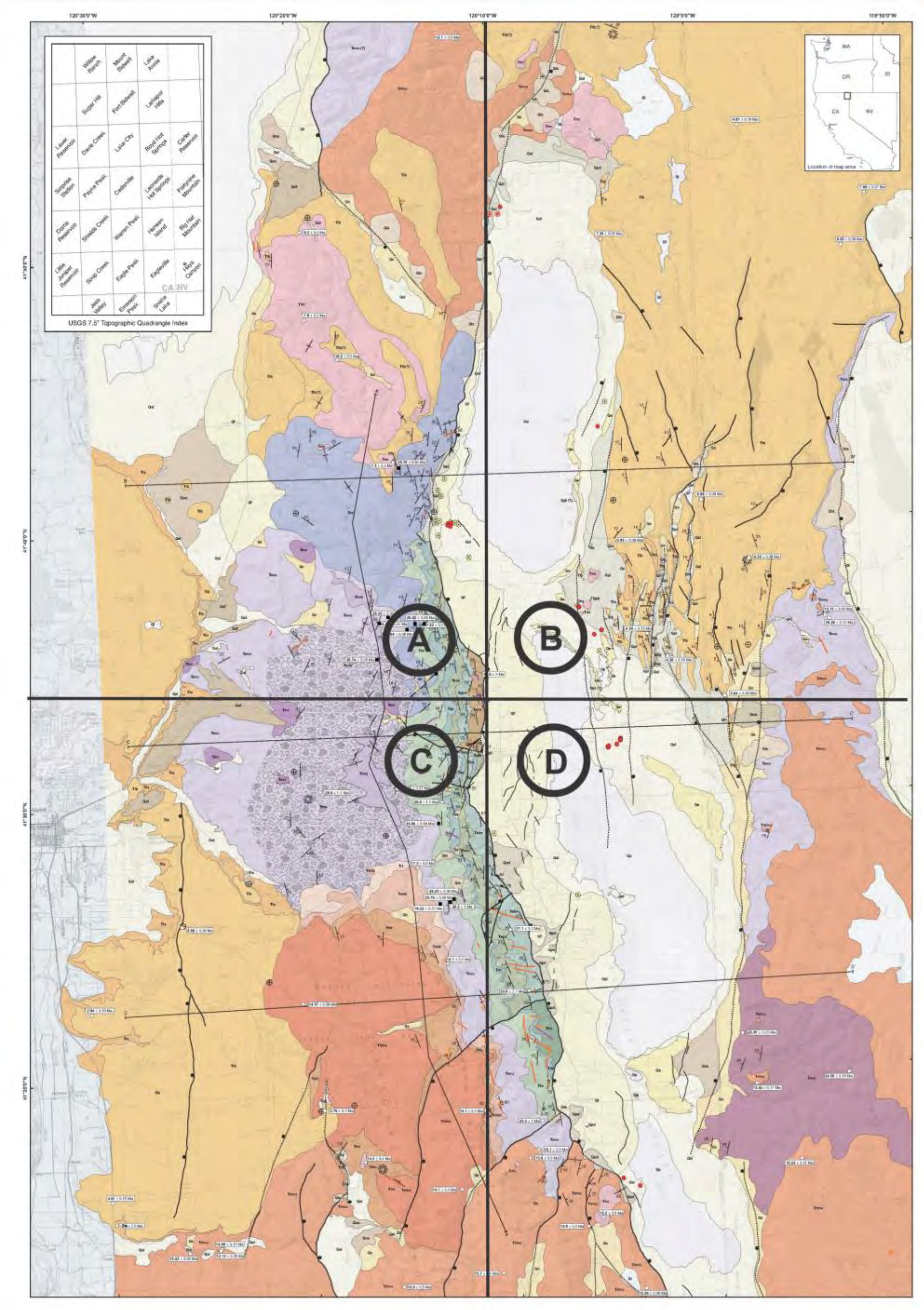

USGS 7.5' Topographic Quadrangle Index
A
B
C
D

LEGEND

Holocene sediments

Qal	Alluvium
Qf	Fan deposits
Qc	Colluvium
Qe	Eolian deposits (sand dunes)
Qhs	Hot spring deposits
Ql/Qp	Lake and playa deposits
Qls	Landslides

Pleistocene sediments

Qoa	Older alluvium
Qof	Older fan deposits
Qols	Older landslide deposits
Qpb	Pleistocene beach gravels of Lake Surprise
Qpd	Pleistocene deltas of Lake Surprise
Qpl	Pleistocene lake sediments of Lake Surprise

Late Miocene-Pliocene volcanic rocks

Tlb	Low-K olivine tholeiitic basalts
Tts	Tuffs and tuffaceous sediments
Tmr	Mid-Late Miocene rhyolites

Mid-Miocene volcanic rocks

Tmbu	Basalt and andesite flows, upper
Tmt	Tuff and reworked tuff
Tmb	Basalt and andesite flows, lower
Tmvu	Mid-Miocene volcanic rocks, undifferentiated

Early Miocene volcanic rocks

Trt	Rhyolitic and andesitic ash flow tuffs

Oligocene volcanic rocks

Tovb	Bald Mountain basalt
Tovp	Payne Peak andesite
Tovh	Hays Volcano
Tovc	Cedar Pass volcanic complex
Tovi	Intrusive rocks of Cedar Pass complex
Tovu	Oligocene volcanic rocks, undifferentiated
Tovl	Lake City basalts

Oligocene sedimentary rocks

Tlw	Lost Woods Formation
Tdc	Deep Creek Formation
Tscc	Steamboat Formation, Cougar Cliffs member
Tsbn	Steamboat Formation, Badger's Nose member
Tsu	Oligocene sedimentary rocks, undifferentiated

Eocene rocks

Tmrv	McCulley Ranch Formation

SYMBOLS

15 Strike and dip of bedding

70 Strike and dip of fault plane

80 Strike and dip of dike

Vertical bedding

Horizontal bedding

Volcanic vent

Drill hole

Hot springs

Contact

Normal fault,
ball on downthrown block

Normal fault, concealed,
ball on downthrown block

Quaternary fault scarp

Maximum lake level, Pleistocene Lake Surprise
(Zimbelman et al., 2008)

14.1 ± 0.4 Ma Geochronological age, symbol indicates source:

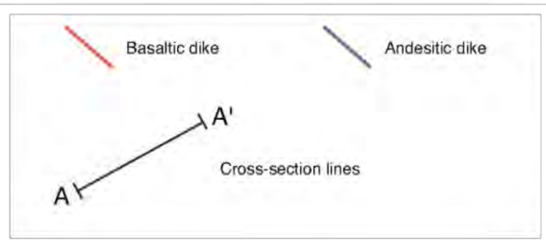

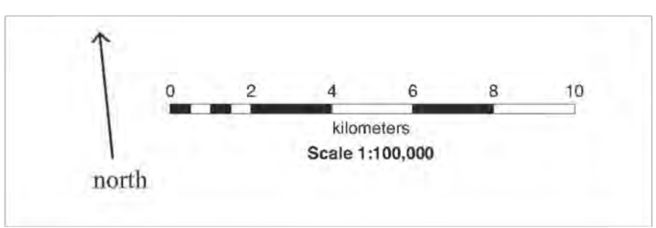

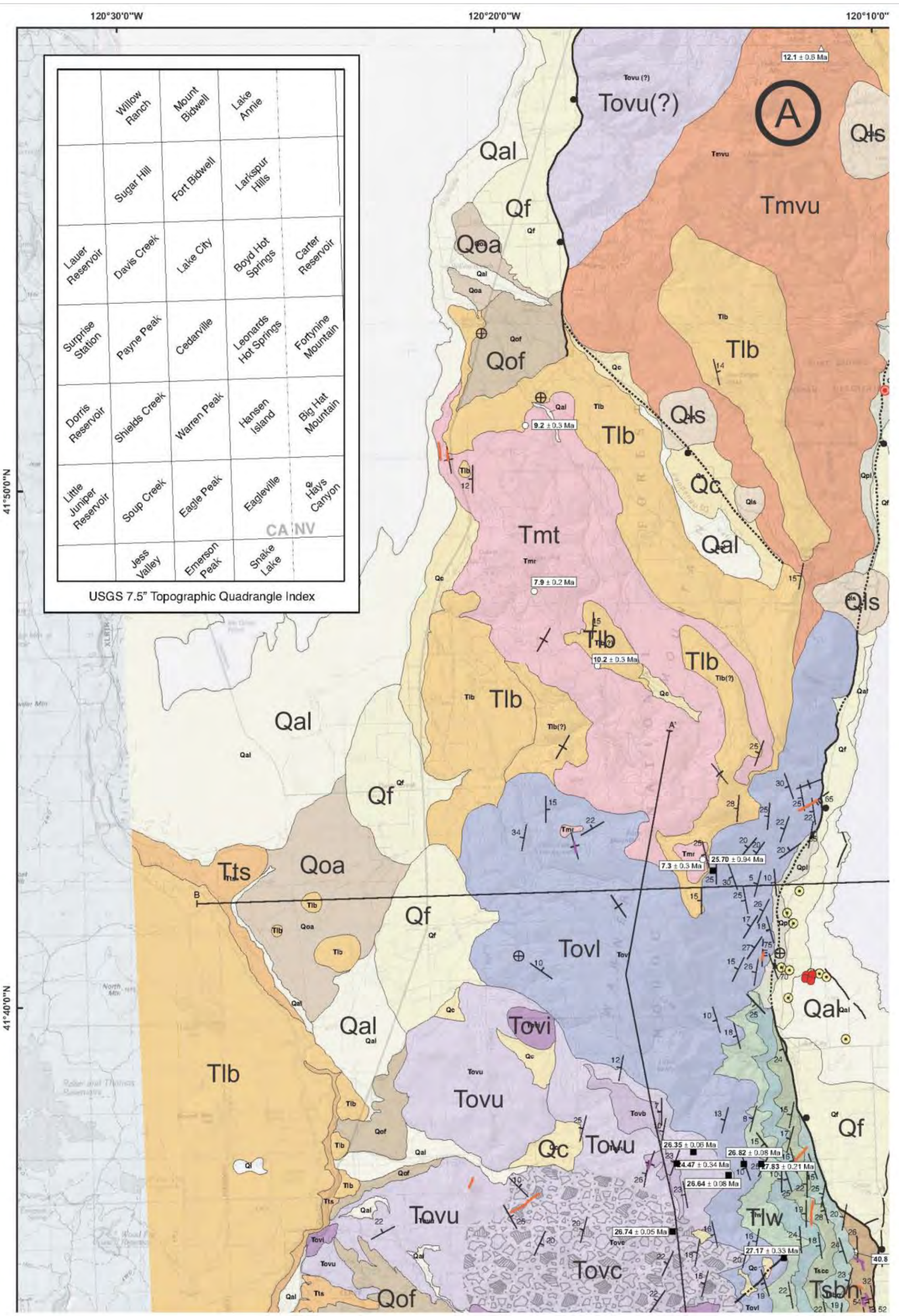
120°30'0"W
120°20'0"W
120°10'0"
41°50'0"N
41°40'0"N
USGS 7.5" Topographic Quadrangle Index
Willow Ranch
Mount Bidwell
Lake Annie
Sugar Hill
Fort Bidwell
Larkspur Hills
Lauer Reservoir
Davis Creek
Lake City
Boyd Hot Springs
Carter Reservoir
Surprise Station
Payne Peak
Cedarville
Leonards Hot Springs
Fortynine Mountain
Dorris Reservoir
Shields Creek
Warren Peak
Hansen Island
Big Hat Mountain
Little Juniper Reservoir
Soup Creek
Eagle Peak
Eagleville
Hays Canyon
CA NV
Jess Valley
Emerson Peak
Snake Lake
A
Tovu(?)
Tmvu
Qls
Qal
Qf
Qoa
Qof
Tlb
Qc
Tmt
Tts
Tovl
Tovi
Tovu
Tovc
Tlw
Tsbh
12.1 ± 0.8 Ma
9.2 ± 0.3 Ma
7.9 ± 0.2 Ma
10.2 ± 0.3 Ma
7.3 ± 0.3 Ma
25.70 ± 0.94 Ma
26.35 ± 0.08 Ma
24.47 ± 0.34 Ma
26.82 ± 0.08 Ma
27.83 ± 0.21 Ma
26.64 ± 0.08 Ma
26.74 ± 0.05 Ma
27.17 ± 0.33 Ma
A'
B

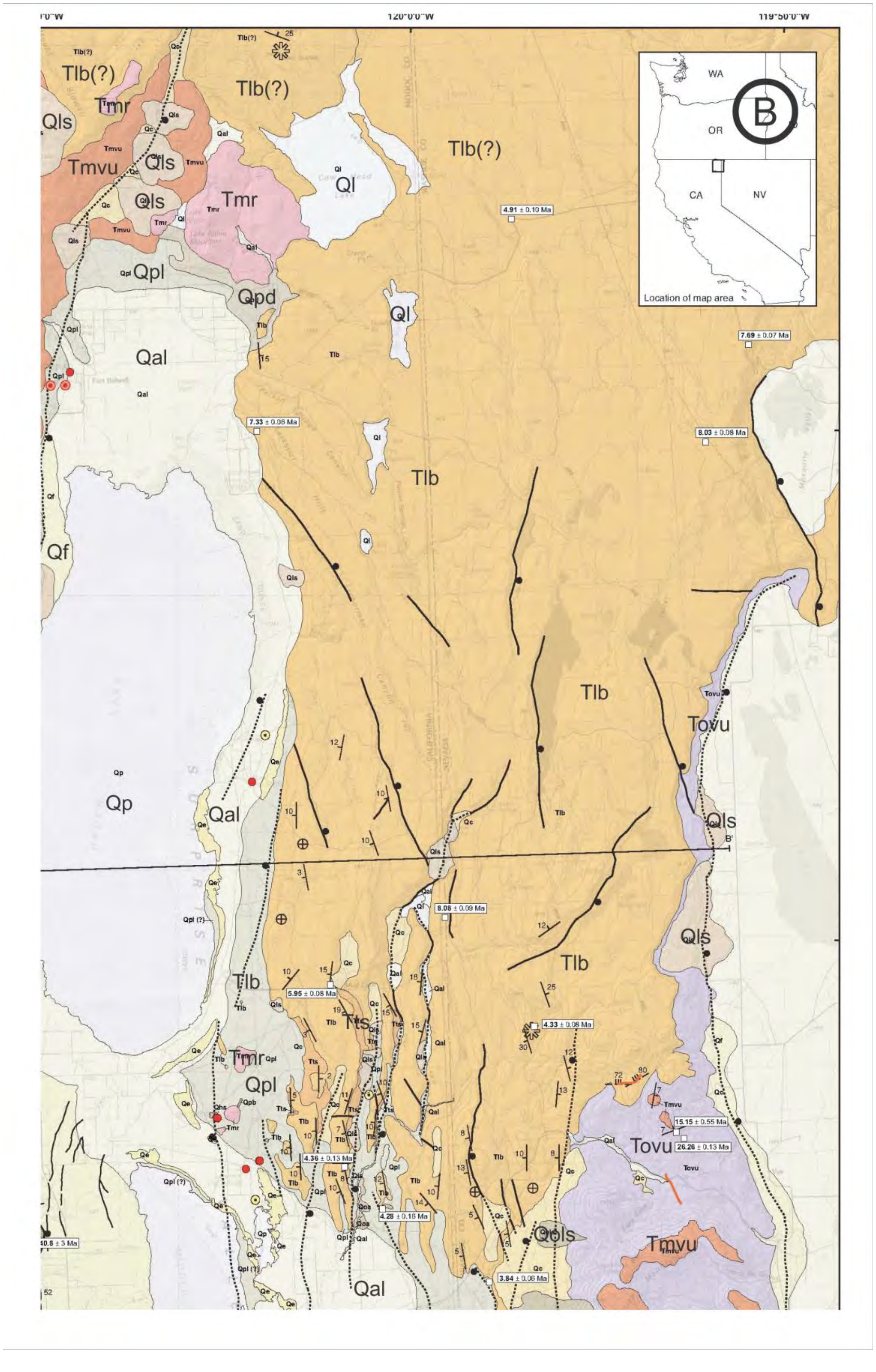
120°0'0"W
119°50'0"W
Tlb(?)
Tmr
Qls
Tmvu
Qpl
Qpd
Ql
Qal
Qf
Qp
Tlb
Tovu
Tts
Tmvu
Qols
WA
OR
CA
NV
Location of map area
B
B'
4.91 ± 0.10 Ma
7.69 ± 0.07 Ma
7.33 ± 0.06 Ma
8.03 ± 0.08 Ma
8.08 ± 0.09 Ma
5.95 ± 0.08 Ma
4.33 ± 0.08 Ma
15.15 ± 0.55 Ma
26.26 ± 0.13 Ma
4.36 ± 0.13 Ma
4.28 ± 0.16 Ma
3.84 ± 0.08 Ma
40.8 ± 3 Ma

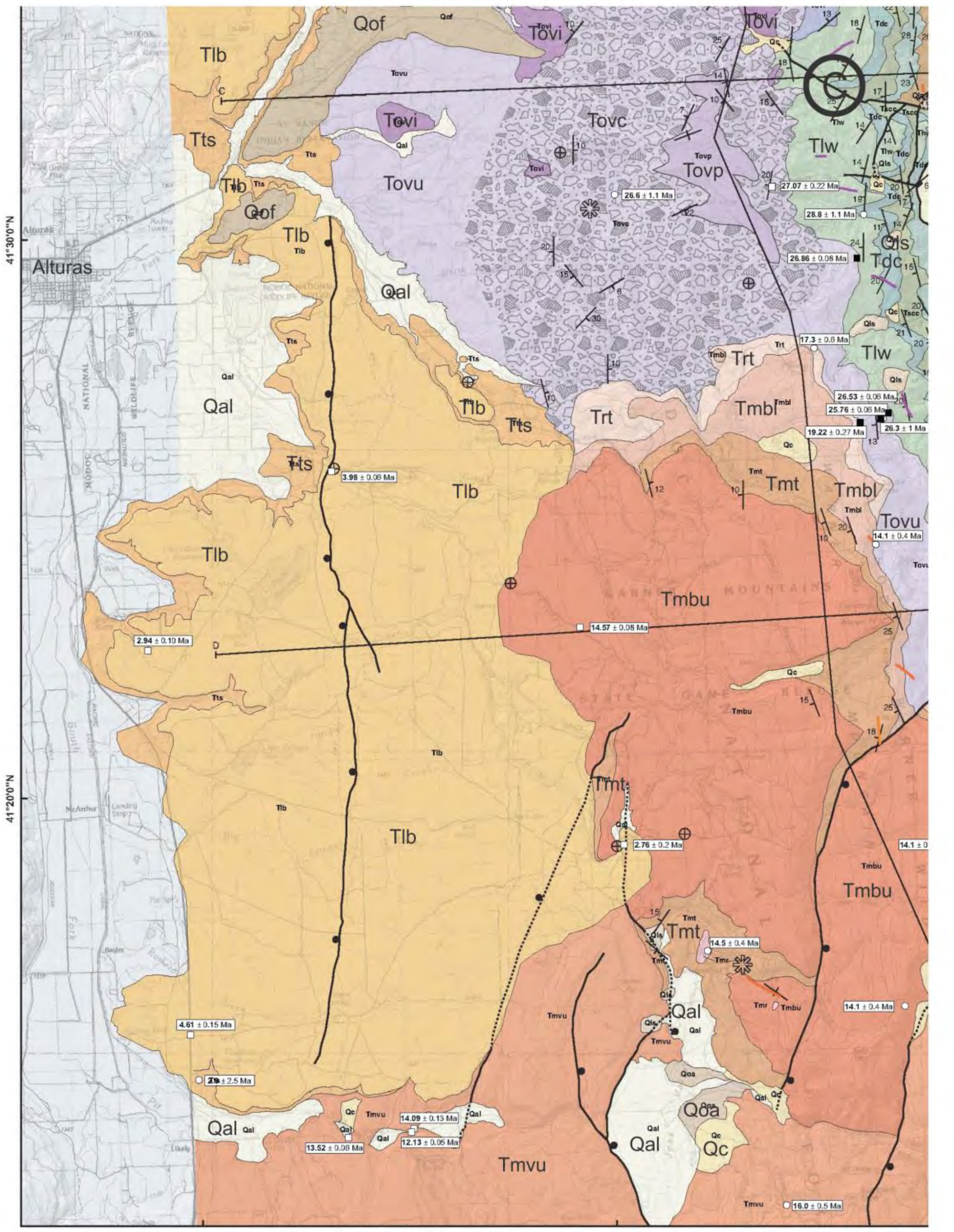

Alturas
41°30'0"N
41°20'0"N
C
D
Qof
Tlb
Tts
Qal
Tovi
Tovu
Tovc
Tovp
Tlw
Tdc
Qls
Qc
Trt
Tmbl
Tmt
Tmbu
Tmvu
Qoa
26.6 ± 1.1 Ma
27.07 ± 0.22 Ma
28.8 ± 1.1 Ma
26.86 ± 0.08 Ma
17.3 ± 0.8 Ma
26.53 ± 0.08 Ma
25.76 ± 0.08 Ma
26.3 ± 1 Ma
19.22 ± 0.27 Ma
3.98 ± 0.08 Ma
14.1 ± 0.4 Ma
14.57 ± 0.08 Ma
2.94 ± 0.10 Ma
2.76 ± 0.2 Ma
14.5 ± 0.4 Ma
4.61 ± 0.15 Ma
14.09 ± 0.13 Ma
12.13 ± 0.05 Ma
13.52 ± 0.08 Ma
16.0 ± 0.5 Ma

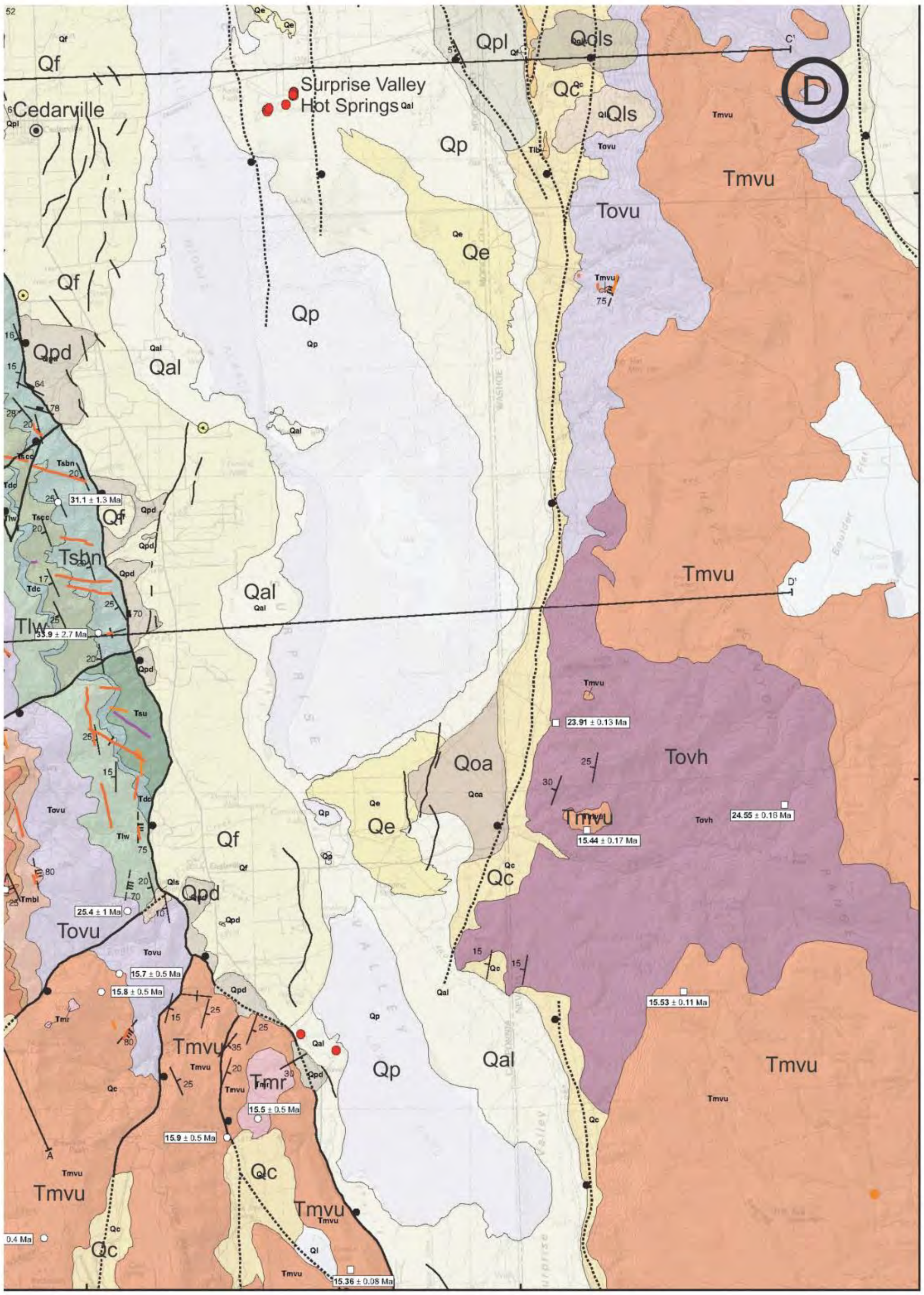
D
C'
D'
Cedarville
Surprise Valley
Hot Springs
Qf
Qpl
Qols
Qc
Qls
Qp
Tmvu
Tovu
Qe
Qpd
Qal
Tsbn
Tlw
Tovh
Qoa
Tmr
31.1 ± 1.3 Ma
33.9 ± 2.7 Ma
23.91 ± 0.13 Ma
24.55 ± 0.16 Ma
15.44 ± 0.17 Ma
25.4 ± 1 Ma
15.7 ± 0.5 Ma
15.8 ± 0.5 Ma
15.53 ± 0.11 Ma
15.5 ± 0.5 Ma
15.9 ± 0.5 Ma
15.36 ± 0.08 Ma

APPENDIX C:

Photographs and Newspaper Articles Associated with Some of the Public Outreach Events

CONGRATULATIONS 2015 GRADUATES

THE MODOC COUNTY

RECORD

ESTABLISHED IN 1892

Vol. 124, No. 1 | Alturas, California | June 4, 2015

Beatty sentenced to 7 years in prison

see Beatty, page 2

Rough . . .

SIX-YEAR-OLD ... Photos by Jamie Hoover

City Sewer rate increase of $10 under proposal

see Sewer, page 4

MHS, SV Graduation ceremonies Friday

SV Geothermal project starting out with a blast

By Jean Bilodeaux
Special to the Record

see Blast, page 4

THE MODOC COUNTY

RECORD

ESTABLISHED IN 1892

SV, MJUSD Geothermal projects moving forward

One contested race for Supervisor on June 7

Steam search. . .

Food "Hub" makes healthy difference a good choice

Town Hall meetings set for BV ambulance election

Storms of past week help snow

Geo from front page

gathering steam.

"Basically it is a group of people from all levels gathering in Sacramento April 13 and organizing in an effort to lobby and educate policy makers at the capital on the importance of "Baseload" energy," Rose said. "Baseload energy means energy being created 24 hours a day, seven days a week, which is what geothermal and biomass do. Not to bash wind and solar, but if you think about it, they only create energy when the wind is blowing or the sun is shining. As California gets ready to require an request for proposal of using 50 percent renewable energy in its portfolio, it is important that Geothermal and Biomass are included."

That meeting is April 13, 9 a.m. to 5 p.m. in the RCRC Conference Rm., 16th Floor Esquire Building, Sacramento.

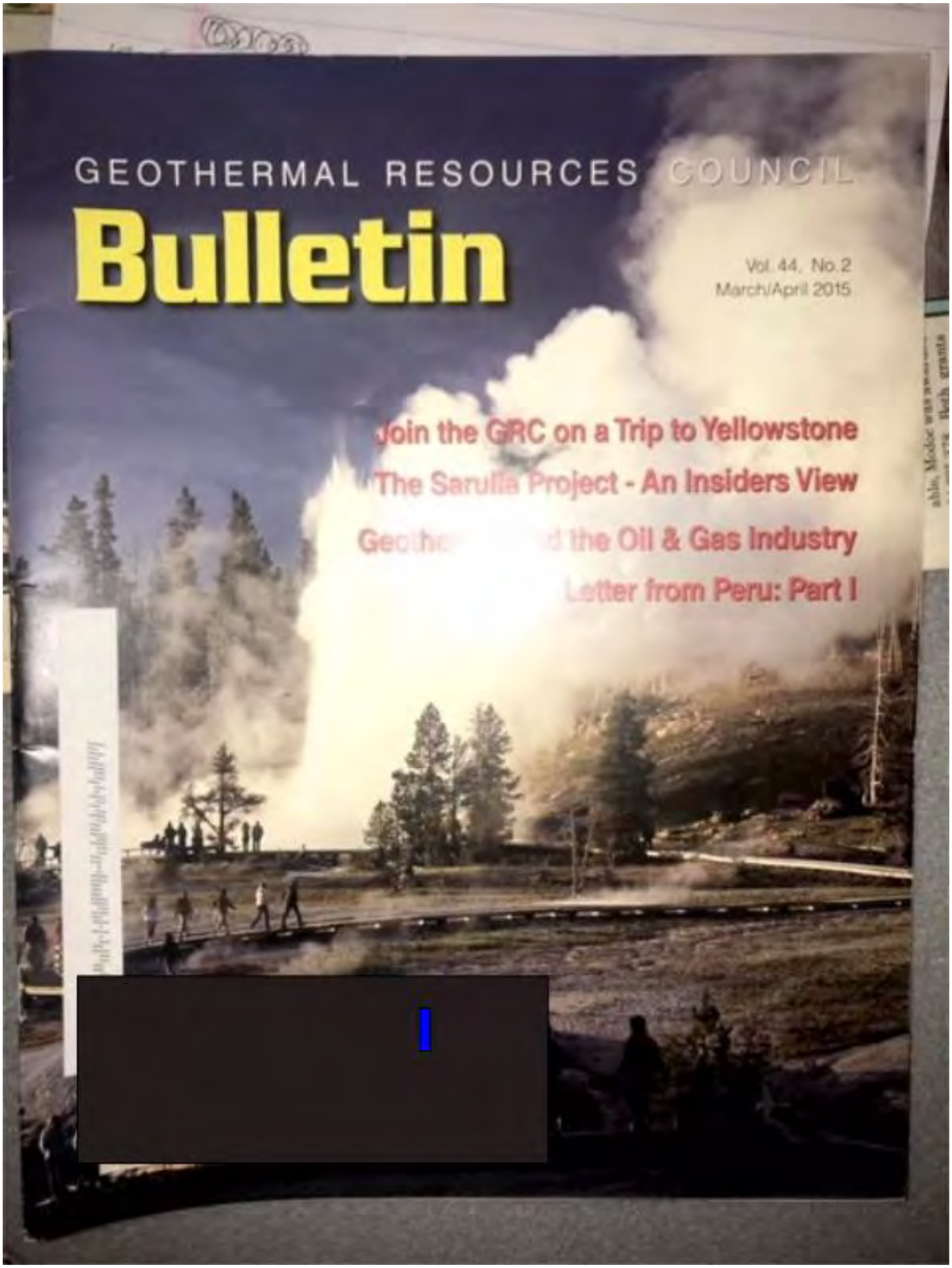
GEOTHERMAL RESOURCES COUNCIL
Bulletin
Vol. 44, No.2
March/April 2015
Join the GRC on a Trip to Yellowstone
The Sarulla Project - An Insiders View
the Oil & Gas Industry
Letter from Peru: Part I
[redacted]

Surprise Valley Geothermal Power Project Gets Million Dollar Grant

The **California Energy Commission** has awarded the **Surprise Valley geothermal project** a grant of over a million dollars.

A **$1,129,619 grant** to conduct geothermal resource assessments and exploratory drilling in the Surprise Valley Hot Springs area is to be given to the **County of Modoc** in north-east California. The project will install and demonstrate **a small geothermal distributed energy unit** to generate electricity at Surprise Valley Hot Springs Resort and conduct a geothermal economic feasibility and market analysis to provide information that can be used in future planning for expanded geothermal development in the area.

The geothermal distributed energy unit is anticipated to offset the electrical load of the Surprise Valley Hot Springs Resort and **save the resort over $10,000** per year in electricity costs.

In addition, the Modoc **Joint Unified School District** is to receive [illegible] **million** to expand the existing **geothermal** [illegible] **system** at Modoc High School to include [illegible] onal schools and the public pool in Altur[illegible] expanded system is projected to **save** the [illegible] **district more than $4.2 million** in fuel and [illegible] city costs over 25 years.

as been found at a
in Nevada. **Dajin**
nada has reported
om a widely
n carried out on
claims in **Mineral**

nt project to
ine borrowed
seems to be
orts *The Desert*

ced it was
um-extraction
un **John L.**
Calipatria,
rnia, with plans
uction. But then
y 40 people from
ys that it is now
ercialize its

da Wells
RC
ive Earth
ered in
nada
f its
da, Inc.
ounced
leases
e
Humboldt
included
ently
sting
ernickel
t and
s. Well
nguished
ver the

Springtime at Surprise Valley Hot Springs [illegible]

COMMUNITY INVITATION

GEOTHERMAL EXPLORATION AND DRILLING OPEN HOUSE

The Warner Mountain Energy and UC Davis Geothermal Exploration Team cordially invites the community to come and learn about the geothermal exploration and drilling project happening around the Surprise Valley Hot Springs area.

DATE: Tuesday, October 18, 2016
TIME: 4:00 – 6:00 p.m.

Enter through the Surprise Valley Hot Springs Resort entrance. Park on the East side of the hot spring resort and walk toward the drilling rig.

Schedule

9:30

Community Drum Circle Welcome

Senior Center – Literary Arts

10 - Fiction Workshop – Caleb Leisure

Caleb Leisure received his MFA in Fiction from New York University. In 2011 he was named a NYC Emerging Writer Fellow at the Center For Fiction, and in 2014 he won the [illegible] at work on his first novel. He lives in [illegible]

inches. The average monthly total is 1.61 inches. The heaviest rain fell Oct. [illegible] inches, and [illegible]. 16 at .27 inches.

Wednesday shooting kills Modoc Deputy

EDITOR'S NOTE: Parts of the story below are from the radio traffic during the incident. The names of the Deputy nor the suspect have been released.

At about 9:45 a.m. Wednesday morning a Modoc Sheriff Deputy radioed in for backup saying "shots fired." [illegible]

[illegible]

see City, page 4

SV Hot Springs hosts productive geothermal open house

By Jean Bilodeaux
Special to the Record

The Modoc County CAO, the Board of Supervisors and interested members of the public attended an open house held on Tuesday afternoon at the Surprise Valley Hot Springs Resort to learn more about the ongoing geothermal project.

[illegible]

THE MODOC COUNTY Board of Supervisors visit the geothermal well drilling site at the Surprise Valley Hot Springs, just as the second test hole is finished. Left to right are: Patricia Cullins, Geri Byrne, Jim Wills, Kathie Rhoads, CAO Chester Robertson, and David Allan.

[illegible]

Geothermal, page 4

Geothermal

from front page

the drilling involved, geothermal is more expensive at first. Geothermal generates power 24 hours a day, so the payback is faster using geothermal," explains Mink.

Solar has the advantage of tax credits. There is a federal and state bias against geothermal and biomass plants. If the playing field were level we'd be competitive," said Robertson.

Geothermal and biomass were left off the present energy bill. Only solar and wind were included for tax credits. Adding geothermal and biomass to the energy bill is still under consideration.

Although generating electricity is the primary focus of this project, there are many other uses for geothermal. This electric plant will only create three jobs, but a greenhouse could employ 15 people. Then there's aquaculture, refrigeration, dehydration and other uses for the geothermal energy.

UC Davis has been a driving force in this project, helping with data and research.

"With this meeting we believe the county and the board of supervisors understand they have a vital role to play. They can assist other landowners in developing their geothermal potential," said Rose.

The current drilling has produced some unexpected surprises. Petrified wood was found at a depth of 130 feet.

"By studying the samples obtained from above and below this wood we should be able to determine how and when this wood got there," said Mink.

Another unexplained sample was obtained from a depth of 170 feet, when metal appeared in the samples.

"The metal is certainly a mystery. We are sending all our samples to UC Davis for further examination," said Lisa Kuscu, project co-manager and head geologist.

The sediment fill in the valley is estimated to be 6,000 feet deep.

The project hopes to educate, to further knowledge and understanding of geothermal with the scientific community and the public. It will serve as a place to do further research and education.

"We are looking at combining resources when necessary. If we find higher temperatures and more flow, we can look at higher production," said Mink.

"The government is looking at honeycombing its electrical generating facilities. In case of a national emergency many smaller plants would stay on the grid where just a few plants could shut everything down," said Rose.

This next Spring the public will be invited to see the new engine and technology being used to power the geothermal electricity. Scientists and project managers will be answering questions about the project and its future for the community and the county.

Correction:

In last week's article on geothermal power drilling, the sentence should have read, "The demonstration plant . . . will be the first installation to generate electricity by using heat from a geothermal resource [in Modoc County]. The power projected to be produced is 25 kw, not 250 kw.

THE MODOC COUNTY

RECORD

ESTABLISHED IN 1892

Local Cops caution about clown hysteria

Drilling begins on SV Hot Springs geothermal project

Soup Complex burned area safety

LISA KUSCU, head geologist and project manager of Warner Mountain Energy washes drilling mud from a sample taken from 600 feet.

SV power from front page

Mink, president of Warner Mountain Energy.

The demonstration plant, using Cornerstone Sustainable Energy's PwrCor engine, will be the first installation to generate electricity by using heat from a geothermal resource. It is projected to produce 250 kilowatts of electric power with 150 gallons per minute of water at 180°F. At that level of output, the Surprise Valley Hot Springs site represents a potential estimated at 1.5 megawatts of constant, uninterrupted electric power.

The footprint of the plant will be about eight by 10 feet and fit inside a cargo container shed.

"This small geothermal power demonstration plant should produce enough electricity to supply the Surprise Valley Hot Springs Resort. We are working with Surprise Valley Electric to sell them any spillover electricity," said Mink.

The scientists are examining the prospect of an even larger project in the future.

"We are evaluating the resources in the whole valley," said UC Davis geophysics professor Jim McClain.

We are very excited to be helping develop economic resources which will benefit the community and the county," said Kuscu.

The team is very pleased with the results of the first well. A pad is being prepared at the second selected site and drilling will commence on Wednesday.

A town meeting to discuss the project and for the public to ask questions is being planned.

Burn from page 3

burns, follow all guidelines outlined (530) 640-2900

MNF

With cooler
weather expect
tumn arrives,
tions will be c
12:01 a.m. on F
7, 2016 in the
tional Forest.
This means
tors may once
campfires out
veloped campg
recreation site

BLM l
fire us
on lan

With cooler
peratures, the
Land Manag
lift fire rest
public lands
the Redding,
and Applegate
effective Frida
6 p.m.
When restr
eased, cam
again be use
developed c
Fire permits
Restrictions
ing and use
combustion e
roads and tr
lifted. Use
after 1 p.m.
allowed
Even with
dangers, of
outdoor enth
homeowners
with fire. C
fully exting
fires when
leaving them

applying for another $1.5 CEC grant that would fund a second phase of the project. It would be used for a deeper exploratory well to reach projected higher temperature water, for improved generation of electricity.

The County's application for geothermal exploration, economic feasibility and market analysis and distributed energy resource demonstration involving Surprise Valley Hot Springs was judged the top application and was awarded $1,129,619 while the MJUSD project for heating Alturas Schools and the swimming pool was judged number two and was awarded $3,155,759.

The County grant has a match of $369,588 and the MJUSD grant has match of $800,000.

The objectives of the County plan ar to fill the data gaps on the east side o Surprise Valley in the vicinity of the SV Hot Springs, using geological approaches including geochemical, geophysical, two-meter soil probes temperature survey, soil gas survey and exploratory drilling; and to install and demonstrate the effectiveness of a distributed energy geothermal unit to generate electricity immediately; to generate an economic feasibility and market analysis to facilitate steps in long-range planning and to effectively engage the public in creating a strong interest in geothermal development.

Power

from page 3

to the surface at temperatures of approximately 190°F, which is considered ultra-low-grade heat. Using just a small fraction of the water flow from the geothermal resource, the PwrCorTM engine is expected to be able to supply 100% of the power used by the resort.

The project will be managed by Warner Mountain Energy Corporation. Warner Mountain Energy specified the PwrCorTM engine, which will be produced and commissioned by CSE. Dr. Roy Mink, Chief Executive of Warner Mountain and former manager of the US Department of Energy geothermal program, explained, "The demonstration project will illustrate how low temperature geothermal heat resources, heretofore not considered economically feasible for power generation for the geothermal industry, can be tapped using this breakthrough technology."

Tom Telegades, CEO of the Company, stated, "We are proud of our executive leadership team which has worked hard to apply this technology to our first geothermal application. This demonstration project, we believe, may very well prove disruptive to the geothermal industry as the cost effective conversion of ultra-low heat from a geothermal resource can now be realized."

The Net: www. modocrecord. com

County agrees to additional geothermal project in SV

We're open. . .

A sweet big secret in little town

WARNER MOUNTAIN ENERGY

GEOTHERMAL EXPLORATION AND DEMONSTRATION PROJECT UPDATE

CEC GRANT GEO-14-003

PRESENTED BY:

MODOC COUNTY – CHESTER ROBERTSON

WARNER MOUNTAIN ENERGY - LISA KUSCU, CURTIS ROSE, MARY MINK

NOVEMBER 29, 2017

Winter glow. . .

THE NIGHT WAS just downright cold Saturday for the Alturas Winterfest and the folks who braved the weather welcomed the bonfire. The Parade of Lights was popular and entrants dressed up their floats and vehicles with flashing and colored lights, trees and people in a variety of costumes. The town Christmas Tree was also lighted in the Alturas Main Street Park as the highlight of the holiday festival. Photos by Claire West

WARNER MOUNTAIN ENERGY's ...

Geothermal project in SV aims to succeed

COMMUNITY

INVITATION

GEOTHERMAL DEMONSTRATION UPDATE AND DISTRIBUTED ENERGY UNIT COMMISSIONING

Co-funded by the California Energy Commission
GRDA Grant GEO-14-003, Modoc County

The Warner Mountain Energy Team cordially invites the community to come and get an update on geothermal demonstration project and Distributed Energy Unit power unit commissioning.

DATE: WEDNESDAY, NOVEMBER 29, 2017
TIME: 7:30-8:30 p.m.
PLACE: Cedarville Senior Center, located on Main Street in Cedarville

September 8, 2015

FOR IMMEDIATE RELEASE

Public Invited to Modoc Geothermal Project Kickoff Meeting

The public is invited to attend an upcoming community meeting to learn more about the Modoc Geothermal Research and Demonstration Project. The meeting will be held **Thursday, September 24, 2015, at 6:00 PM at the Community Church, Cedarville, CA. The church is located on the corner of Bonner and Center Street.**

The County of Modoc received grant funding from the California Energy Commission to conduct a research and demonstration project to determine the viability of generating geothermal power in Surprise Valley. The County is partnering on the project with Warner Mountain Energy (WME), UC Davis, Surprise Valley Electric and other stakeholders. The two-year undertaking will include installation of a small distributed energy geothermal unit and completion of an economic feasibility and market analysis.

Chester Robertson, County Administrative Officer, will explain why the production of geothermal energy could be of benefit to the county as a whole and the County's role in securing grant funding for the research project. WME representatives will speak about each of the project components, timelines and progress to date. A question and answer period will follow the presentation.

No pre-registration is required for the meeting. For more information contact Curt Rose at (775) 527-3345 or e-mail: svgeothermal@yahoo.com

###

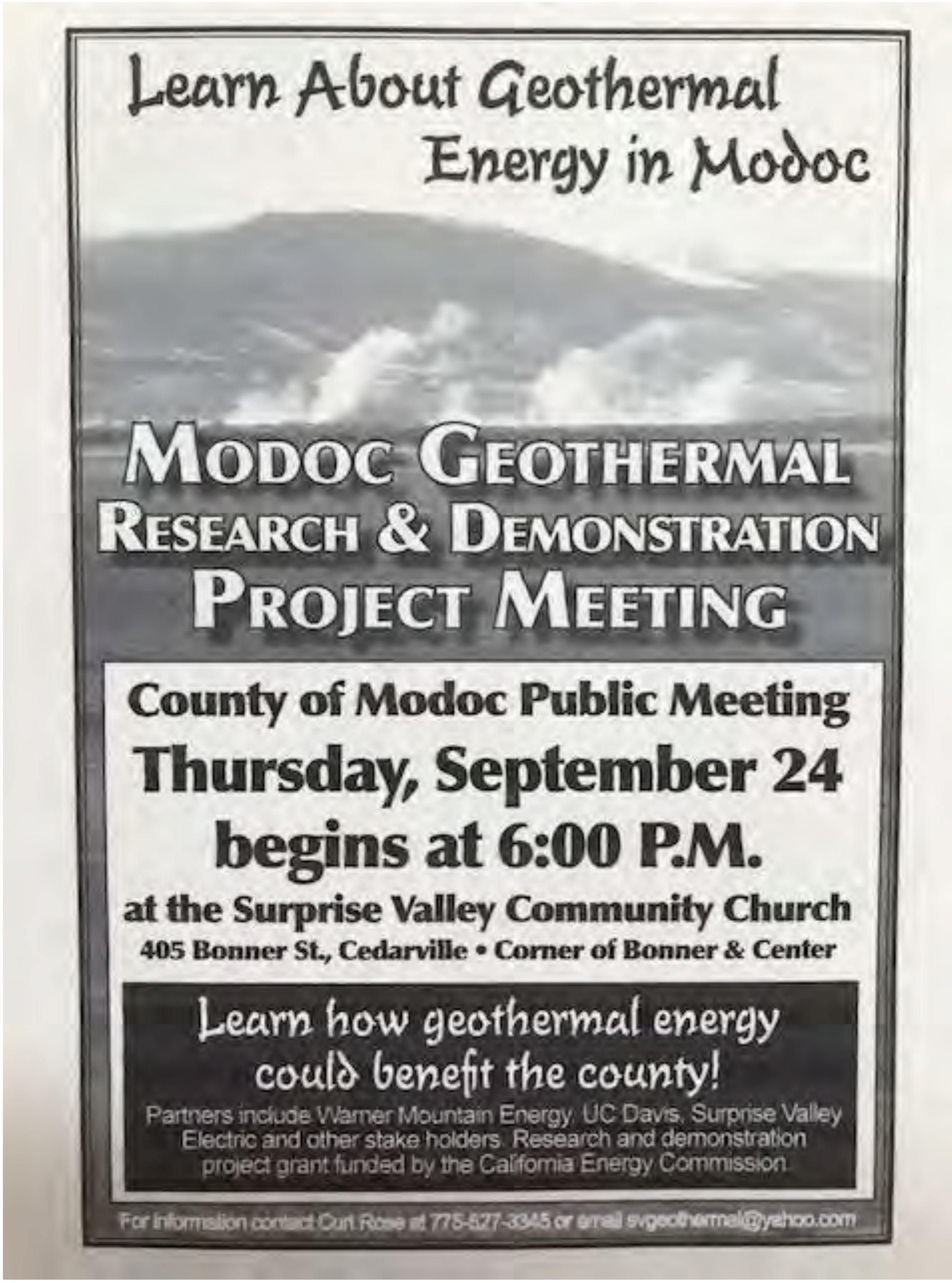

Learn About Geothermal
Energy in Modoc
MODOC GEOTHERMAL
RESEARCH & DEMONSTRATION
PROJECT MEETING
County of Modoc Public Meeting
Thursday, September 24
begins at 6:00 P.M.
at the Surprise Valley Community Church
405 Bonner St., Cedarville • Corner of Bonner & Center
Learn how geothermal energy
could benefit the county!
Partners include Warner Mountain Energy, UC Davis, Surprise Valley Electric and other stake holders. Research and demonstration project grant funded by the California Energy Commission.
For information contact Curt Rose at 775-527-3345 or email svgeothermal@yahoo.com

NS31A-1948 Investigation of the heat source(s) of the Surprise Valley Geothermal System, Northern California

Nicole Tanner[1], *Chris Daniel Holt*[1], *Samuel Hawkes*[1], *James S McClain*[1], *Lisa Safford*[2], *Leland L Mink*[2], *Curtis Rose*[3] *and Robert A Zierenberg*[4], *(1)University of California Davis, Davis, CA, United States, (2)Blackrock Geoscience, Pocatello, ID, United States, (3)Surprise Valley Hot Springs, Cedarville, CA, United States, (4)University of California Davis, Earth and Planetary Sciences, Davis, CA, United States*

Copy of research paper.

NS31A-1948: Investigation of the heat source(s) of the Surprise Valley Geothermal System, Northern California

Concerns about environmental impacts and energy security have led to an increased interest in sustainable and renewable energy resources, including geothermal systems. It is essential to know the permeability structure and possible heat source(s) of a geothermal area in order to assess the capacity and extent of the potential resource.

We have undertaken geophysical surveys at the Surprise Valley Hot Springs in Cedarville, California to characterize essential parameters related to a fault-controlled geothermal system. At present, the heat source(s) for the system are unknown. Igneous bodies in the area are likely too old to have retained enough heat to supply the system, so it is probable that fracture networks provide heat from some deeper or more distributed heat sources. However, the fracture system and permeability structure remain enigmatic. The goal of our research is to identify the pathways for fluid transport within the Surprise Valley geothermal system using a combination of geophysical methods including active seismic surveys and short- and long-period magnetotelluric (MT) surveys.

We have collected 14 spreads, consisting of 24 geophones each, of active-source seismic data. We used a "Betsy Gun" source at 8 to 12 locations along each spread and have collected and analyzed about 2800 shot-receiver pairs. Seismic velocities reveal shallow lake sediments, as well as velocities consistent with porous basalts. The latter, with velocities of greater than 3.0 km/s, lie along strike with known hot springs and faulted and tilted basalt outcrops outside our field area. This suggests that basalts may provide a permeable pathway through impermeable lake deposits.

We conducted short-period (10Hz-60kHz) MT measurements at 33 stations. Our short-period MT models indicate shallow resistive blocks (>100Ωm) with a thin cover of more conductive sediments (~10Ωm) at the surface. Hot springs are located in gaps between resistive blocks and are connected to deeper low resistivity zones (~1Ωm), suggestive of a fluid pathway. In order to refine these models and extend them to greater depths, we have deployed long-period (0.002Hz-10Hz) MT instruments in three locations. The data were collected over several weeks and are currently being processed and analyzed.

Authors:

N. Tanner, C. D. Holt, S. Hawkes, J.S. McClain, L. Safford, L.L. Mink, C. Rose, R. Zierenberg,

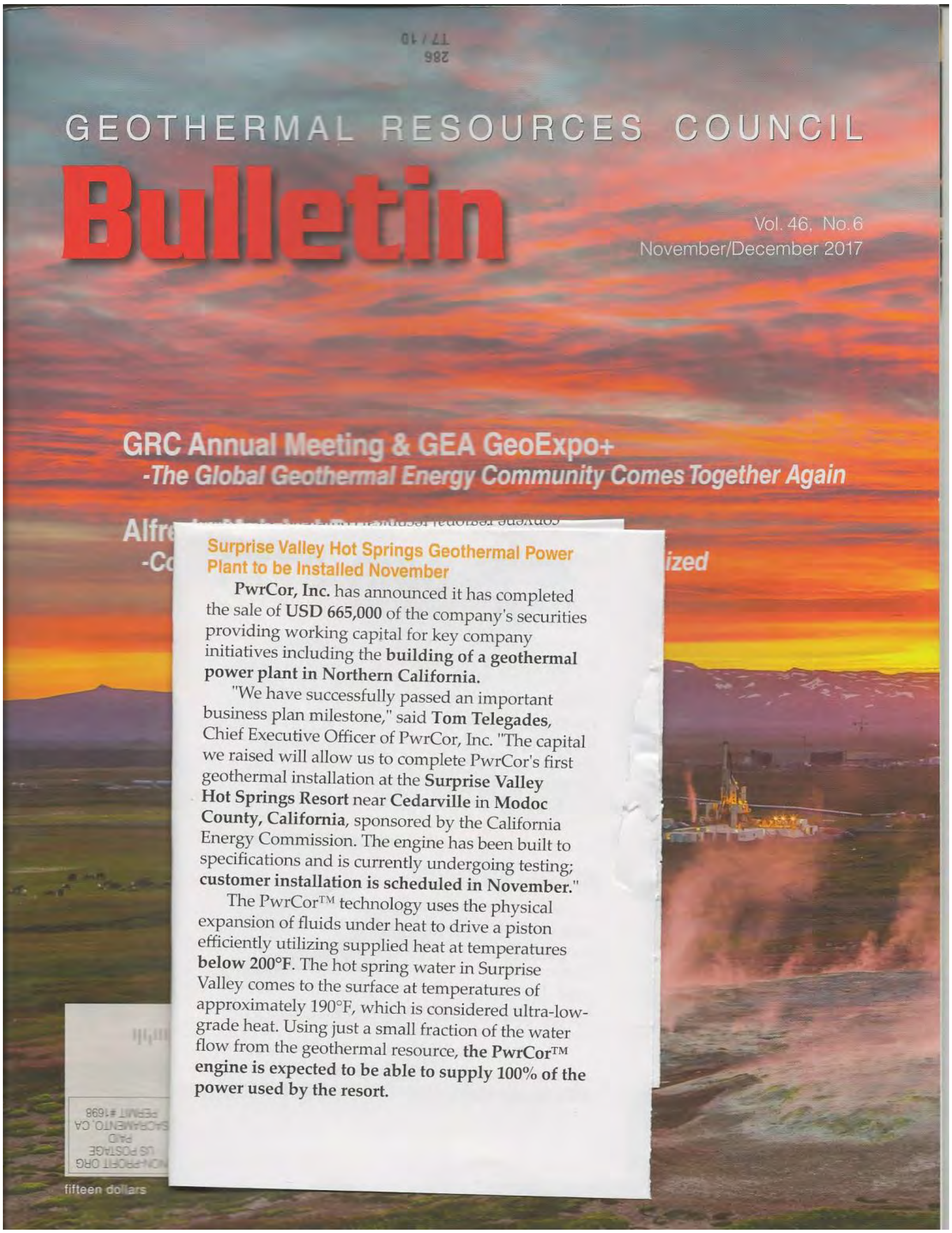

Surprise Valley Hot Springs Geothermal Power Plant to be Installed November

PwrCor, Inc. has announced it has completed the sale of **USD 665,000** of the company's securities providing working capital for key company initiatives including the **building of a geothermal power plant in Northern California.**

"We have successfully passed an important business plan milestone," said **Tom Telegades**, Chief Executive Officer of PwrCor, Inc. "The capital we raised will allow us to complete PwrCor's first geothermal installation at the **Surprise Valley Hot Springs Resort** near **Cedarville** in **Modoc County, California**, sponsored by the California Energy Commission. The engine has been built to specifications and is currently undergoing testing; **customer installation is scheduled in November.**"

The PwrCor™ technology uses the physical expansion of fluids under heat to drive a piston efficiently utilizing supplied heat at temperatures **below 200°F**. The hot spring water in Surprise Valley comes to the surface at temperatures of approximately 190°F, which is considered ultra-low-grade heat. Using just a small fraction of the water flow from the geothermal resource, **the PwrCor™ engine is expected to be able to supply 100% of the power used by the resort.**